ARCHIVES OF MECHANICS **Appears since 1949**



**Aims and Scope**

ARCHIVES OF MECHANICS provides a forum for original research on mechanics of solids, fluids and discrete systems, including the development of mathematical methods for solving mechanical problems. The journal encompasses all aspects of the field, with the emphasis placed on:

- mechanics of materials: elasticity, plasticity, time-dependent phenomena, phase transformation, damage, fracture; physical and experimental foundations, micromechanics, thermodynamics, instabilities
- methods and problems in continuum mechanics: general theory and novel applications, thermomechanics, structural analysis, porous media, contact problems
- dynamics of material systems
- fluid flows and interactions with solids



Address of the Editorial Office:
Institute of Fundamental Technological Research
Świętokrzyska 21
PL 00-049 Warsaw, Poland

Tel.(48-22) 826 60 22, Fax (48-22) 826 98 15, E-mail: publikac@ippt.gov.pl

**Abstracted/indexed in:**

Applied Mechanics Reviews, Current Mathematical Publications, Mathematical Reviews, MathSci, Zentralblatt für Mathematik, UnCover, Inspec.

http://am.ippt.gov.pl/

Polish Academy of Sciences
Institute of Fundamental Technological Research



# Archives of Mechanics

## Archiwum Mechaniki Stosowanej

volume 54 issue 1

## SUBSCRIPTIONS

Address of the Editorial Office: Archives of Mechanics
Institute of Fundamental Technological Research, Świętokrzyska 21
PL 00-049 Warsaw, Poland
Tel. 48 (*prefix*) 22 826 60 22, Fax 48 (*prefix*) 22 826 98 15,
e-mail:publikac@ippt.gov.pl

**Subscription orders for all journals edited by IFTR may be sent directly to the Editorial Office of the Institute of Fundamental Technological Research**

**Subscription rates**

Annual subscription rate (2002) including postage is US $ 240.
Please transfer the subscription fee to our bank account: Payee: IPPT PAN,
Bank: PKO SA. IV O/Warszawa,
Account number 12401053-40054492-3000-401112-001.

All journals edited by IFTR are available also through:

- Foreign Trade Enterprise ARS POLONA Krakowskie Przedmieście 7,
  00-068 Warszawa, Poland fax 48 (*prefix*) 22 826 86 73
- RUCH S.A. ul. Towarowa 28,
  00-958 Warszawa, Poland fax 48 (*prefix*) 22 620 17 62
- International Publishing Service Sp. z o.o. ul. Noakowskiego 10 lok. 38
  00-664 Warszawa, Poland tel./fax 48 (*prefix*) 22 625 16 53, 625 49 55

## Warunki prenumeraty

**Redakcja przyjmuje prenumeratę na wszystkie czasopisma wydawane przez IPPT PAN. Bieżące numery można nabyć, a także zaprenumerować roczne wydanie Archiwum Mechaniki Stosowanej bezpośrednio w Dziale Wydawnictw IPPT PAN, Świętokrzyska 21, 00-049 Warszawa, Tel. 48 (*prefix*) 22 826 60 22; Fax 48 (*prefix*) 22 826 98 15.**
Cena rocznej prenumeraty z bonifikatą (na rok 2002) dla krajowego odbiorcy wynosi 300 PLN

Również można je nabyć, a także zamówić (przesyłka za zaliczeniem pocztowym) we Wzorcowni Ośrodka Rozpowszechniania Wydawnictw Naukowych PAN,
00-818 Warszawa, ul. Twarda 51/55, tel. 48 (*prefix*) 22 697 88 35.
Wpłaty na prenumeratę przyjmują także jednostki kolportażowe RUCH S.A. Oddział Krajowej Dystrybucji Prasy, 00-958 Warszawa, ul. Towarowa 28. Konto: PBK. S.A. XIII Oddział Warszawa nr 11101053-16551-2700-1-67. Dostawa odbywa się pocztą lotniczą, której koszt w pełni pokrywa zleceniodawca. Tel. 48 (*prefix*) 22 620 10 39, Fax 48 (*prefix*) 22 620 17 62

Arkuszy wydawniczych 10. Arkuszy drukarskich 8.3
Papier offset. kl III 70g. B1.
Oddano do składania w grudniu 2001 r. Druk ukończono w lutym 2002 r.
Skład i łamanie: E. Jaczyńska.
Druk i oprawa: Drukarnia Braci Grodzickich, Piaseczno ul. Geodetów 47A.

Arch. Mech., 54, 1, pp. 3–13, Warszawa 2002



# On nonlinear waves in elastic conductors under a magnetic field

S. CHAKRABORTY

*St. Xavier's College*
*30 Park Street, Calcutta 700016, India*

A STUDY OF THE BEHAVIOR of magneto-elastic waves in a nonlinear isotropic elastic conductor by applying the method of multiple scales and perturbation has been made for a general displacement wave, under the action of an arbitrarily directed, uniform magnetic field. While in the case of transverse magnetic field the shock the waves are formed, it has been shown here that, under an oblique magnetic field, the wave is distorted without the formation of shocks.

## 1. Introduction

THE STUDY OF ONE-DIMENSIONAL waves in nonlinear elastic media were investigated by many authors such as NAYFEH [1], LARDNER [2,3]. They considered longitudinal and transverse waves and examined the growth of amplitude and formation of shock waves, using the methods of perturbation and multiple scales. MAUGIN [4] considered the effect of a bias magnetic field on the problems of propagation of harmonic waves in hyperelastic dielectrics and in perfectly conducting nonlinear elastic conductor. HEFNI *et al.* [5] have studied general one-dimensional bulk waves in a non-linear magneto-elastic conductor. They considered both the linear and nonlinear waves from the general formulation of the constitutive equations. CHAKRABORTY [6] recently considered the problem of distortion of waves in a nonlinear magneto-elastic conductor wherein it has been shown that shock waves may be formed in a traveling wave signal, depending on the elastic coefficients and the magnetic field, the direction of the bias magnetic field being transverse to the direction of the wave propagation. In the present paper we consider the bias magnetic field to have an arbitrary direction. The method of perturbation and multiple scales have been used. Equations of motion of different orders have been obtained. Several particular cases have been considered. For the bias magnetic field oblique to the direction of wave propagation, it is seen here that no shocks are formed.

## 2. Basic equations

Maxwell's equations of the electromagnetic field in which the displacement current has been neglected are, in the usual notations, the following:

$$\begin{aligned} \operatorname{div}\mathbf{B} &= 0, \\ \operatorname{div}\mathbf{D} &= \rho_e, \\ \operatorname{curl}\mathbf{H} &= J, \\ \operatorname{curl}\mathbf{E} + \mathbf{B}_t &= 0, \end{aligned} \tag{2.1}$$

($\rho_e$ is the electrostatic charge density). The constitutive equations of the medium are taken as

$$\begin{aligned} \mathbf{B} &= \mu\mathbf{H}, \\ \mathbf{D} &= \varepsilon_1\mathbf{E} \end{aligned} \tag{2.2}$$

while Ohm's law in the generalized form is

$$\mathbf{J} = \sigma\left[\mathbf{E} + \mathbf{u}_t \times \mathbf{B}\right] \tag{2.3}$$

$\sigma$ being the electrical conductivity, $\mathbf{u}_t \left(\equiv \dfrac{\partial \mathbf{u}}{\partial t}\right)$ being velocity of the material point of the medium.

The motion of the medium is governed by the stress equations of motion by including the Lorentz force of electromagnetic origin:

$$L_{ij}\,,\, j + (\mathbf{J} \times \mathbf{B})_i = \rho_0 \frac{\partial^2 u_i}{\partial t^2}, \qquad i = 1,2,3\,, \tag{2.4}$$

$\sigma$ is the mass per unit volume in the undeformed state and $L_{ij}$ is the PIOLA-KIRCHHOFF tensor derived from the strain energy W per unit volume [BLAND (7)], given by

$$L_{ij} = \frac{\partial W}{\partial u_{i,j}}, \qquad i,j = 1,2,3\,. \tag{2.5}$$

The expression for $W$ for a nonlinear elastic solid is taken in the form

$$W = \frac{1}{2}\lambda I_1 + GI_2 + \alpha I_1^3 + \beta I_1 I_2 + \gamma I_3, \tag{2.6}$$

where $\lambda$, $G$ correspond to elastic constants in the linear theory, and $\alpha, \beta, \gamma$ are higher order elastic coefficients, $I_1$, $I_2$, $I_3$ are the three independent strain-invariants given by

$$I_1 = e_{ii}, \quad I_2 = e_{ij}e_{ij}, \quad I_3 = e_{ij}e_{jk}e_{ki}, \qquad i,j,k = 1,2,3\,, \tag{2.7}$$

while the strain tensor $e_{ij}$ in terms of displacement $u_i(x_1, x_2, x_3, t)$ is given by

$$e_{ij} = \left(\frac{1}{2}\right)(u_{i,j} + u_{j,i} + u_{k,i}u_{k,j}), \qquad i, j, k = 1, 2, 3. \tag{2.8}$$

The term $\mathbf{J} \times \mathbf{B}$ in (2.4) is the Lorentz force per unit volume due to the magnetic field $\mathbf{B}$ and the current density $\mathbf{J}$.

### 2.1. Formulation

The displacement wave travels in the $x_1$ direction and the medium is acted upon by a uniform bias magnetic field $\mathbf{H}^0$ in an arbitrary direction. Let us choose the $x_2$-axis such that $\mathbf{H}^0$ lies in the $x_1x_1$ plane (this is always possible whatever would be the direction of $\mathbf{H}^0$). Hence we have

$$\mathbf{H}^0 = (H_1^0, H_2^0, 0). \tag{2.9}$$

The perturhed magnetic field is

$$\mathbf{H} = \mathbf{H}^0 + \mathbf{h} \tag{2.10}$$

where

$$\mathbf{h} = (h_1, h_2, h_3). \tag{2.11}$$

For a spatially one-dimensional problem, we write equation (2.10) as

$$\mathbf{H} = H_1, H_2, H_3 \tag{2.12}$$

and

$$H_i = H_i^0 + h_i(x_1, t,) \qquad i = 1, 2, 3. \tag{2.13}$$

The displacement components $(u_1, u_2, u_3)$ are functions of $x_1$ and time $t$ only. The equations of motion (2.4) are simplified to

$$\frac{\partial}{\partial x_1} L_{i1} + (\mathbf{J} \times \mathbf{B})_i = \rho_0 \frac{\partial^2 u_i}{\partial t^2}, \qquad i = 1, 2, 3. \tag{2.14}$$

From Eqs. (2.5) and (2.6),

$$\begin{aligned} L_{11} &= \frac{\partial W}{\partial I_1}\frac{\partial I_1}{\partial u_{1,1}} + \frac{\partial W}{\partial I_2}\frac{\partial I_2}{\partial u_{1,1}} + \frac{\partial W}{\partial I_3}\frac{\partial I_3}{\partial u_{1,1}} \\ &= \left(\lambda I_1 + 3\alpha I_1^2 + \beta I_2\right)(1 + u_{1,1}) + (G + \beta I)\,(2e_{11}(1 + u_{1,1})) \\ &\quad + \gamma\left[\left(3e_{11}^2 + 3e_{12}^2 + 3e_{13}^2\right)(1 + u_{1,1})\right], \end{aligned} \tag{2.15}$$

$$L_{21} = \frac{\partial W}{\partial u_{2,1}} = \left(\lambda I_1 + 3\alpha I_1^2 + \beta I_2\right) u_{2,1} + (G + \beta I_1)\ (2e_{11}u_{2,1} + 2e_{12}) + \gamma \left[3e_{11}^2 + 3e_{12}^2 + 3e_{13}^2 + \left(\frac{3}{2}\right) e_{11}\right] u_{2,1}, \tag{2.16}$$

$$L_{31} = \left(\lambda I_1 + 3\alpha I_1^2 + \beta I_2\right) u_{3,1} + (G + \beta I_1)\ (1 + 2e_{11})\ u_{3,1} + \gamma \left[\left(3e_{11}^2 + 3e_{12}^2 + 3e_{13}^2\right) + \frac{3}{2} e_{11}\right] u_{3,1}. \tag{2.17}$$

The Lorentz force-components in our problem reduce to

$$(\mathbf{J} \times \mathbf{B})_1 = -\mu h_3 h_{3,1} - \mu\ \left(H_2^0 + h_2\right) + h_{2,1}, \tag{2.18}$$

$$(\mathbf{J} \times \mathbf{B})_2 = \mu\ \left(H_1^0 h_{2,1} + h_1 h_{2,1}\right), \tag{2.19}$$

$$(\mathbf{J} \times \mathbf{B})_3 = \mu h_{3,1}\ \left(H_1^0 + h_1\right), \tag{2.20}$$

where

$$h_{2,1} = \frac{\partial h_2}{\partial x_1}, \qquad h_{3,1} = \frac{\partial h_3}{\partial x_1}. \tag{2.21}$$

For a perfectly conducting solid, we get from equations $(2.1)_4$ and (2.3):

$$\frac{\partial}{\partial t}\mathbf{h} = \operatorname{curl}(\mathbf{u}_t \times \mathbf{H}) \tag{2.22}$$

But curl $(\mathbf{u}_t \times \mathbf{H})$ in our problem has the components

$$0,\ u_{1_{tx_1}} H_2 - u_{1_t} h_{2_{x_1}} + u_{2_{tx_1}} H_1 + u_{2_t} h_{1_{x_1}} \quad u_{3_{tx_1}} H_1 + u_{3_t} h_{1_{x_1}} - u_{1_t} h_{3_{x_1}} \tag{2.23}$$

where

$$u_{1_t} = \frac{\partial u_1}{\partial t}, u_{1_{tx_1}} = \frac{\partial^2 u_1}{\partial t \partial x_1} \quad \text{etc.} \tag{2.24}$$

From Maxwell's equation $(2.1)_1$ and the component of (2.22), we get

$$\frac{\partial h_1}{\partial x_1} = 0 \quad \text{and} \quad \frac{\partial h_1}{\partial t} = 0 \tag{2.25}$$

We conclude from (2.25) that

$$h_1 = 0. \tag{2.26}$$

For applying the method of perturbation, parameter $\varepsilon$ is used to denote the order of magnitude of the displacement. We also use the slowness parameters $\xi$, $\eta$ defined by

$$\xi = \varepsilon x_1, \ \eta = \varepsilon^2 x_1 . \tag{2.27}$$

The displacement components can now written as

$$u_i(x_1,t) = \varepsilon\, u_{i0}(x_1,t,\xi,\eta) + \varepsilon^2 u_{i1}(x_1,t,\xi,\eta) + \varepsilon^3 u_{i2}(x_1,t,\xi,\eta) + 0(\varepsilon^4), \quad i = 1,2,3. \tag{2.28}$$

Since the magnetic perturbation arises from the motion, $h_2, h_3$ are of the order of $\varepsilon$. We write

$$h_\alpha(x_1,t) = \varepsilon\, h_{\alpha 0}(x_1,t,\xi,\eta) + \varepsilon^2 h_{\alpha 1}(x_1,t,\xi,\eta) + \varepsilon^3 h_{\alpha 2}(x_1,t,\xi,\eta) + 0(\varepsilon^4) \quad \alpha = 2,3. \tag{2.29}$$

As a consequence of the introduction of the slowness parameters $\xi, \eta$ as variables in the functions $u_{10}$,$u_{11}$ etc., the partial derivative $\dfrac{\partial}{\partial x_1}$ in the equations (2.1) to (2.21) is to be replaced by the operator

$$\frac{\partial}{\partial x_1} + \varepsilon \frac{\partial}{\partial \xi} + \varepsilon^2 \frac{\partial}{\partial \eta}. \tag{2.30}$$

Substituting in (2.22) the expressions from equations (2.23), (2.28) and (2.29) and equating the terms with different powers of $\varepsilon$, on integrating w.r.t. time, we obtain

$$h_{20} = -u_{10} H_2^0 + u_{20_{x_1}} H_1^0 \tag{2.31}$$

$$h_{21} = -H_2^0 u_{11_{x_1}} - H_2^0 u_{10_\xi} + H_1^0 u_{20_\xi} + H_1^0 u_{21_{x_1}} + H_2^0 \int \left(u_{10_t} u_{10_{x_1}}\right)_{x_1} dt - H_1^0 \int \left(u_{10_t} u_{20_{x_1}}\right)_{x_1} dt \tag{2.32}$$

$$h_{22} = -H_1^0 u_{12_{x_1}} + H_2^0 u_{11_\xi} + H_1^0 u_{22_{x_1}} + H_1^0 u_{21_\xi} + H_1^0 u_{20_\eta} + \int F dt \tag{2.33}$$

where

$$F = -u_{10_{tx_1}} h_{21} - h_{20} u_{11_{tx_1}} - h_{20} u_{10_{\xi\xi}} + u_{20_{tx_1}} - h_{21_{x_1}} u_{10_t} - u_{11_t} h_{20_{x_1}} - h_{20_\xi} u_{10_t},$$

$$h_{30} = H_1^0 u_{30_{x_1}}, \tag{2.34}$$

$$h_{31} = -h_{30} u_{10_{x_1}} + H_1^0 u_{30_\xi} + H_1^0 u_{31_{x_1}} + H_1^0 \int u_{10_{x_1}} u_{30_{tx_1}} dt, \tag{2.35}$$

$$h_{32_t} = H_1^0 u_{30_{t\eta}} + H_1^0 u_{32_{tx_1}} + H_1^0 u_{31_{t\xi}} - (u_{11_t} h_{30})_{x_1} - (u_{10_t} h_{30})_\xi - (u_{10_t} h_{31})_{x_1}. \tag{2.36}$$

On substituting from equations (2.15) to (2.20), (2.28) to Eq. (2.35) in each of the three equations of (2.14), and then equating the coofficients of $\varepsilon, \varepsilon^2$ and $\varepsilon^3$ on both sides, we get the following equations:

$$0(\varepsilon) : D_1 u_{10} = \frac{P_2}{2} u_{20_{x_1 x_1}}, \tag{2.37}$$

$$0(\varepsilon^2) : D_1 u_{11} - D_3 u_{21} = P_1 u_{10_{x_1 \xi}} + P_2 u_{20_{x_1 \xi}} + T_1, \tag{2.38}$$

$$0(\varepsilon) : D_2 u_{20} = \frac{P_2}{2} u_{10_{x_1 x_1}}, \tag{2.39}$$

$$0(\varepsilon^2) : D_2 u_{21} - D_3 u_{11} = P_2 u_{20_{x_1 \xi}} + P_3 u_{10_{x_1 \xi}} + T_2, \tag{2.40}$$

$$\begin{aligned} 0(\varepsilon^3) : D_2 u_{22} = {} & P_2 u_{21_{x_1 \xi}} + P_2 u_{20_{x_1 \eta}} + \frac{P_3}{2} u_{11_{x_1 \xi}} + \frac{P_2}{2} u_{20_{\xi\xi}} \\ & - c_3^2 (u_{20_\xi} u_{10_{x_1}} + u_{10_{x_1}} u_{21_{x_1}} + u_{10_\xi} u_{20_{x_1}} + u_{11_{x_1}} u_{20_{x_1}})_{x_1} \\ & - \frac{P_3}{2} \left(u_{10_{x_1 \eta}} + u_{12_{x_1 x_1}}\right) - \frac{P_3}{2} \int \left(u_{10_t} u_{10_{x_1}}\right)_{x_1} dt + a_1^2 \int \left(u_{10_t} u_{20_{x_1}}\right)_{x_{1\xi}} dt \\ & - \frac{\mu H_1^0}{P_0} \int F_x dt - c_4^2 \left(u_{20_{x_1}} u_{10_{x_1}}^2 + u_{20_{x_1}}^3 + u_{30_{x_1}}^2 u_{20_{x_1}}\right)_{x_1}. \end{aligned} \tag{2.41}$$

$$0(\varepsilon) : D_2 u_{30} = 0, \tag{2.42}$$

$$0(\varepsilon^2) : D_2 u_{31} = -P_2 u_{30_{x_1\xi}} + T_3, \tag{2.43}$$

where

$$D_1 \equiv \left(c_1^2 + a_2^2\right) \frac{\partial^2}{\partial x_1 \partial x_1} - \frac{\partial^2}{\partial t^2}, \tag{2.44}$$

$$D_2 \equiv \left(c_2^2 + a_1^2\right) \frac{\partial^2}{\partial x_1 \partial x_1} - \frac{\partial^2}{\partial t^2}, \tag{2.45}$$

$$D_3 \equiv a_1 a_2 \frac{\partial^2}{\partial x_1 \partial x_1}, \tag{2.46}$$

$$P_1 = -2\left(c_1^2 + a_2^2\right), \tag{2.47}$$

$$P_2 = -2\left(c_2^2 + a_1^2\right), \tag{2.48}$$

$$P_3 = 2a_1 a_2, \tag{2.49}$$

$$\begin{aligned} T_1 = &- \left(2c_2^2 + 2c_4^2 - a_2^2\right) u_{10_{x_1}} u_{10_{x_1x_1}} - \left(c_3^2 - a_1^2\right) \\ &\cdot \left(u_{20_{x_1x_1}} u_{20_{x_1}} + u_{30_{x_1x_1}} u_{30_{x_1}}\right) - a_1 a_2 \left(u_{10_{x_1x_1}} u_{20_{x_1}} + u_{10_{x_1}} u_{20_{x_1x_1}}\right) \\ &+ a_2^2 \int \left(u_{10_t} u_{10_{x_1}}\right)_{x_1x_1} dt - a_1 a_2 \int \left(u_{10_t} u_{20_{x_1}}\right)_{x_1x_1} dt, \end{aligned} \tag{2.50}$$

$$\begin{aligned} T_2 = &-c_3^2 \left(u_{10_{x_1}} u_{20_{x_1}}\right)_{x_1} - a_1 a_2 \int \left(u_{10_t} u_{10_{x_1}}\right)_{x_1x_1} dt \\ &+ a_1^2 \int \left(u_{10_t} u_{20_{x_1}}\right)_{x_1x_1} dt, \end{aligned} \tag{2.51}$$

$$\begin{aligned} T_3 = &\, a_1^2 \left(u_{10_{x_1x_1}} u_{30_{x_1}} + u_{30_{x_1x_1}} u_{10_{x_1}}\right) - c_3^2 \left(u_{10_{x_1}} u_{30_{x_1}}\right)_{x_1} \\ &+ a_1^2 \int \left(u_{10_t} u_{30_{x_1}}\right)_{x_1x_1} dt. \end{aligned} \tag{2.52}$$

$$c_1^2 = (\lambda + 2G)/\rho_0, \quad c_2^2 = G/\rho_0, \tag{2.53}$$

$$c_3^2 = (\lambda + 2G + \beta + 3\gamma/2)/\rho_0, \tag{2.54}$$

$$c_4^2 = (\lambda/2 + G + 3\alpha + 3\beta + 3\gamma)/\rho_0, \tag{2.55}$$

$$a_1^2 = \mu H_1^{0^2}/\rho_0, \quad a_2^2 = \mu H_2^{0^2}/\rho_0. \tag{2.56}$$

Here $c_1, c_2$ are the $P$ and $S$ wave velocities in linear elasticity, while $a_1, a_2$ are the Alfven wave velocities. We know that $c_1 > c_2$ while $a_1$ and $a_2$ are much less than $c_2$. We consider the cases :

CASE 1. $a_1 \neq 0, a_2 \neq 0$. This occurs when the magnetic field $H^0$ is oblique i.e. it has non-zero components $H_1^0$ and $H_2^0$. From equations (2.37), (2.39) and (2.41) we notice that $u_{10}$ and $u_{20}$ satisfy two coupled equations while $u_{30}$ satisfies a single equation. For linear wave solutions in the form

$$u_{10} = A_{10} \exp\left[ik\,(x - Vt)\right], \tag{2.57}$$

$$u_{20} = A_{20} \exp\left[ik\,(x - Vt)\right], \tag{2.58}$$

$$u_{30} = A_{30} \exp\left[ik\left(x - \sqrt{c_2^2 + a_1^2}\,t\right)\right], \tag{2.59}$$

the velocity $V$ is a solution of the biquadratic equation

$$V^4 - V^2\left(c_1^2 + c_2^2 + a_1^2 + a_2^2\right) + \left(c_1^2 + a_2^2\right)\left(c_2^2 + a_1^2\right) - a_1^2 a_2^2 = 0. \tag{2.60}$$

The two solutions, say $V_1, V_2$, are given by

$$V_{1,2} = \left[\left(c_1^2 + c_2^2 + a_1^2 + a_2^2\right)/2 \pm \frac{1}{2}\left(\left(c_1^2 + a_2^2 - c_2^2 - a_1^2\right)^2 + 4a_1^2 a_2^2\right)^{1/2}\right]^{1/2} \tag{2.61}$$

Since $c_1^2 > c_2^2$, it is possible that $c_1^2 + a_2^2 > c_2^2 + a_1^2$. Then we get from (2.61) the bounds for $V_1, V_2$ :

$$c_1^2 + a_2^2 < V_1^2 < c_1^2 + a_2^2 + a_1 a_2 \tag{2.62}$$

and

$$c_2^2 + a_1^2 - a_1 a_2 < V_2^2 < c_2^2 + a_1^2. \tag{2.63}$$

One effect of the oblique magnetic field is therefore that there exist two possible waves, one travelling with velocity greater than $\sqrt{c_1^2 + a_2^2}$, while the other has the velocity less than $\sqrt{c_2^2 + a_1^2}$.

To assess the nonlinear wave components we notice that $u_{11}, u_{21}$ here are involved in two equations (2.38) and (2.40). A comparison of these equations with the case treated in [6] shows that distortion of the wave

$$u_{10} = A_{10}(\xi, \eta)\, e^{ik(x - V_1 t)}, \tag{2.64}$$

$$u_{20} = A_{20}(\xi, \eta)\, e^{ik(x - V_1 t)}, \tag{2.65}$$

with distance takes place, but no shock is formed since $V_1$ or $V_2$ are different from $\sqrt{c_1^2 + a_2^2}$ and $\sqrt{c_2^2 + a_1^2}$. We therefore conclude that the presence of an oblique magnetic field prevents the formation of shock in the propagation of a magnetoelastic wave.

CASE 2. $a_1 = 0$, $a_2 \neq 0$, i.e. $H_1^0 = 0$, $H_2^0 \neq 0$. This case has been treated by Chakraborty [6] in which the possibility of a shock for a longitudinal wave was studied in detail.

CASE 3. $a_2 = 0$, $a_1 \neq 0$, i.e, $H_2^0 = 0$, $H_1^0 \neq 0$. In this case the longitudinal wave $u_{10}$ is a purely elastic one, while the transverse wave $u_{20}$ travels with velocity $\left(c_2^2 + a_1^2\right)^{\frac{1}{2}}$ Taking $u_{10} = u_{11} = u_{12} = u_{30} = 0$, i.e. assuming that no elastic longitudinal wave propagates, equation (2.41) gives, ignoring the slowness parameter $\xi$ as it has no effect here,

$$D_2 u_{22} = P_2 u_{20\eta x_1} - c_4^2 \left(u_{20_{x_1}}^3\right)_{x_1}. \tag{2.66}$$

On substituting in (2.66)

$$u_{20} = G(\theta, \eta) \tag{2.67}$$

with

$$\theta = t - x_1 \Big/ \sqrt{c_2^2 + a_1^2}, \tag{2.68}$$

$$\phi = t + x_1 \Big/ \sqrt{c_2^2 + a_1^2} \tag{2.69}$$

being a solution of equation (2.39) for a progressive transverse wave, equation (2.66) becomes

$$u_{22\theta\phi} = -\frac{\sqrt{c_2^2 + a_1^2}}{2} G_{\theta\eta} + \frac{3}{4} \frac{c_4^2}{\left(c_2^2 + a_1^2\right)^2} G_\theta^2 G_{\theta\theta}. \tag{2.70}$$

Integrating (2.70) w. r. t. $\theta$, we get

$$u_{22\phi} = -\frac{\sqrt{c_2^2 + a_1^2}}{2} G_\eta + \frac{1}{4} \frac{c_4^2}{\left(c_2^2 + a_1^2\right)^2} G_\theta^3. \tag{2.71}$$

In order to be sure that integration of (2.71) w. r. t. $\phi$ gives an equation that keeps $u_{22}$ finite, we get the secular equation

$$-\frac{\sqrt{c_2^2 + a_1^2}}{2} G_\eta + \frac{c_4^2}{4\left(c_2^2 + a_1^2\right)^2} G_\theta^3 = 0. \tag{2.72}$$

Differentiating (2.72) w. r. t. $\theta$ and putting $G_\theta = g$, we get the equation

$$g_\eta - M_1 g^2 g_\theta^2 = 0 \tag{2.73}$$

where

$$M_1 = \frac{3c_4^2}{2\left(c_2^2 + a_1^2\right)^{\frac{5}{2}}}. \tag{2.74}$$

The solution of (2.73) corresponding to the initial condition

$$g(\theta, 0) = m(\theta) \tag{2.75}$$

$$g(\theta, \eta) = m(\theta_1) \tag{2.76}$$

where $\theta_1$ is given by (WHITHAM [8])

$$\theta_1 = \theta + M_1 m^2(\theta_1)\, \eta. \tag{2.77}$$

Equation (2.77) shows that the magneto elastic quasi-transverse wave is distorted and shock waves are possible under suitable initial condition (LARDNER [3]).

## 3. Conclusion

The effect of a bias magnetic field acting obliquely to the direction of a wave propagating in a nonlinear elastic medium is to prevent the shock formation of waves with displacement in its plane.

## Acknowledgement

The author thanks (Retd.) Professor S. K.Chakraborty, Department of Mathematics, University of Burdwan, for help and encouragement while working on the problem.

## References

1. A. H. NAYFEH, *Finite amplitude longitudinal waves in a non-uniform bar,* J. Sound and Vibration, **42**, 3, 357-361, 1975.
2. R. W. LARDNER, *Non-linear surface waves in an elastic solid,* Int. J. Engng. Sc. **21**, 1331-1342, 1983.
3. R. W. LARDNER, *Non-linear effects on transverse shear waves in an elastic medium,* J. Elasticity, **15**, 53-57, 1985.
4. G. A. MAUGIN, *Wave motion in magnetizable deformable solids (Review article),* Int. J. Engng. Sc. **19**, 321, 1981.
5. A. Z. HEFNI, A. F. GALEB, and G. A. MAUGIN, *One-dimensional bulk waves in a non-linear magnetoelastic conductor of finite conductivity,* Int. J. Engng. Sc. **33**, 14, 2067-2084, 1995.
6. S. CHAKRABORTY, *On distortion of waves in non-linear magnetoelastic conductor,* Arch. Mech., **50**, 6, 945-951, Warszawa 1998.
7. D. R. BLAND, *Non-linear dynamic elasticity,* Blaisdell, Waltham, Mass, 1969.
8. G. B. WHITHAM, *Linear and non-linear waves,* John Wiley and Sons, 1974.

*Received July 28, 1999; revised version July 7, 2001.*

Arch. Mech., **54**, 1, pp. 15–33, Warszawa 2002

# A domain of influence theorem in linear thermo-elasticity with thermal relaxation and internal variable

V. A. CIMMELLI and P. ROGOLINO

*Dept. of Mathematics, University of Basilicata,*
*Contrada Macchia Romana,*
*85100, Potenza-Italy*
*e-mail:cimmelli@unibas.it*
*e-mail:patrizia@dipmat.unime.it*

A DOMAIN OF INFLUENCE theorem is proved for a linear thermoelastic solid with a Cattaneo's type heat conduction law and a scalar internal variable. The obtained result is applied to prove the hyperbolicity of a semiempirical heat conduction theory, describing the propagation of thermal waves in crystals at low temperatures.

## 1. Introduction

A DOMAIN OF INFLUENCE theorem is one of the basic results of classical isothermal elastodynamics [1, 2]. It asserts that for a finite time $t > 0$ a solution of a given initial and boundary value problem, corresponding to the data which are defined in a bounded support, vanishes outside a bounded domain $D(t)$. Its physical interpretation is that an initial perturbation of a bounded elastic domain gives rise to an elastic disturbance which for any $t > 0$ cannot occupy the whole space, i. e. it propagates with a finite speed. Such a theorem cannot be proved in classical linear coupled thermoelasticity since the Fourier law of heat conduction implies an infinite speed of thermal disturbances [3]. LORD and SHULMAN [4] proposed a generalized dynamical theory of thermoelasticity which is based on a generalized heat conduction law [3]. Some domain of influence theorems in the framework of the afore-mentioned theory has been proved in [5 - 8]. Different authors [9 - 14] approach the problem of finite speed of thermal waves by introducing into the constitutive equation some additional internal variables related to the thermal inertia of the body at hand. The ensuing initial and boundary value problems are transformed from the mixed hyperbolic-parabolic type to the hyperbolic type. This situation is typical of the internal variables theory since very often additional variables are introduced to eliminate the paradox of infinite speed of propagation [15, 16]. For linear and quasi-linear systems of evolution equations the hyperbolicity is assured if a given matrix, related to the coefficients of the system, admits real eigenvalues and a corresponding complete

set of eigenvectors spanning the space of states [17, 18]. However, this property in general cannot be assured by *a priori* conditions but very often these conditions depend on the solution itself. In other words, these should be regarded as compatibility conditions in the sense that those solutions which do not verify them do not lead to a finite speed of propagation of thermomechanical disturbances. In many cases the notion of domain of influence yields the possibility of establishing a priori conditions ensuring the hyperbolicity. This renders the study of wave propagation more perspicuous.

In this paper we prove a domain of influence theorem for a linear thermoelastic solid obeying a generalized heat conduction equation and with an additional scalar internal variable. The physical nature of this variable will be not specified, allowing thus the model to describe a wide class of phenomena. In Sec. 2 we specify the model and its thermodynamic properties. In Sec. 3, after posing the initial and boundary value problem we are faced with, we enunciate our main hypotheses on the data and on the material functions. Then, in Sec. 4, we apply the technique developed in [8] to establish *a domain of dependence inequality* which, in Sec. 5, is used to prove our main result, i.e. a domain of influence theorem. Finally, in Sec. 6, the obtained result is applied to the so-called *semi-empirical heat conduction model*, introduced by Kosiński and co-workers [10, 12, 19], to describe non-Fourier heat conduction in solids.

## 2. The physical model

Let us consider a linear thermoelastic body $B$ which is identified with an open and connected region $C$ of the Euclidean three-dimensional point space $E_3$. The set $C$ is supposed to be regular and, generally, unbounded. The fundamental system of equations governing the time evolution of $B$ consists of:

1. The equation of motion

$$\rho\ddot{\mathbf{u}} = \operatorname{div}\mathbf{S} + \mathbf{b}, \tag{2.1}$$

where $\rho$ is the mass density, $\mathbf{u}$ the field of displacement, $\mathbf{S}$ the stress tensor, $\mathbf{b}$ the body force;

2. The balance of energy

$$\rho\dot{\epsilon} = \mathbf{S}\cdot\dot{\mathbf{E}} - \operatorname{div}\mathbf{q} + \rho r, \tag{2.2}$$

where $\epsilon$ means the specific internal energy, $\mathbf{E} \equiv \frac{1}{2}(\nabla\mathbf{u} + \nabla\mathbf{u}^T)$ is the strain tensor, $\mathbf{q}$ the heat flux vector and $r$ the radiating heat supply;

3. The second law of thermodynamics, expressed by the Clausius-Duhem inequality

$$\rho\dot{\eta} + \operatorname{div}\frac{\mathbf{q}}{\theta} - \rho\frac{r}{\theta} \geq 0, \tag{2.3}$$

where $\eta$ is the specific entropy and $\theta$ the absolute temperature;

4. The Maxwell-Cattaneo heat conduction equation

$$t_0\dot{\mathbf{q}} + \mathbf{q} = -\mathbf{K}\nabla\theta, \tag{2.4}$$

where constant $t_0$ is a suitable relaxation time and $\mathbf{K}$ the conductivity tensor;

5. The evolution equation for a temperature-dependent scalar internal variable $\alpha$ which in the present paper is set in the form

$$\dot{\alpha} = m\theta + n\alpha. \tag{2.5}$$

The scalar functions $m$ and $n$ express suitable material properties whose physical nature will remain unspecified. However, we observe that at the equilibrium ($\dot{\alpha} = 0$), $\alpha$ is proportional to the absolute temperature.

Taking into account (2.2), inequality (2.3) may be set in the form

$$-\rho(\dot{\Psi} + \eta\dot{\theta}) + \mathbf{S}\cdot\dot{\mathbf{E}} - \frac{1}{\theta}\mathbf{q}\cdot\nabla\theta \geq 0, \tag{2.6}$$

where

$$\Psi \equiv \epsilon - \theta\eta \tag{2.7}$$

is the Helmholtz free energy. Finally, a set of constitutive equations of the type

$$\Phi = \Phi^*(\theta, \nabla\theta, \mathbf{E}, \alpha, \nabla\alpha), \tag{2.8}$$

where $\Phi$ is an element of the set $\{\mathbf{S}, \epsilon, \Psi, \mathbf{q}\}$, characterizes the model under analysis. Compatibility of (2.8) with (2.6) implies the thermodynamical restrictions [20]

$$\eta = -\frac{\partial\Psi}{\partial\theta}, \tag{2.9}$$

$$\mathbf{S} = \rho\frac{\partial\Psi}{\partial\mathbf{E}}, \tag{2.10}$$

$$\Psi = \Psi(\theta, \mathbf{E}, \alpha, \nabla\alpha), \tag{2.11}$$

$$A\dot{\alpha} + \tilde{\mathbf{A}}\nabla\dot{\alpha} - \frac{1}{\theta}\mathbf{q}\cdot\nabla\theta \geq 0, \tag{2.12}$$

where $A \equiv \rho \dfrac{\partial \Psi}{\partial \alpha}$ is the so-called *affinity* representing the generalized force conjugated to $\alpha$ and $\tilde{A} \equiv \rho \dfrac{\partial \Psi}{\partial \nabla \alpha}$ [21, 22].

We pursue our analysis under the additional hypotheses that the stress tensor does not depend on $\alpha$ or on $\nabla \alpha$ and the internal energy does not depend on $\nabla \alpha$.

In such a case, the linearization procedure [20] leads to the following constitutive equation for $\mathbf{S}$ :

$$\mathbf{S} = \mathbf{C}[\mathbf{E}] + \theta \mathbf{M}, \tag{2.13}$$

where $\mathbf{C}$ is the classical fourth order tensor of linear elasticity while $\mathbf{M}$ is a second order symmetric tensor accounting for the stress-temperature relation. From (2.13) and (2.2) we get

$$c_e \dot{\theta} + c_\alpha \dot{\alpha} = \theta_0 \mathbf{M} \cdot \dot{\mathbf{E}} - \operatorname{div} \mathbf{q} + \rho r, \tag{2.14}$$

where $c_e \equiv \rho \dfrac{\partial \epsilon}{\partial \theta}$ is the heat capacity per unit of volume and $c_\alpha \equiv \rho \dfrac{\partial \epsilon}{\partial \alpha}$ is the latent heat per unit of volume related to the presence of the internal variable. Moreover, (2.10) and (2.13) yield

$$\Psi(\theta, \mathbf{E}, \alpha) = \frac{1}{2\rho} \mathbf{E} \cdot \mathbf{C}[\mathbf{E}] + \frac{1}{\rho} \theta \mathbf{M} \cdot \mathbf{E} + \Psi_0(\alpha, \theta, \nabla \alpha), \tag{2.15}$$

where $\Psi_0$ is the free energy corresponding to a rigid motion.

## 3. The initial and boundary value problem: basic assumptions and postulates

The fields $\rho$, $c_e$, $c_\alpha$, $m$, $n$, $\mathbf{K}$, $\mathbf{M}$ and $\mathbf{C}$ represent the material thermomechanical properties of $B$ and are supposed to be prescribed. The mass density $\rho$ and the specific and latent heats $c_e$ and $c_\alpha$, respectively, and the parameter $m$ are assumed to be positive fields on $\bar{C}$, i.e.

$$m > 0, \quad \rho > 0, \quad c_e > 0, \quad c_\alpha > 0 \ \text{ on } \bar{C}. \tag{3.1}$$

Requirements of stability for the solution of (2.5) force $n$ to be negative.

The elasticity tensor is symmetric and positive semidefinite so that [1)]

$$\mathbf{A} \cdot \mathbf{C}[\mathbf{B}] = \mathbf{B} \cdot \mathbf{C}[\mathbf{A}], \forall \mathbf{A}, \mathbf{B} \in Lin, \tag{3.2}$$

$$\mathbf{A} \cdot \mathbf{C}[\mathbf{A}] \geq 0 \ \forall \mathbf{A} \in Lin. \tag{3.3}$$

[1)] We denote by $V$ the basic Euclidean three-dimensional vector space and by $Lin$ the nine-dimensional vector space of all linear mappings from $V$ to $V$ (second order tensors on $V$).

Analogous relations are required to be satisfied by $\mathbf{K}$ and $\mathbf{M}$:

$$\mathbf{a} \cdot \mathbf{Kb} = \mathbf{b} \cdot \mathbf{Ka}; \quad \mathbf{a} \cdot \mathbf{Mb} = \mathbf{b} \cdot \mathbf{Ma} \quad \forall \mathbf{a}, \mathbf{b} \in V,$$

$$\mathbf{a} \cdot \mathbf{Ka} \geq 0 \quad \forall \mathbf{a} \in V.$$

These relations imply the inequalities [1]

$$2\mathbf{A} \cdot \mathbf{C}[\mathbf{B}] \leq \xi^{-1}\mathbf{A} \cdot \mathbf{C}[A] + \xi \mathbf{B} \cdot \mathbf{C}[\mathbf{B}] \quad \forall \mathbf{A}, \mathbf{B} \in Lin, \ \forall \xi > 0 \tag{3.4}$$

$$2\mathbf{a} \cdot \mathbf{Kb} \leq \xi^{-1}\mathbf{a} \cdot \mathbf{Ka} + \xi \mathbf{b} \cdot \mathbf{Kb} \quad \forall \mathbf{a}, \mathbf{b} \in V, \ \forall \xi > 0. \tag{3.5}$$

We also assume that $\rho^{-1}(\mathbf{x})$, $c_e^{-1}(\mathbf{x})$, $c_\alpha^{-1}(\mathbf{x})$, $|\mathbf{C}(\mathbf{x})|$, $|\mathbf{K}(\mathbf{x})|$ and $|\mathbf{M}(\mathbf{x})|$ are bounded on $\bar{C}$. The elasticity tensor $\mathbf{C}$ maps $Lin$ into the subspace $Sym$ of all symmetric elements of $Lin$: its kernel is the whole subspace $Skw$ of all skew-symmetric elements of $Lin$. Finally, we assume that the material fields have the following regularity properties:

$$\rho, \ c_e, \ c_\alpha, \ m, \ n, \ \in C^0(\bar{C}), \ \mathbf{K}, \ \mathbf{M} \in C_2^1(\bar{C}), \ \mathbf{C} \in C_4^1(\bar{C}), \tag{3.6}$$

where, as usual, $\bar{C} = C \cup \partial C$. Moreover we suppose that the external fields $\mathbf{b}(\mathbf{x}, t)$ and $r(\mathbf{x}, t)$ are such that

$$\mathbf{b} \in C^1(Q), \ r \in C^1(\bar{Q}), \tag{3.7}$$

where $\bar{Q} = \bar{C} \times [0, +\infty[$. As far as the field equations are concerned, let us observe that equations (2.4) and (2.14) imply

$$c_e \dot{\hat{\theta}} + c_\alpha \dot{\hat{\alpha}} = \theta_0 \mathbf{M} \cdot \nabla \dot{\hat{\mathbf{u}}} + \operatorname{div}(\mathbf{K} \nabla \theta) + \hat{\mathrm{r}}, \tag{3.8}$$

where

$$\hat{f} = f + t_0 \dot{f} \tag{3.9}$$

and $\theta_0$ is a suitable reference temperature. Hence, our system of equations becomes now

$$\rho \ddot{\mathbf{u}} = \operatorname{div}(\mathbf{C}[\mathbf{E}] + \theta \mathbf{M}) + \mathbf{b}, \tag{3.10}$$

$$c_e \dot{\hat{\theta}} + c_\alpha \dot{\hat{\alpha}} = \theta_0 \mathbf{M} \cdot \nabla \dot{\hat{\mathbf{u}}} + \operatorname{div}(\mathbf{K} \nabla \theta) + \hat{\mathrm{r}}, \tag{3.11}$$

$$\dot{\alpha} = m\theta + n\alpha. \tag{3.12}$$

Let now $\{\partial_1 C, \partial_2 C\}$ and $\{\partial_3 C, \partial_4 C\}$ be two partitions of the boundary $\partial C$ of $C$ such that

$$\partial C = \partial_1 C \cup \partial_2 C = \partial_3 C \cup \partial_4 C,$$
$$\partial_1 C \cap \partial_2 C = \emptyset, \ \partial_3 C \cap \partial_4 C = \emptyset.$$

A solution of the mixed coupled thermoelasticity with thermal relaxation and an internal variable consists of a triple $\{\mathbf{u}, \theta, \alpha\}$ such that:

1. Equations (3.10)-(3.12) are satisfied;

2.

$$\begin{aligned} &\mathbf{u} = \mathbf{u}_0, \ \dot{\mathbf{u}} = \dot{\mathbf{u}}_0, \\ &\theta = \theta_0, \ \dot{\theta} = \dot{\theta}_0, \qquad \text{on } C \times \{0\} \\ &\alpha = \alpha_0, \end{aligned}$$

where $\mathbf{u}_0$, $\dot{\mathbf{u}}_0$, $\theta_0$, $\dot{\theta}_0$ and $\alpha_0$ are given initial conditions;

3.

$$\begin{aligned} &\mathbf{u} = \mathbf{u}^* \text{ on } \partial_1 C \times [0, +\infty[, \\ &\mathbf{Sn} \equiv (\mathbf{C}[\nabla \mathbf{u}] + \mathbf{M}\theta)\mathbf{n} = \mathbf{s}^* \text{ on } \partial_2 C \times [0, +\infty[, \\ &\theta = \theta^* \text{ on } \partial_3 C \times [0, +\infty[, \\ &-\mathbf{K}\nabla\theta \cdot \mathbf{n} = q^* \text{ on } \partial_4 C \times [0, +\infty[, \end{aligned}$$

with $\mathbf{n}$ being the outward unit normal to $\partial C$.

In the next section we will prove a suitable inequality representing a link between the support of the data $\mathbf{u}^*$, $\mathbf{s}^*$, $\theta^*$, $q^*$, $\mathbf{u}_0$, $\dot{\mathbf{u}}_0$, $\theta_0$, $\dot{\theta}_0$, $\alpha_0$, $r$ and $\mathbf{b}$, and the support of the solution $(\mathbf{u}, \theta, \alpha)$ at each instant $t > 0$.

## 4. A domain of dependence inequality

The present section is devoted to prove a domain of dependence inequality for a solution $(\mathbf{u}, \theta, \alpha)$ of the initial and boundary value problem of Sec. 3.

Let us first observe that, if we multiply the equations (3.10) and (3.12) by $t_0$, then differentiate with respect to $t$ and finally add the derived equations to the original ones, we may rewrite system (3.10)-(3.12) as follows:

$$\rho\ddot{\hat{\mathbf{u}}} = \operatorname{div}\{\mathbf{C}[\nabla\hat{\mathbf{u}}] + \hat{\theta}\mathbf{M}\} + \hat{\mathbf{b}}, \tag{4.1}$$

$$c_e\dot{\hat{\theta}} + c_\alpha\dot{\hat{\alpha}} = \theta_0\mathbf{M} \cdot \nabla\dot{\hat{\mathbf{u}}} + \operatorname{div}(\mathbf{K}\nabla\theta) + \hat{\mathrm{r}}, \tag{4.2}$$

$$\dot{\hat{\alpha}} = m\hat{\theta} + n\,\hat{\alpha}. \tag{4.3}$$

For this system we prove the following

THEOREM 1. *(Domain of dependence inequality). Let* $(\mathbf{u}, \theta, \alpha)$ *be a solution of the initial and boundary value problem specified in Sec. 3, and let* $c$ *be a positive constant of the velocity dimension, such that*

$$c^{-1}|\mathbf{A}| + \{(c_e\rho^{-1})\theta_0\}^{\frac{1}{2}}|\mathbf{M}| \leq c, \tag{4.4}$$

$$(c\,c_e\,t_0)^{-1}|\mathbf{K}| + \{(c_e\rho)^{-1}\theta_0\}^{\frac{1}{2}}|\mathbf{M}| \leq c, \tag{4.5}$$

*where* $\mathbf{A}$ *is the"acoustic tensor" in the direction of propagation* $\mathbf{m}$, *defined by*

$$\mathbf{A}(\mathbf{x}, \mathbf{m}) = \rho^{-1}(\mathbf{x})\mathbf{C}[\mathbf{a} \otimes \mathbf{m}] \quad \forall \mathbf{x} \in E_3, \ \forall \mathbf{a} \in V; \tag{4.6}$$

*then the following domain of dependence inequality holds true:*

$$\begin{aligned} &\int\limits_{C(\mathbf{x}_0,R)} \eta(\mathbf{x},t)dv + \theta_0^{-1}\int\limits_0^t ds \int\limits_{C[\mathbf{x}_0,R+c(t-s)]} (\nabla\theta \cdot \mathbf{K}\nabla\theta)(\mathbf{x},s)dv \\ &+ \theta_0^{-1}\int\limits_0^t ds \int\limits_{C[\mathbf{x}_0,R+c(t-s)]} c_\alpha \frac{1}{m}\dot{\hat{\alpha}}^2(\mathbf{x},s)dv \leq \int\limits_{C[\mathbf{x}_0,R+ct]} \eta(\mathbf{x}_0,0)dv \\ &+ \int\limits_0^t ds \int\limits_{C[\mathbf{x}_0,R+c(t-s)]} (\hat{\mathbf{b}} \cdot \hat{\mathbf{u}} + \theta_0^{-1}\hat{r}\hat{\theta})(\mathbf{x},s)dv \\ &+ \int\limits_0^t ds \cdot \int\limits_{\partial C \cap S[\mathbf{x}_{0,R+c(t-s)}]} (\dot{\hat{\mathbf{u}}} \cdot \hat{\mathbf{s}} - \theta_0^{-1}\hat{\theta}\hat{q})(\mathbf{x},s)d\sigma \end{aligned} \tag{4.7}$$

$\forall t > 0, \ \forall R > 0$ *and* $\forall \mathbf{x}_0 \in C$,
*where*

$$\eta(\mathbf{x},s) = \frac{1}{2}\Big(\rho\dot{\hat{\mathbf{u}}}^2 + \nabla\hat{\mathbf{u}} \cdot \mathbf{C}[\nabla\hat{\mathbf{u}}] + c_e\theta_0^{-1}\hat{\theta}^2 + t_0\theta_0^{-1}\nabla\theta \cdot \mathbf{K}\nabla\theta - c_\alpha\theta_0^{-1}\frac{n}{m}\hat{\alpha}^2\Big)(\mathbf{x},s) \tag{4.8}$$

*while*

$$S(\mathbf{x}_0,d) = \{\mathbf{x} \in E_3 : |\mathbf{x} - \mathbf{x}_0| < d\},$$

$$C(\mathbf{x}_0,d) = C \cap S(\mathbf{x}_0,d)$$

$\forall d \in R^+$ *and, moreover,*

$$(\mathbf{C}[\nabla \hat{\mathbf{u}}] + \mathbf{M}\hat{\theta})\,\mathbf{n} = \hat{\mathbf{s}}, \tag{4.9}$$

$$-(\mathbf{K}\nabla\hat{\theta}) \cdot \mathbf{n} = \hat{q}. \tag{4.10}$$

P r o o f. Let $g_\delta : \lambda \in R \to g_\delta(\lambda) \in [0,1]$ such that

$$\begin{aligned} &g_\delta(\lambda) = 0 \quad if \quad \lambda \in ]-\infty, 0], \\ &g_\delta(\lambda) = 1 \quad if \quad \lambda \in [\delta, +\infty[, \quad \delta \geq 0, \\ &g'_\delta(\lambda) = \frac{dg_\delta(\lambda)}{d\lambda} \geq 0 \quad \forall \lambda \in R, \end{aligned} \tag{4.11}$$

and let us define

$$g(\mathbf{x}, s) \equiv g_\delta(c^{-1}[R + c(t-s) - |\mathbf{x} - \mathbf{x}_0|]), \tag{4.12}$$

where $R$ is a positive constant of the length dimension while $t$ and $\mathbf{x}_0$ are arbitrarily fixed. Function $g$ is defined on $E_3 \times [0, +\infty[$ and its support is

$$\Sigma = \bigcup_{s \in [0,t]} S[\mathbf{x}_0, R + c(t-s)]. \tag{4.13}$$

Moreover, $g$ is smooth on $E_3 \times [0, +\infty[$ and $\nabla g$ vanishes identically on the following set

$$\Sigma_0 = \bigcup_{s \in [0,t]} S[\mathbf{x}_0, R + c(t-s-\delta)] \tag{4.14}$$

in which

$$g(\mathbf{x}, s) = 1 \quad \forall \mathbf{x} \in S[\mathbf{x}_0, R + c(t-s-\delta)]. \tag{4.15}$$

Clearly, $\delta$ is to be choosen so small as to assure that $R + c(t-s-\delta) > 0$ for any $s \in [0,t]$. Now if we multiply both sides of (4.1) by $g\dot{\hat{\mathbf{u}}}$ and use the vectorial identity relative to the divergence of an inner product, we obtain

$$\begin{aligned} \frac{1}{2} g \frac{d}{dt}\left[\rho \dot{\hat{\mathbf{u}}} \cdot \dot{\hat{\mathbf{u}}}\right] &= g\hat{\mathbf{b}} \cdot \hat{\mathbf{u}} + \nabla \cdot \{(\mathbf{C}[\nabla \hat{\mathbf{u}}] + \hat{\theta}\mathbf{M})\, g\dot{\hat{\mathbf{u}}}\} \\ &\quad - g\{\mathbf{C}[\nabla \hat{\mathbf{u}}] + \hat{\theta}\mathbf{M}\} \cdot \nabla \dot{\hat{\mathbf{u}}} - \dot{\hat{\mathbf{u}}} \cdot \{\mathbf{C}[\nabla \hat{\mathbf{u}}] + \hat{\theta}\mathbf{M}\} \nabla g. \end{aligned} \tag{4.16}$$

As a further step, we multiply (4.2) by $\hat{\theta}$ and take into account the definition of $\hat{\theta}$ in order to get

$$(4.17)\quad \hat{\theta}\nabla\dot{\hat{\mathbf{u}}}\cdot\mathbf{M}-c_\alpha\dot{\hat{\alpha}}\hat{\theta}\theta_0^{-1}=(2\theta_0)^{-1}\frac{d}{dt}(c_e\hat{\theta}^2)-\theta_0^{-1}\nabla\cdot(\hat{\theta}\mathbf{K}\nabla\theta)$$
$$+\theta_0^{-1}\nabla\theta\cdot\mathbf{K}\nabla\theta+t_0(2\theta_0)^{-1}\frac{d}{dt}(\nabla\theta\cdot\mathbf{K}\nabla\theta)-\hat{r}\hat{\theta}\theta_0^{-1}.$$

Finally, we substitute equation (4.17) in (4.16) and integrate on $C\times[0,t]$. Then, by applying the divergence theorem and taking into account (4.9) and (4.10), we may write

$$(4.18)\quad \int_C\Big[\frac{1}{2}g\rho\dot{\hat{\mathbf{u}}}^2\Big]_0^t dv+\int_C\Big[\frac{1}{2}g\,c_e\theta_0^{-1}(\hat{\theta})^2\Big]_0^t dv$$
$$+\int_C\Big[\frac{1}{2}gt_0\theta_0^{-1}(\nabla\theta\cdot\mathbf{K}\nabla\theta)\Big]_0^t dv$$
$$+\int_C\Big[\frac{1}{2}g\,\nabla\hat{\mathbf{u}}\cdot\mathbf{C}[\nabla\hat{\mathbf{u}}]\Big]_0^t dv+\theta_0^{-1}\int_0^t ds\int_C(g\nabla\theta\cdot\mathbf{K}\nabla\theta)(\mathbf{x},s)dv,$$

$$=\int_0^t ds\int_C\Big[\frac{1}{2}\rho\dot{\hat{\mathbf{u}}}^2\dot{g}+\frac{1}{2}\theta_0^{-1}c_e\hat{\theta}^2\dot{g}+\frac{1}{2}t_0\theta_0^{-1}\nabla\theta\cdot\mathbf{K}\nabla\theta\dot{g}+\frac{1}{2}\nabla\hat{\mathbf{u}}\cdot\mathbf{C}[\nabla\hat{\mathbf{u}}]\dot{g}\Big]dv+$$
$$-\int_0^t ds\int_C\dot{\hat{\mathbf{u}}}\cdot(\mathbf{C}[\nabla\hat{\mathbf{u}}]+\hat{\theta}\mathbf{M})\nabla g dv-\int_0^t ds\int_C\theta_0^{-1}\hat{\theta}\nabla g\cdot\mathbf{K}\nabla\theta dv$$
$$+\int_0^t ds\int_{\partial C}g[\dot{\hat{\mathbf{u}}}\cdot\hat{\mathbf{s}}-\theta_0^{-1}\hat{\theta}\hat{q}]d\sigma+\int_0^t ds\int_C[g(\hat{\mathbf{b}}\cdot\hat{\mathbf{u}}+\hat{r}\hat{\theta}\theta_0^{-1})]\,dv+$$
$$-\int_0^t ds\int_C g(c_\alpha\dot{\hat{\alpha}}\hat{\theta}\theta_0^{-1})dv.$$

On the other hand, from (4.3) it follows that

$$\hat{\theta}\dot{\hat{\alpha}} = \tau\dot{\hat{\alpha}}^2 - \sigma\hat{\alpha}\dot{\hat{\alpha}} \tag{4.19}$$

with

$$\tau \equiv \frac{1}{m}, \quad \sigma \equiv \frac{n}{m}. \tag{4.20}$$

Then, due to (4.19), the last integral of (4.18) takes the form

$$\int_0^t ds \int_C g c_\alpha \theta_0^{-1} \dot{\hat{\alpha}}\hat{\theta}\, dv = \int_0^t ds \int_C g c_\alpha \theta_0^{-1} \tau \dot{\hat{\alpha}}^2\, dv + \tag{4.21}$$

$$- \frac{1}{2}\int_C [g c_\alpha \theta_0^{-1}\sigma\hat{\alpha}^2]_0^t dv + \frac{1}{2}\int_0^t ds \int_C c_\alpha \theta_0^{-1}\sigma\hat{\alpha}^2 \dot{g}\, dv.$$

Owing to the definition of $\eta$ and taking into account the equalities presented above, the following relation holds true:

$$\int_C g\eta(\mathbf{x},t)\, dv + \theta_0^{-1}\int_0^t ds \int_C (g\nabla\theta \cdot \mathbf{K}\nabla\theta)(\mathbf{x},s) dv \tag{4.22}$$

$$= \int_C g\eta(\mathbf{x},0)\, dv + \int_0^t ds \int_C (\dot{g}\eta)(\mathbf{x},s)\, dv - \int_0^t ds \int_C \dot{\hat{\mathbf{u}}} \cdot \{\mathbf{C}[\nabla\hat{\mathbf{u}}] + \hat{\theta}\mathbf{M}\}\nabla g\, dv +$$

$$- \int_0^t ds \int_C \theta_0^{-1}\hat{\theta}\nabla g \cdot \mathbf{K}\nabla\theta\, dv + \int_0^t ds \int_{\partial C} g(\hat{\mathbf{u}} \cdot \hat{\mathbf{s}} - \theta_0^{-1}\hat{\theta}\hat{q}) d\sigma$$

$$+ \int_0^t ds \int_C g(\hat{\mathbf{b}} \cdot \dot{\hat{\mathbf{u}}} + \theta_0^{-1}\hat{r}\hat{\theta})\, dv - \int_0^t ds \int_C g c_\alpha \theta_0^{-1}\tau\dot{\hat{\alpha}}^2 dv.$$

The third and the fourth integrals at the right-hand side of equation (4.22) may be estimated by using the following inequality, which follows from (3.4), (3.5), (4.4), (4.5) together with the definition of $g(\mathbf{x},s)$ and $\mathbf{A}(\mathbf{x},\mathbf{m})$ :

$$(4.23)\quad -\dot{\hat{\mathbf{u}}}\cdot\mathbf{C}[\nabla\hat{\mathbf{u}}]\nabla g-\dot{\hat{\mathbf{u}}}\cdot\mathbf{M}\nabla g-\theta_0^{-1}\hat{\theta}\nabla g\cdot(\mathbf{K}\nabla\theta)$$

$$\leq\frac{1}{2}g'_\delta\Big\{\nabla\hat{\mathbf{u}}\cdot\mathbf{C}[\nabla\hat{\mathbf{u}}]+(c^{-2}\dot{\hat{\mathbf{u}}}\cdot\mathbf{C}[\dot{\hat{\mathbf{u}}}\otimes\mathbf{e}_{\mathbf{r}}^0]\mathbf{e}_{\mathbf{r}}^0)\Big\}$$

$$+\frac{1}{2}g'_\delta\Big\{c^{-1}|\mathbf{M}|[(c_e\rho)^{-1}\theta_0]^{\frac{1}{2}}(\rho\dot{\hat{\mathbf{u}}}^2+\theta_0^{-1}c_e\hat{\theta}^2)$$

$$+(c^2t_0\theta_0)^{-1}\hat{\theta}^2\mathbf{e}_r^0\cdot\mathbf{K}\mathbf{e}_r^0+\theta_0^{-1}t_0\nabla\theta\cdot\mathbf{K}\nabla\theta\Big\}$$

$$\leq\frac{1}{2}g'_\delta\Big\{\nabla\hat{\mathbf{u}}\cdot\mathbf{C}[\nabla\hat{\mathbf{u}}]+(c^{-2}|\mathbf{A}|+c^{-1}|\mathbf{M}|\Big\{(c_e\rho)^{-1}\theta_0\Big\}^{\frac{1}{2}})\rho\dot{\hat{\mathbf{u}}}^2$$

$$+[(c^2t_0c_e)^{-1}|\mathbf{K}|+c^{-1}|\mathbf{M}|\Big\{(c_e\rho)^{-1}\theta_0\Big\}^{\frac{1}{2}}]c_e\theta_0^{-1}\hat{\theta}^2+\theta_0^{-1}t_0\nabla\theta\cdot\mathbf{K}\nabla\theta\Big\}\leq g'_\delta\eta.$$

Here

$$\mathbf{e}_r^0=|\mathbf{x}-\mathbf{x}_0|^{-1}(\mathbf{x}-\mathbf{x}_0).$$

Let us observe now that function $g$ is not decreasing and hence the relation

$$(4.24)\qquad g'_\delta(\lambda)=-\dot{g}(\mathbf{x},s)$$

implies that $\dot{g}$ is negative. As a consequence, owing to (4.23), the sum of the second, third and fourth integrals on the right-hand side of (4.22) is negative, so that from (4.22) it follows:

$$(4.25)\quad\int_C g\eta(\mathbf{x},t)dv+\theta_0^{-1}\int_0^t ds\int_C(g\nabla\theta\cdot\mathbf{K}\nabla\theta)(\mathbf{x},s)dv$$

$$+\theta_0^{-1}\int_0^t ds\int_C gc_\alpha\tau\dot{\hat{\alpha}}^2(\mathbf{x},s)dv\leq\int_C g\eta(\mathbf{x},0)dv$$

$$+\int_0^t ds\int_{\partial C}g(\hat{\mathbf{u}}\cdot\dot{\hat{\mathbf{u}}}\cdot\mathbf{s}-\theta_0\hat{\theta}\hat{q})d\sigma+\int_0^t ds\int_C(\hat{\mathbf{b}}\cdot\dot{\hat{\mathbf{u}}}+\theta_0^{-1}\hat{r}\hat{\theta})dv.$$

Finally, since

$$g(\mathbf{x},s)=g_\delta(c^{-1}[R+c(t-s)-|\mathbf{x}-\mathbf{x}_0|]),$$

$$g_\delta(\lambda)=1\ \ \forall\lambda\in[\delta,+\infty[$$

and $g$ having support $\Sigma$ defined by (4.13), we may conclude that, as $\delta$ tends to zero, function $g$ tends to the characteristic function of the set $\Sigma$. Then, it is allowed to calculate the limit of (4.25) as $\delta$ tends to 0. It yields exactly (4.7), q.e.d.

## 5. Domain of influence theorem

In this section we prove that from the domain of dependence inequality, together with the hypotheses of Sec. 2 and 3, a domain of influence theorem follows. Let $\tilde{C}(t)$, $t > 0$, be the set of the points $\mathbf{x} \in \bar{C}$ such that:

1. $\mathbf{x} \in C \Rightarrow \mathbf{u}_0 \neq 0 \quad \text{or} \quad \dot{\mathbf{u}}_0 \neq 0, \quad \text{or} \quad \theta_0 \neq 0 \quad \text{or} \quad \dot{\theta}_0 \neq 0 \quad \text{or} \quad \alpha_0 \neq 0;$

   moreover $\exists \bar{t} \in [0,t] : \mathbf{b}(\mathbf{x},t) \neq 0 \quad \text{or} \quad r(\mathbf{x},\bar{t}) \neq 0;$

2. $\mathbf{x} \in \partial_1 C \Rightarrow \exists \bar{t} \in [0,t] : \mathbf{u}^*(\mathbf{x},\bar{t}) \neq \mathbf{0};$

3. $\mathbf{x} \in \partial_2 C \Rightarrow \exists \bar{t} \in [0,t] : \mathbf{s}^*(\mathbf{x},\bar{t}) \neq \mathbf{0};$

4. $\mathbf{x} \in \partial_3 C \Rightarrow \exists \bar{t} \in [0,t] : \theta^*(\mathbf{x},\bar{t}) \neq 0;$

5. $\mathbf{x} \in \partial_4 C \Rightarrow \exists \bar{t} \in [0,t] : q^*(\mathbf{x},\bar{t}) \neq 0.$

The set

$$C^* = \{\mathbf{x}_0 \in \bar{C} : \tilde{C}(t) \cap \bar{S}(\mathbf{x}_0, ct) \neq \emptyset\}, \tag{5.1}$$

where $c$ is the same of equations (4.4)-(4.5), is the *domain of influence* of the data at the instant $t$. We prove now the following

THEOREM 2. *(Domain of influence theorem). Let* $(\mathbf{u}, \theta, \alpha)$ *be a solution of the initial and boundary value problem (3.10)-(3.12). Then* $\mathbf{u} = \mathbf{0}$, $\theta = 0$ *and* $\alpha = 0$ *on the set* $\bar{Q} = \{\bar{C} - C^*\} \times [0,t]$.

P r o o f. Let $\mathbf{x}_0 \in \bar{C} - C^*(t)$ and let $\lambda \in [0,t]$. We apply the domain of dependence inequality with $t = \lambda$ and $R = c(t-\lambda)$ in order to get

$$\int_{C[\mathbf{x}_0,c(t-\lambda)]} \eta(\mathbf{x},\lambda)dv + \theta_0^{-1}\int_0^\lambda ds \int_{C[\mathbf{x}_0,c(t-s)]} (\nabla\theta\cdot\mathbf{K}\nabla\theta)(\mathbf{x},s)dv$$

$$+\theta_0^{-1}\int_0^\lambda ds \int_{C[\mathbf{x}_0,c(t-s)]} (c_\alpha\tau\dot{\hat{\alpha}}^2)(\mathbf{x},s)\mathrm{dv} \le \int_{C(\mathbf{x}_0,ct)} \eta(\mathbf{x},0)\mathrm{dv}$$

$$+\int_0^\lambda ds \int_{C[\mathbf{x}_0,c(t-s)]} (\dot{\hat{\mathbf{b}}}\cdot\dot{\hat{\mathbf{u}}} + \hat{\theta}_0^{-1}\hat{r}\hat{\theta})(\mathbf{x},s)dv$$

$$+\int_0^\lambda ds \int_{\partial C\cap S[\mathbf{x}_0,c(t-s)]} (\dot{\hat{\mathbf{u}}}\cdot\hat{\mathbf{s}} - \theta_0^{-1}\hat{\theta}\hat{q})(\mathbf{x},s)d\sigma. \tag{5.2}$$

The right hand-side of (5.2) is zero. In fact, because $\mathbf{x}_0 \in (\bar{C} - B^*(t))$, by equation (3.10) restricted to the set $C(\mathbf{x}_0,ct)\times\{0\}$ and by Hypothesis 1, it follows $\ddot{\mathbf{u}}_0 = \mathbf{0}$ and hence $\dot{\hat{\mathbf{u}}} = \mathbf{0}$ on $C(\mathbf{x}_0,ct)$. Also by Hypothesis 1 we have $\hat{\theta}_0 = 0$, $\nabla\hat{\mathbf{u}} = \mathbf{0}$ and $\nabla\theta_0 = \mathbf{0}$ on $C(\mathbf{x}_0,ct)$. This is enough to conclude that

$$\int_{C(\mathbf{x}_0,ct)} \eta(\mathbf{x},0)dv = 0. \tag{5.3}$$

Furthermore $r(\mathbf{x},s)$ and $\mathbf{b}(\mathbf{x},s)$ vanish on $C(\mathbf{x}_0,ct)\times[0,t]$ so that $\dot{\mathbf{b}}(\mathbf{x},s)$ and $\dot{r}(\mathbf{x},s)$ are zero on the same set. As a consequence, $\dot{\hat{\mathbf{b}}}(\mathbf{x},s)$ and $\dot{\hat{r}}(\mathbf{x},s)$ identically vanish on $C(\mathbf{x}_0,ct)\times[0,t]$, so that

$$\int_0^\lambda ds \int_{C[\mathbf{x}_0,c(t-s)]} (\dot{\hat{\mathbf{b}}}\cdot\dot{\hat{\mathbf{u}}} + \hat{\theta}_0^{-1}\hat{r}\hat{\theta})(\mathbf{x},s)dv = 0. \tag{5.4}$$

In order to evaluate the last integral in (5.2) we rewrite it in the form

$$(5.5)\quad \int_0^\lambda ds \int_{\partial C\cap S[\mathbf{x}_0,c(t-s)]} (\dot{\hat{\mathbf{u}}}\cdot\hat{\mathbf{s}} - \theta_0^{-1}\hat{\theta}\hat{q})(\mathbf{x},s)d\sigma$$

$$= \int_0^\lambda \Bigg[ \int_{\partial_1 C\cap S[\mathbf{x}_0,c(t-s)]} (\dot{\mathbf{u}} + t_0\ddot{\mathbf{u}})\cdot\hat{\mathbf{s}}d\sigma + \int_{\partial_2 C\cap S[\mathbf{x}_0,c(t-s)]} \dot{\hat{\mathbf{u}}}\cdot(\mathbf{s}_0 + t_0\dot{\mathbf{s}})d\sigma +$$

$$- \theta_0^{-1} \int_{\partial_3 C\cap S[\mathbf{x}_0,c(t-s)]} (\theta + t_0\dot{\theta})\hat{q}d\sigma - \theta_0^{-1} \int_{\partial_4 C\cap S[\mathbf{x}_0,c(t-s)]} \hat{\theta}\hat{q}d\sigma \Bigg] ds.$$

Since $\lambda \leq t$ and $C(\mathbf{x}_0, ct) \subset \{\bar{C} - \tilde{C}(t)\}$, due to Conditions 2-5, the right-hand side of (5.5) also vanishes. Then, inequality (5.2) reduces to

$$(5.6)\quad \int_C \eta(\mathbf{x},\lambda)dv + \theta_0^{-1}\int_0^\lambda ds \int_{C[\mathbf{x}_0,c(t-\lambda)]} (\nabla\theta\cdot\mathbf{K}\nabla\theta)(\mathbf{x},s)dv +$$

$$+ \theta_0^{-1}\int_0^\lambda ds \int_{C[\mathbf{x}_0,c(t-\lambda)]} c_\alpha\tau\dot{\hat{\alpha}}^2(\mathbf{x},s)dv \leq 0.$$

Let us recall now that tensor $\mathbf{K}$ is positive semidefinite and from (5.6) it follows that

$$(5.7)\quad \int_{C[\mathbf{x}_0,c(t-\lambda)]} \eta(\mathbf{x},\lambda)dv \leq 0.$$

Finally, since $\eta$ is non-negative, we have

$$(5.8)\quad \eta(\mathbf{x},\lambda) = 0.$$

Taking into account the definition of $\eta$ we deduce

$$(5.9)\quad \dot{\hat{\mathbf{u}}}(\mathbf{x}_0,\lambda) = \mathbf{0}, \quad \hat{\theta}(\mathbf{x}_0,\lambda) = 0, \quad \text{and} \quad \hat{\alpha}(\mathbf{x}_0,\lambda) = 0.$$

Moreover, Condition 1 implies

$$(5.10)\quad \hat{\mathbf{u}}(\mathbf{x}_0,0) = \mathbf{0}, \quad \theta(\mathbf{x}_0,0) = 0, \quad \alpha(\mathbf{x}_0,0) = 0 \quad \forall\mathbf{x}_0 \in \bar{C} - C^*(t).$$

Hence, from the uniqueness theorem of the solution of ordinary differential equations it follows

$$\hat{\mathbf{u}}(\mathbf{x}_0, \lambda) = \mathbf{0},\ \theta(\mathbf{x}_0, \lambda) = 0,\ \alpha(\mathbf{x}_0, \lambda) = 0\ \forall (\mathbf{x}_0, \lambda) \in \{\bar{C} - C^*(t)\} \times [0, t]. \tag{5.11}$$

Finally, the ordinary differential equation

$$\hat{\mathbf{u}}(\mathbf{x}_0, \lambda) = \mathbf{0}, \tag{5.12}$$

with the initial condition

$$\mathbf{u}(\mathbf{x}_0, 0) = \mathbf{0}, \tag{5.13}$$

admits the unique solution

$$\mathbf{u}(\mathbf{x}_0, \lambda) = \mathbf{0}\ \forall \lambda \in [0, t]. \tag{5.14}$$

This is enough to conclude that

$$\mathbf{u}(\mathbf{x}, \lambda) = \mathbf{0}\ \forall (\mathbf{x}, \lambda) \in \{\bar{C} - C^*(t)\} \times [0, t]. \tag{5.15}$$

The theorem has been proved.

## 6. The semi-empirical heat conduction model

One of the most fundamental and delicate concepts of non-equilibrium thermodynamics is that of absolute temperature. Its definition is well founded at the equilibrium or even for small deviations from an equilibrium state. However, it becomes questionable for arbitrary states and processes when the Clausius integral extended to a closed process is not zero [23]. On the other hand, it becomes necessary to consider non-equilibrium states and processes if one wants to describe some important thermodynamic phenomena. One of these is just the propagation of thermal waves at a low temperature. Kosiński and co-workers approached the problem by introducing a new temperature $\beta$, called semi-empirical, as a scalar internal state variable, [10, 12]. It is related to the absolute temperature, $\theta$, by a suitable ordinary differential equation of the type

$$\dot{\beta} = f(\theta, t) \tag{6.1}$$

and a given initial condition

$$\beta(t_0) = \beta_0. \tag{6.2}$$

Obviously, the new theory is hyperbolic but it must also allow a passage to the classical parabolic case given by Fourier's law. By design, when relaxed $\beta$

coincides with the absolute temperature $\theta$, otherwise $\beta$ follows after $\theta$ with a certain delay, controlled by a small parameter $\tau$, called relaxation time. This delay introduces hyperbolicity and, if chosen to be small, controls the passage to the classical case. A general model of anisotropic thermoelastic solids with semi-empirical temperature has been introduced in [12]. In the linear case, numerical solutions to an initial and boundary value problem of the type considered in the present paper have been found in [19]. These solutions confirm that the model admits hyperbolic heat propagation. In this section we apply the result of Sec. 5 in order to prove the hyperbolicity of the theory via a domain of influence theorem. To this end let us consider a linear thermoelastic solid described by a set of constitutive equations having the form

$$\Phi = \Phi^*(\theta, \beta, \nabla\theta, \nabla\beta, \mathbf{E}). \tag{6.3}$$

The additional hypotheses quoted below specify better the model.

a) The stress tensor depends on $\beta$ only through $\theta$ and is given by the constitutive equation

$$\mathbf{S}(\mathbf{E}, \theta) = \mathbf{C}[\nabla\mathbf{u}] + \mathbf{M}\theta, \tag{6.4}$$

where $\mathbf{C}$ and $\mathbf{M}$ are the same of Sec. 2.

b) The evolution of the semi-empirical temperature is determined by the linear differential equation

$$\dot{\beta} = \frac{1}{\tau}\theta - \frac{1}{\sigma}\beta, \tag{6.5}$$

where the material scalar parameters $\tau = \tau(x)$ and $\sigma = \sigma(x)$ are positive and have both the dimensions of time.

c) The heat flux is given by the Fourier's type heat conduction law

$$\mathbf{q} = -\mathbf{K}\nabla\beta, \tag{6.6}$$

where $\mathbf{K}(x)$ is the the heat conductivity tensor defined in Sec. 2.

d) The specific internal energy $\epsilon$ does not depend on $\nabla\beta$ [2], i.e.

[2] Let us recall that the second law of thermodynamics prevents $\epsilon$ from depending on $\nabla\theta$.

$$\epsilon = \epsilon(\theta, \beta, \mathbf{E}). \tag{6.7}$$

Equation (6.5) may be rewritten as follows

$$\tau\dot{\beta} = \theta - \frac{\tau}{\sigma}\beta. \tag{6.8}$$

Taking the gradient of (6.8) and applying to the obtained equation the operator $-\mathbf{K}$, we get

$$\sigma\dot{\mathbf{q}} + \mathbf{q} = -\tilde{\mathbf{K}}\nabla\theta, \tag{6.9}$$

with $\tilde{\mathbf{K}} = \dfrac{\sigma}{\tau}\mathbf{K}$. Equation (6.9) is of the Cattaneo's type and it may be put in the form

$$\hat{\mathbf{q}} = -\tilde{\mathbf{K}}\nabla\theta, \tag{6.10}$$

with

$$\hat{f} = f + \sigma\dot{f}. \tag{6.11}$$

The same procedure developed in Sec. 3 allows us to write our system of equations in the form

$$\rho\ddot{\mathbf{u}} = \operatorname{div}\{\mathbf{C}[\nabla\mathbf{u}] + \theta\mathbf{M}\} + \mathbf{b}, \tag{6.12}$$

$$c_e\dot{\hat{\theta}} + c_\beta\dot{\beta} = \theta_0\mathbf{M}\cdot\nabla\dot{\mathbf{u}} + \operatorname{div}\{\tilde{\mathbf{K}}\nabla\theta\} + \hat{r}, \tag{6.13}$$

$$\dot{\beta} = \frac{1}{\tau}\theta - \frac{1}{\sigma}\beta, \tag{6.14}$$

where $c_\beta$ is the latent heat relative to the semi-empirical temperature $\beta$. We assume for the functions $\dfrac{1}{\tau}$, $-\dfrac{1}{\sigma}$ and $c_\beta$ the same properties of $m$, $n$ and $c_\alpha$, respectively. Then, we consider the problem of finding a solution $(\mathbf{u}, \theta, \beta)$ of equations (6.12)-(6.14) such that

$$\mathbf{u} = \mathbf{u}_0,\ \dot{\mathbf{u}} = \dot{\mathbf{u}}_0,\ \theta = \theta_0,\ \dot{\theta} = \dot{\theta}_0\ \ \beta = \beta_0 \ \text{ on } \ C \times \{0\}, \tag{6.15}$$

where $\mathbf{u}_0$, $\dot{\mathbf{u}}_0$, $\theta_0$, $\dot{\theta}_0$ and $\beta_0$ are given initial functions, and

$$\begin{aligned} \mathbf{u} &= \mathbf{u}^* \ \text{ on } \partial_1 C \times [0, +\infty[, \\ (\mathbf{C}[\nabla\mathbf{u}] + \mathbf{M}\theta)\mathbf{n} &= \mathbf{s}^* \ \text{ on } \partial_2 C \times [0, +\infty[, \\ \theta &= \theta^* \ \text{ on } \partial_3 C \times [0, +\infty[, \\ -\mathbf{K}\nabla\theta\cdot\mathbf{n} &= q^* \ \text{ on } \partial_4 C \times [0, +\infty[. \end{aligned} \tag{6.16}$$

It is immediately seen that, by identifying $\beta$ with $\alpha$, the above mentioned initial and boundary value problem is the same as that of Sec. 3. Then, we define the domain of influence $C^*$ of the data in the same manner as in Sec. 5. Theorem 4. admits the following corollary:

THEOREM 3. *Let* $(\mathbf{u}, \theta, \beta)$ *be a solution of the initial and boundary value problem (6.12)-(6.16). Then*

$$\mathbf{u} = 0, \quad \theta = 0 \text{ and } \beta = 0 \tag{6.17}$$

*on the domain*

$$\tilde{Q} = \{\bar{C} - C^*\} \times [0, t]. \tag{6.18}$$

## Acknowledgement

Work performed under the auspices of University of Basilicata, research program in Mathematical Physics D. R. 204/99.

## References

1. M. E. GURTIN, *The linear theory of elasticity*, Handbuch der Physik, band VIa/2, 1-295, Springer-Verlag, Berlin, 1972.
2. A. C. ERINGEN and S. SUHUBI, *Elastodynamics*, **2**, Academic Press, New York, 1975.
3. C. CATTANEO, *Sulla conduzione del calore*, Atti Sem. Mat. Fis. Univ. Modena **3**, 83-101, 1948.
4. H. W. LORD and Y SHULMAN, *A generalized dynamical theory of thermoelasticity*, J. Mech. Phys. Solids, **15**, 229-309, 1967.
5. J. IGNACZAK, *Domain of influence theorem in linear thermoelasticity*, Int. J. Engng. Sci., **16**, 139-145, 1978.
6. J. IGNACZAK and J. BIALY, *Domain of influence in thermoelasticity with one relaxation time*, J. Therm. Stresses, **3**, 391-399, 1980.
7. B. CARBONARO and R. RUSSO, *Energy inequalities and the domain of influence theorem in classical elastodynamics*, J. Elast., **14**, 163-174, 1984.
8. J. IGNACZAK, B. CARBONARO and R. RUSSO, *Domain of influence theorem in thermoelasticity with one relaxation time*, J. Therm. Stresses, **9**, 79-91, 1986.
9. A. MORRO and T. RUGGERI, *Second sound and internal energy in solids*, Int. J. Non-Lin. Mech., **22**, 1, 27-36, 1987.
10. V. A. CIMMELLI and W. KOSIŃSKI, *Non-equilibrium semi-empirical temperature in materials with thermal relaxation*, Arch. Mech., **43**, 6, 753-767, 1991.
11. G. CAVIGLIA, A. MORRO and B. STRAUGHAN, *Thermoelasticity at cryogenic temperatures*, Int. J. Non-Lin. Mech., **27**, 2, 251-263, 1992.

12. V. A. CIMMELLI, *Thermodynamics of anisotropic solids near absolute zero*, Math. Comput. Modelling, **28**, 3, 79-89, 1998.

13. G. A. KLUITENBERG and V. CIANCIO, *On linear dynamical equations of state for isotropic media I*, Physica, 93A, 273-286, 1978.

14. D. S. CHANDRASEKHARAIAH, *Hyperbolic thermoelasticity: A review of recent literature*, Appl. Mech. Rev., **51**, no. 12, part 1, 1998.

15. F. BAMPI and A. MORRO, *Non-equilibrium thermodynamics: a hidden variable approach*; [in:] Recent Developments in Non-Equilibrium Thermodynamics, J. CASAS-VAZQUEZ, D. JOU and G. LEBON [Eds.], 211-232, Springer-Verlag, Berlin 1984.

16. F. BAMPI and A. MORRO, *Relaxation phenomena in irreversible thermodynamics*, Atti Sem. Mat. Fis. Univ. Modena, **XXX**, 1-15, 1981.

17. G. BOILLAT, *La propagation des ondes*, Traité de physique theorique et de physique mathematique, Gauthier-Villars, Paris, 1965.

18. T. RUGGERI, *Thermodynamics and symmetric hyperbolic systems*, Rend. Sem. Mat. Univ. Pol. Torino, Fascicolo Speciale, 167-183, 1988.

19. K. FRISCHMUTH and V. A. CIMMELLI, *Coupling in thermomechanical wave propagation in NaF at low temperature*, Arch. Mech., **50**, 703-713, 1998.

20. D. E. CARLSON, *Linear thermoelasticity*, Handbuch der Physik, Band VIa/2, 297-345, Springer-Verlag, Berlin, 1972.

21. G.A. MAUGIN and W. MUSCHIK, *Thermodynamics with internal variables. Part I. General Concepts*, J. Non-Equilib. Thermodyn., **19**, 217-249, 1994.

22. W. MUSCHIK, *Non-equilibrium thermodynamics with applications to solids*, CISM Courses and Lectures, no. 336, Springer-Verlag, Berlin, 1994.

23. M. PITTERI, *On the axiomatic foundations of temperature*, Appendix G 6 of Rational Thermodynamics, C. TRUESDELL [Ed.], Springer Verlag, Berlin, 1984.

*Received December 22, 2000; revised version July 17, 2001.*

Arch. Mech., 54, 1, pp. 35–54, Warszawa 2002

# Partial material replacement without stress redistribution

A. MATUSZAK

*Cracow University of Technology,*
*Institute of Computer Methods in Civil Engineering*
*ul. Warszawska 24, 31-155 Kraków*
*e-mail : max@twins.pk.edu.pl*

A PARTIAL MATERIAL replacement causes stress redistribution in comparison to the original structure made of a homogeneous material. The article presents a possibility to design a geometry of the replacement which keeps the state of stress unchanged. It is shown that for a class of two-dimensional configurations, it is possible to find a solution of this problem. Conditions for the existence of an appropriate geometry are given. A method to obtain the shape of the replaced part is proposed.

## 1. Introduction

WE CONSIDER AN ELASTIC body initially made of one material and subjected to a single load system. Then some part of the body is replaced by a part of the same shape but made of another material. This partial material replacement usually causes essential stress redistribution in comparison to the same structure made of one material. The choice of the shape of a bimaterial interface significantly influences the redistribution. Defining any norm (measure) of the stress change, we can consider a function which maps the set of all possible interfaces into the value of the stress redistribution norm. Considering the lowest possible value of this norm it is clear that since the norm is nonnegative, the lowest (theoretical) value is zero. The physical interpretation of this value requires the existence of an interface which does not cause the stress redistribution in the whole domain. We are going to analyze the possibility of existence of the replacement shape which preserves the stress state unchanged.

Such a problem seems to lead to a contradiction. The solution of a Boundary Value Problem (BVP) of elasticity is dependent on the distribution of material properties. The change of mechanical properties in any part of the domain should lead to significant changes in the BVP solution. Considering the problem of the body with a replaced part from the viewpoint of mechanics, it is obvious that the stress redistribution depends on the mechanical properties of materials, the geometry of the body, the shape of a material interface, the applied loads and kinematic boundary conditions.

We are going to show in the paper that, even if the properties of the original and new material are given and the geometry of the domain is determined, there may exist a shape of the interface which does not lead to any change of stress distribution. We will show cases when such an interface exists. Then we will try to establish a simple method of finding such an interface for a limited class of problems.

The idea of this research was introduced by the analysis of biomechanical problems related to the stability of an implant–bone system. An inserted implant (the replacement) causes stress redistribution which initiates the process of bone material adaptation known as *remodeling*. This process causes essential structural changes in the bone material and these changes belong to important factors limiting the implant service time [3]. The majority of known remodeling theories assume that the process is caused by stress/strain redistribution [7]. The most effective way to avoid an unwanted effect is to prevent its cause. A design which would cause no redistribution of stress would prevent any mechanically induced remodeling and eliminate one of the reasons of implant loosening. However, at this stage of development, the presented theory is of a purely theoretical significance for biomechanics, since assumptions adopted in this paper are too restrictive for their practical application.

Apart from biomechanics, the presented results can be interesting for any problem where a bimaterial interface occurs and a single load system dominates. At the bimaterial interface high stress concentrations occur [6]. The existence of such a special shape of the interface which does not cause the stress redistribution allows one to obtain a structure made of two materials but maintaining the same stress state as the structure made of one material, and therefore free of any stress concentrations caused by the bimaterial interface.

Finally, what is most important, this solution presents some unexpected properties of elasticity which contradict our belief and is interesting *per se*.

## 2. Problem formulation and trivial solutions

### 2.1. Primary problem

We define a primary problem considering a body occupying domain $\mathcal{D}$, with prescribed boundary conditions: kinematic on $\partial\mathcal{D}_u$ of boundary $\partial\mathcal{D}$ and static on part $\partial\mathcal{D}_\sigma$, as depicted in Fig. 1. The linear elastic material properties are described by the tensor $E_{ijkl}$.

This is the classical BVP of the theory of elasticity. The problem is well-posed and can be solved for the unknown fields of displacements $u_i^I$, stresses $\sigma_{ij}^I$ and strains $\varepsilon_{ij}^I$.

In what follows we assume that the solution of the primary problem i.e. fields $u_i^I$, $\sigma_{ij}^I$ and $\varepsilon_{ij}^I$ are known.

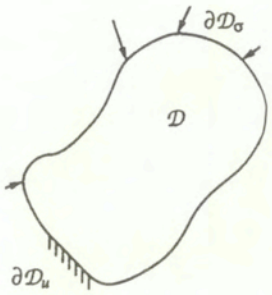


FIG. 1. Primary problem

### 2.2. Secondary problem

Let us modify the primary problem assuming the existence of an interface $\Gamma$ which forms two subdomains $\mathcal{D}_1$ and $\mathcal{D}_2$ of domain $\mathcal{D}$, as shown in Fig. 2.

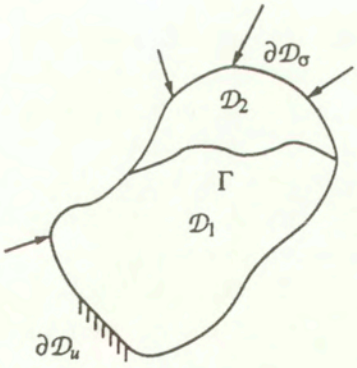


FIG. 2. Secondary problem

The material properties in subdomain $\mathcal{D}_1$ remain the same as in the primary problem, while in subdomain $\mathcal{D}_2$ the material properties are described by another elasticity tensor $\tilde{E}_{ijkl}$.

Kinematic boundary conditions are prescribed on boundary part $\partial\mathcal{D}_{1u}$ of subdomain $\mathcal{D}_1$ and static boundary conditions are prescribed on $\partial\mathcal{D}_{1\sigma}$. Only static boundary conditions are prescribed on boundary $\partial\mathcal{D}_2$ of subdomain $\mathcal{D}_2$.

This new BVP will be called a secondary problem. The secondary problem is still well-posed and can also be solved for the fields: displacements $u_i^{II}$, stresses $\sigma_{ij}^{II}$ and strains $\varepsilon_{ij}^{II}$. One primary problem can generate a series of secondary problems with different locations of $\Gamma$. Each of the secondary problems has a solution $u_i^{II}$, $\sigma_{ij}^{II}$, $\varepsilon_{ij}^{II}$.

We expect that the solution of a secondary problem is highly dependent on the location of $\Gamma$. It is also expected that the introduction of another material causes redistribution of stresses, i.e. everywhere in $\mathcal{D}$

$$\Delta\sigma_{ij} = \sigma_{ij}^{II} - \sigma_{ij}^{I} \neq 0. \tag{2.1}$$

### 2.3. Redistribution problem

Our objective is to find a special case of the secondary problem with such a shape of interface $\Gamma$ which gives no stress redistribution

$$\Delta\sigma_{ij} = 0 \tag{2.2}$$

in the whole domain $\mathcal{D}$ provided that such a line $\Gamma$ exists. This is equivalent to the condition:

$$\sigma_{ij}^{II} = \sigma_{ij}^{I}. \tag{2.3}$$

In what follows we will refer to this problem as the problem of stress redistribution or shortly, as the problem of redistribution.

In order to distinguish the solution of the secondary problem from its special case when condition Eq. (2.3) is met, another notation is introduced. For the solution of the stress redistribution problem we denote the solution of the secondary problem in subdomain $\mathcal{D}_1$ (where material properties are $E_{ijkl}$) by $u_i$, $\sigma_{ij}$, $\varepsilon_{ij}$ and in subdomain $\mathcal{D}_2$ (where material properties are $\tilde{E}_{ijkl}$) by $\tilde{u}_i, \tilde{\sigma}_{ij}, \tilde{\varepsilon}_{ij}$.

Due to the properties of Eq. (2.3) we have: $\sigma_{ij} \equiv \sigma_{ij}^{I}$ in $\mathcal{D}_1$, $\tilde{\sigma}_{ij} \equiv \sigma_{ij}^{I}$ in $\mathcal{D}_2$ and therefore we could use $\sigma_{ij}^{I}$ as the distribution of stresses in the solution of the redistribution problem, but we will use the notation $\sigma_{ij}$ and $\tilde{\sigma}_{ij}$ in order to emphasize which subdomain is considered.

It should be noted that for a known shape of $\Gamma$, the verification of Eq. (2.3) can be performed by a direct solution of the primary and secondary problems.

### 2.4. Trivial solutions

It is unbelievable that the redistribution problem may possess a solution. The solution of the problem which satisfies condition Eq. (2.3) contradicts our experience. In order to prove that the considered problem is solvable, a few simple solutions should be presented prior to the formulation of a consistent theory.

Let us consider a rectangular panel subjected to pure tension in plane stress conditions. The panel is made of two linear, elastic, isotropic and homogenous materials with a material interface perpendicular to the axis of tension, as shown in Fig. 3. In order to preserve the pure tension condition, we assume that the kinematic boundary conditions at the left-hand edge of the panel should allow for free expansion in direction $y$.

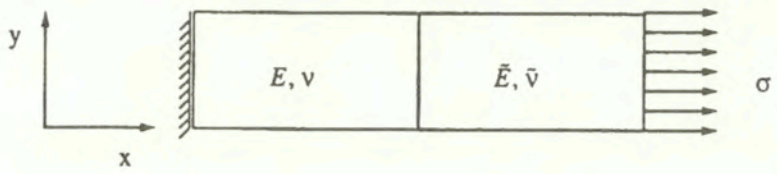


FIG. 3. Panel with straight interface

Let us virtually separate the panel along the material interface and assume pure tension in both parts. Then both parts of the panel deform independently. The elongation of each part in the direction of tension is governed by Young's modulus. In the direction perpendicular to the axis of tension, the value of Poisson's ratio governs the width change of each part. The strain value in the direction perpendicular to the axis of tension (in the system of coordinates shown in Fig. 3) is given by:

$$\varepsilon_{yy} = -\frac{\nu}{E}\sigma \tag{2.4}$$

where the values of $E$ and $\nu$ are taken for the relevant material.

If both sides of the interface shrank in the same way, the displacements along both sides of the interface would be compatible and both parts would deform in the same way, either separately or as a whole. Therefore we can join them back because both the displacement continuity and equilibrium are satisfied and the complete solution of BVP is obtained.

The condition of equal transverse shrinking of both parts leads to the following relation between the material constants:

$$\frac{\tilde{E}}{E} = \frac{\tilde{\nu}}{\nu}. \tag{2.5}$$

The above solution can be viewed as a solution of the redistribution problem while the primary problem would concern the same panel made of one material. This gives us an example of a material replacement without stress redistribution, but in fact this problem is different from that originally specified, since it imposes

conditions on the material properties instead of conditions on the shape of the interface.

In order to find an interface shape which gives no redistribution after material replacement, it is sufficient to consider a straight but inclined interface in the previously considered example, see Fig. 4. It could be shown that it is sufficient to consider the condition of equal elongations of both sides of the interface. After rewriting the strain tensor in a local set of coordinates chosen in such a way that the first local axis $\xi$ coincides with the direction of the interface, the elongation of the interface is given by:

$$\varepsilon_{\xi\xi} = \varepsilon_{xx} \cos^2 \alpha + \varepsilon_{yy} \sin^2 \alpha. \tag{2.6}$$

where $\alpha$ is the angle between the global axis $x$ and the local axis $\xi$.

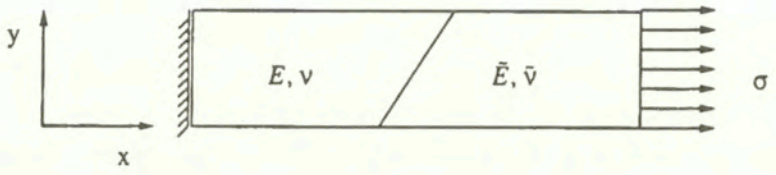


FIG. 4. Panel with inclined interface

The condition of equal elongation of both sides of the interface leads to the following formula for the inclination angle:

$$\tan^2 \alpha = \frac{\tilde{E} - E}{\tilde{E}\nu - E\tilde{\nu}}. \tag{2.7}$$

It can be verified that the solution of the primary and the secondary problem with the inclination angle given by Eq. (2.7) yields the same stress field. This means that for a given primary problem such as the panel made of one material subjected to pure tension, one can replace a part of this panel with another material and, as long as the interface is a straight line with an inclination given by Eq. (2.7), there will be no stress redistribution. This is a simple example of a solution of the main problem considered in this paper. It is also a proof that the problem has a solution at least in one case.

It is worth noting that, while in the secondary problem the stress field is homogeneous, the field of strain is not. There is a jump of strains along the material interface. As a consequence of this, the deformation is non-symmetric, as depicted in Fig. 5.

It has been shown that a solution of the problem exists in the case of the pure tension. Another simple example could also be demonstrated, the case of

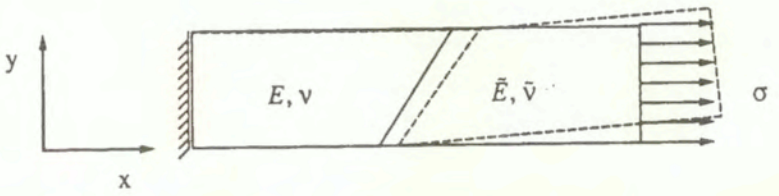


FIG. 5. Undeformed (solid line) and deformed (dashed line) shape of panel with inclined interface

uniform tension (compresion) state of stress where a solution does not exist (the simple proof will be given later in this paper).

At this point it is clear that the problem of stress redistribution can possess a solution but it is also possible that even in a simple case, such a solution may not exists. Therefore, it is difficult to find a condition which gives us information about the existence of the solution for a given case.

Instead of searching for the universal condition which asserts existence, in the following part we focus our attention on a more practical problem, how to find the interface location. We assume that this interface exists and try to establish the conditions which allow us to find its location.

## 3. Interface location

The problem of finding the shape of such a replacement in the most general case is far too difficult to consider. In this paper we simplify the problem essentially (and therefore restrict the validity of our solution) by adopting the following assumptions:

(a) displacements and strains are small,

(b) plane stress conditions are adopted,

(c) materials are homogeneous, isotropic and linear elastic, therefore tensor $E_{ijkl}$ is completely defined by Young's modulus $E$ and Poisson's ratio $\nu$, and the tensor $\tilde{E}_{ijkl}$ by values $\tilde{E}$ and $\tilde{\nu}$,

(d) body forces are neglected,

(e) a single load is applied to the structure,

(f) the interface of materials is perfectly bonded,

(g) the replacement is external, which means that a part of the structure made from the new material includes a boundary of the domain $\partial\mathcal{D}_2 \cap \partial\mathcal{D} \neq \emptyset$; in other words, the replacement is not completely surrounded by the body,

(h) there are no kinematic boundary conditions placed on the part of boundary which belongs to the replacement $\partial\mathcal{D}_{2\sigma} = \partial\mathcal{D}_2$.

We restrict our aim to establishing the theoretical formulation. The numerical application of the presented idea is not straightforward and has been described separately [5].

The stress redistribution problem leads to searching for the unknown interface line $\Gamma$. The formulation of the problem provides us a simple condition for verification if a particular line is an actual solution of the redistribition problem (by means of condition (2.3)) but it does not give us any practical method of searching for the interface location.

In the following part of the paper we will try to anlyse the consequences of the existence of the stress redistribution problem in order to find an auxiliary condition which helps us to determine the interface location.

It is useful to consider the problem as given in two subdomains. The solution of the whole redistribution problem can be split into two smaller problems given in two subdomains $\mathcal{D}_1$ and $\mathcal{D}_2$ defined by line $\Gamma$. Then we have two BVPs and in addition, we have to specify the interface conditions which couple the solutions of the subproblems to obtain a proper solution of BVP in whole domain domain $\mathcal{D}$.

Interface conditions [1] require:
continuity of displacements along interface $\Gamma$:

$$u_i = \tilde{u}_i; \tag{3.1}$$

equilibrium of interface

$$\sigma_{ij}n_j = \tilde{\sigma}_{ij}n_j. \tag{3.2}$$

Standard interface conditions of type Eq. (3.1) and Eq. (3.2) introduce $\tilde{u}_i$, $u_i$, $\sigma_{ij}n_j$ and $\tilde{\sigma}_{ij}n_j$ as unknowns of the problem at each point of $\Gamma$. None of these variables is prescribed along $\Gamma$ and there are six independent components of the stress tensors, while formula Eq. (3.2) gives only two equations which relate them.

For the redistribution problem the stresses along the interface are not unknown, since stresses should be the same as in the primary problem everywhere in $\mathcal{D}$ and therefore also along $\Gamma$. Then, in addition to Eq. (3.2), because of condition Eq. (2.3) we also have

$$\sigma_{ij}n_j = \sigma^I_{ij}n_j. \tag{3.3}$$

Therefore, the interface equilibrium Eq. (3.2) is satisfied as an identity, but because of condition Eq. (3.3), the value of $\sigma_{ij}n_j$ and $\tilde{\sigma}_{ij}n_j$ along $\Gamma$ becomes prescribed. We obtain prescribed static boundary conditions at the boundary $\Gamma$ of both subdomains.

Now the problem can be seen as two, almost uncoupled, BVPs with prescribed tractions along $\Gamma$ (as shown in Fig. 6) and with an additional condition given by Eq. (3.1).

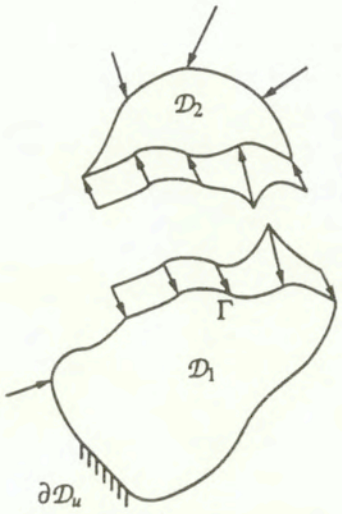


FIG. 6. Problem separated into two problems in subdomains

In subdomain $\mathcal{D}_1$ a separate BVP can be formulated, with prescribed tractions Eq. (3.3) along $\Gamma$. The material is the same as in the primary problem, therefore the whole solution of BVP is identical to the solution of the primary problem in subdomain $\mathcal{D}_1$. The field of stress $\sigma_{ij}$ is the same as $\sigma_{ij}^I$, the field of strain $\varepsilon_{ij}$ is the same as $\varepsilon_{ij}^I$ and the field of displacement $u_i$ is the same as $u_i^I$. The last statement leads to the conclusion that displacements along $\Gamma$ are also known, so we can write in addition to Eq. (3.1) that along $\Gamma$:

$$u_i = u_i^I. \tag{3.4}$$

Next, we can consider the second subdomain. The boundary of $\mathcal{D}_2$ is formed by part $\partial\mathcal{D}_{2\sigma}$ and by interface $\Gamma$. At boundary $\partial\mathcal{D}_{2\sigma}$, the tractions are prescribed. At boundary $\Gamma$ the static boundary conditions are also prescribed, since substituting Eq. (3.3) into Eq. (3.2) we obtain:

$$p_i = \tilde{\sigma}_{ij} n_j = \sigma_{ij}^I n_j. \tag{3.5}$$

Moreover, at $\Gamma$ also the kinematic boundary conditions are prescribed. Substituting Eq. (3.4) into Eq. (3.1) we obtain:

$$\tilde{u}_i = u_i^I. \tag{3.6}$$

Therefore, in the second subdomain we have a BVP with both kinematic and static boundary conditions prescribed along $\Gamma$. For a problem of linear elasticity, exactly one type of boundary conditions should be prescribed. When both types are specified, it can (and usually will) lead to a contradiction and can form an ill-posed problem.

The problem formulated in subdomain $\mathcal{D}_1$ is an example of a BVP problem which can formally be specified with an excessive number of boundary conditions and which does not lead to a contradiction. Formally, in this BVP problem in $\mathcal{D}_1$ we can have along $\Gamma$ given tractions Eq. (3.3) and displacements Eq. (3.4), but a solution satysfying both conditions exists.

This is the unique possibility. For prescribed tractions there is exactly one function of displacements which gives the proper solution. Conversely, for prescribed displacements there is exactly one function of tractions which does not lead to contradiction.

The application of the same reasoning to $\mathcal{D}_2$ leads to an alternative method of verification if a given $\Gamma$ is a solution of the redistribution problem. We can specify one of boundary conditions Eq. (3.5) or Eq. (3.6) along $\Gamma$, solve the BVP in $\mathcal{D}_2$ and check if the second condition is satisfied. Then with both equilibrium and continuity along $\Gamma$ satisfied, we can join both subdomains to form one body and obtain a complete solution which satisfies Eq. (2.3).

When the interface line $\Gamma$ is unknown, we can assume that one of these boundary conditions is specified and use the other one to determine the shape of $\Gamma$ if it exists. The choice which boundary condition is prescribed is arbitrary. In the following considerations tractions along $\Gamma$ are specified.

Now, we focus our attention on the virtually separated subdomain $\mathcal{D}_2$. Taking assumption (h) into account, the BVP in $\mathcal{D}_2$ is given in stresses. Because of assumptions (a)–(d), the stress distribution in such a problem is independent of material properties of the body. It is then clear that the state of stress $\tilde{\sigma}_{ij}$ is the same as the state of stress $\sigma^I_{ij}$ in the solution of the primary problem in subdomain $\mathcal{D}_2$, while the same stress $\tilde{\sigma}_{ij}$ with new material of properties $\tilde{E}$, $\tilde{\nu}$ gives a different strain $\tilde{\varepsilon}_{ij}$. It is also clear that the field of displacements will change, however displacements for the secondary problem in $\mathcal{D}_2$ can be obtained with an accuracy corresponding to unknown rigid body motions since the problem is given in stresses.

This leads us to another formulation of the redistribution problem:

> Find such a line $\Gamma$ defining subdomain $\mathcal{D}_2$ that for given stresses $\sigma^I_{ij}$ and material properties $\tilde{E}$, $\tilde{\nu}$ we can satisfy prescribed displacements Eq. (3.6) along $\Gamma$.

## 4. Displacements along $\Gamma$

Now, we focus our attention on the separated BVP given in $\mathcal{D}_2$ with an additional condition of prescribed displacement Eq. (3.6) which has to be satisfied along part $\Gamma$ of the boundary.

We analyse the consequences of this problem in order to find the unknown shape of $\Gamma$ in the redistribution problem.

Equation (3.6) is formulated in terms of displacements and is not convenient for further analysis. A better possibility is given by rewriting this equation in terms of displacement differentials. The displacement along any curve $C$ can be expressed as

$$u_i(x_C) = u_i(x_{C_0}) + \int_{x_{C_0}}^{x_C} du_i. \tag{4.1}$$

Applying Eq. (4.1) to $\Gamma$ it can be stated that, assuming the existence of one point $x_0 \in \Gamma$ where equation Eq. (3.6) is satisfied, it is *equivalent* to compare the displacement differentials along $\Gamma$:

$$d\tilde{u}_i = du_i^I. \tag{4.2}$$

For any field, the differentials of displacements can be expressed in terms of derivatives using the chain rule, and can be expressed in terms of small strain and small rotation tensors. In an extended form it gives (all superscripts are dropped):

$$\begin{aligned} du_1 &= \varepsilon_{11} dx_1 + \varepsilon_{12} dx_2 + \omega_{12} dx_2, \\ du_2 &= \varepsilon_{12} dx_1 + \varepsilon_{22} dx_2 - \omega_{12} dx_1. \end{aligned} \tag{4.3}$$

For the plane stress conditions the tensor of small rotation $\omega_{ij}$ has only two nonzero components, each of the same absolute value but with an opposite sign, so it can be described by a single scalar value $\omega$:

$$\omega = \omega_{12} = -\omega_{21}. \tag{4.4}$$

Rearranging equation Eq. (4.2) and taking into account Eqs. (4.3) and Eq. (4.4) we obtain:

$$\begin{aligned} (\varepsilon_{11} - \tilde{\varepsilon}_{11})\, dx_1 + (\varepsilon_{12} - \tilde{\varepsilon}_{12} + \omega - \tilde{\omega})\, dx_2 &= 0, \\ (\varepsilon_{12} - \tilde{\varepsilon}_{12} - \omega + \tilde{\omega})\, dx_1 + (\varepsilon_{22} - \tilde{\varepsilon}_{22})\, dx_2 &= 0. \end{aligned} \tag{4.5}$$

Now, we introduce an additional notation in order to simplify the equations. We define the difference of strains as:

$$e_{ij} = \varepsilon_{ij} - \varepsilon_{ij}. \tag{4.6}$$

It should be noted that $e_{ij}$ depends on the properties of both materials. In a similar manner we define the difference of rotations:

$$\Omega = \omega - \tilde{\omega}. \tag{4.7}$$

Rewriting the set of Eqs. (4.5) with the new notation we obtain:

$$\begin{aligned} e_{11}dx_1 + (e_{12} + \Omega)\, dx_2 = 0. \\ (e_{12} - \Omega)\, dx_1 + e_{22}dx_2 = 0. \end{aligned} \tag{4.8}$$

The set of Eqs. (4.8) is a system of linear homogeneous equations with unknowns $dx_1$ and $dx_2$. Such a system always possesses the trivial solution with the unknowns equal to zero. It has a nontrivial solution if the determinant of the system is equal to zero. This happens only if value of $\Omega$ satisfies the condition:

$$\Omega^2 = e_{12}^2 - e_{11}e_{22}. \tag{4.9}$$

Since Eq. (3.6) and its equivalent form Eq. (4.8) are well–defined only along $\Gamma$, the unknowns $dx_1$ and $dx_2$ define increments along $\Gamma$. Then, the local slope of $\Gamma$ at a given point is:

$$\frac{dx_2}{dx_1} = -\frac{e_{11}}{e_{12} + \Omega} = \frac{\Omega - e_{12}}{e_{22}}. \tag{4.10}$$

The rightmost term of Eq. (4.10) is valid except for the case $e_{22} = 0$. In order to handle properly any case of $e_{ij}$, we have to examine special cases:

1. If $e_{22} = 0$ and $e_{12} \neq 0$, then we obtain inclination

$$\frac{dx_2}{dx_1} = -\frac{e_{11}}{2e_{12}}. \tag{4.11}$$

2. If $e_{22} = 0$ and $e_{12} = 0$, then we obtain a vertical line

$$dx_1 = 0. \tag{4.12}$$

It should be noted that Eq. (4.10) (and its special cases) is a first order differential equation which can be used for finding $\Gamma$ if proper initial conditions can be specified. This requires that at least a single point belonging to $\Gamma$ is known.

### 4.1. Remarks

Equation (4.9) gives us a value of $\Omega$ squared. This makes it necessary to determine when the RHS of Eq. (4.9) is nonnegative. The sign of the RHS of Eq. (4.9) depends on the state of stress and material constants of both materials. This makes it dependent on seven variables: three components of stress tensor $\tilde{\sigma}_{ij}$ and four material constants. Such a function is far too complex to be analysed. However, the properties of this function with respect to the stress state can be examined. In order to simplify the analysis we consider the stress tensor in its principal directions. This does not restrict the generality of our considerations since the existence of a solution does not depend on the choice of a coordinate system.

After rewriting equation Eq. (4.9) in terms of principal stresses, the condition for the nonnegative value of RHS of Eq. (4.9) leads to the following inequality:

$$0 \geq [k\sigma_1 - \sigma_2][k\sigma_2 - \sigma_1] \tag{4.13}$$

where

$$k = \frac{\tilde{E} - E}{\tilde{E}\nu - E\tilde{\nu}}. \tag{4.14}$$

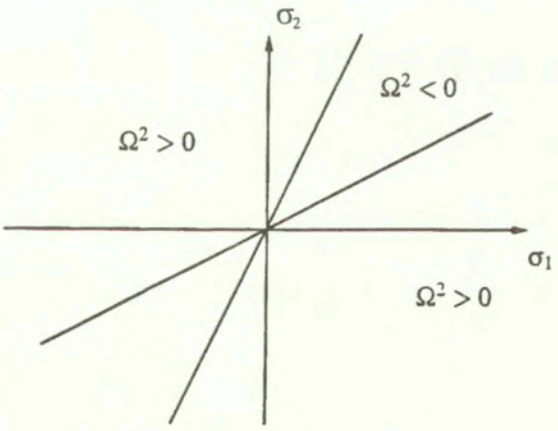


FIG. 7. Existence of solution on the plane of principal stresses

Inequality Eq. (4.13) splits the plane $\sigma_1$, $\sigma_2$ into four parts as depicted in Fig. 7. In the part where condition Eq. (4.13) is not satisfied, the solution does not exist. This means that such a point of domain can not belong to $\Gamma$. When at a given point the value of $\Omega$ can be computed, the existence of $\Gamma$ is not guaranteed yet and must be investigated using further conditions.

It is clear from Fig. 7 that in the case of uniform tension or compression ($\sigma_1 = \sigma_2$) the solution does not exist.

Equation (4.6) defines a tensor of strain differences $e_{ij}$. The RHS of Eq. (4.9) is the value of the second invariant of $e_{ij}$ taken with a negative sign. This makes it clear that condition Eq. (4.9) is independent of the choice of a coordinate system.

### 4.2. Interpretations

Now, we review some interpretations of the obtained formulae Eq. (4.9) and Eq. (4.10). By definition Eq. (4.7) $\Omega$ is a difference between the value of rotation in the primary problem and the value of rotation in the secondary problem. The rotation tensor component $\omega$ can be interpreted as the angle of rotation of an infinitesimally small segment between the undeformed and deformed state. Therefore, in case of the secondary problem, any curve crossing interface which is smooth before deformation, exhibits a slope discontinuity at $\Gamma$ after deformation.

The physical interpretation of the equations describing the continuity of displacements along the material interface is also worth examining. It becomes quite clear after assuming that Eqs. (4.8) are written in a local set of coordinates with the first axis coinciding with the tangent to the curve $\Gamma$ ($dx_2 = 0$). The first Eq. $(4.8)_1$ then becomes a condition of equal elongation of both sides of the interface. The second one becomes a condition of equal displacements in the direction perpendicular to the interface. This condition is dependent on $\Omega$, therefore the value of $\Omega$ is responsible for a gap or overlap.

### 4.3. Final condition

We now extend the meaning of Eq. (4.9). This equation must be satisfied along the material interface $\Gamma$. It has been pointed out that the RHS of Eq. (4.9) can be computed everywhere in domain $\mathcal{D}$. Then, it is useful to introduce a new field $\bar{\Omega}$ such that:

$$\bar{\Omega}^2 = e_{12}^2 - e_{11}e_{22} \tag{4.15}$$

in $\mathcal{D}$. The value of $\bar{\Omega}^2$ can be computed from the solution of the primary problem without knowing $\Gamma$. Then, condition Eq. (4.9) can be rewritten as:

$$\Omega^2 = \bar{\Omega}^2 \tag{4.16}$$

and must be satisfied along $\Gamma$.

We note that the sign of $\bar{\Omega}$ computed from Eq. (4.15) is in fact undetermined. Since along $\Gamma$ the sign of $\Omega$ should remain the same, setting the sign at any arbitrary point determines the whole solution. This is the reason why

both possible signs of $\bar{\Omega}$ should be examined as separate solutions. Then we will rewrite Eq. (4.16) in the form:

$$\Omega = \bar{\Omega} \tag{4.17}$$

to be satisfied along $\Gamma$, keeping in mind that it actually shows two possibilities

$$\bar{\Omega} = \pm\sqrt{e_{12}^2 - e_{11}e_{22}}. \tag{4.18}$$

Let us look at the definition of $\Omega$ given by equation Eq. (4.7). The value of the rotation, either $\omega$ or $\tilde{\omega}$, is not independent of the strain field. It is given by the following relation [2]:

$$\omega = \omega_0 + \int (\varepsilon_{11,2} - \varepsilon_{12,1})dx_1 + (\varepsilon_{12,2} - \varepsilon_{22,1})dx_2. \tag{4.19}$$

This means that for a given strain field the whole field of rotation is determined over the domain (or subdomain) except for the unknown value of $\omega_0$. The field of $\omega$ is determined by the solution of the primary problem since the value of $\omega_0$ can be computed from boundary conditions on $\partial\mathcal{D}_u$. The field of $\tilde{\omega}$ is not completely defined, since the value of $\tilde{\omega}_0$ is unknown. This value can easily be computed from the condition of displacement continuity if at least one point of curve $\Gamma$ is known. In the case of unknown $\Gamma$ and the secondary problem given in stresses, the value of $\tilde{\omega}$ is determined with a parameter. This means that at any point that is supposed to belong to $\Gamma$, the value of $\tilde{\omega}_0$ can be chosen to satisfy condition Eq. (4.17). Then, at any other point of $\Gamma$ the value of $\tilde{\omega}$ is fixed.

Thus, the field of $\Omega$ over the whole domain is determined with a single unknown scalar parameter. This is the reason why a directional derivative of $\Omega$ is used. Since condition Eq. (4.17) has to be satisfied only along $\Gamma$, the increments of both sides of Eq. (4.17) should be equal along $\Gamma$:

$$\frac{d\Omega}{ds} = \frac{d\bar{\Omega}}{ds}. \tag{4.20}$$

After expanding both sides of equation Eq. (4.20) according to the chain rule we obtain:

$$\frac{\partial\Omega}{\partial x_1}dx_1 + \frac{\partial\Omega}{\partial x_2}dx_2 = \frac{\partial\bar{\Omega}}{\partial x_1}dx_1 + \frac{\partial\bar{\Omega}}{\partial x_2}dx_2. \tag{4.21}$$

After substituting the definition of $\bar{\Omega}$ Eq. (4.15) and its derivatives, taking into account Eqs. (4.7), (4.19) and rearranging Eq. (4.21), we obtain the following condition to be satisfied along $\Gamma$:

$$\left(\bar{\Omega}_{,1} - e_{11,2} + e_{12,1}\right)dx_1 + \left(\bar{\Omega}_{,2} - e_{12,2} + e_{22,1}\right)dx_2 = 0. \tag{4.22}$$

The relation between $dx_1$ and $dx_2$ is determined from the local slope of $\Gamma$ and is given by Eq. (4.10)

$$e_{22}\left(\bar{\Omega}_{,1}-e_{11,2}+e_{12,1}\right)+\left(\bar{\Omega}_{,2}-e_{12,2}+e_{22,1}\right)\left(\bar{\Omega}-e_{12}\right)=0. \tag{4.23}$$

In special cases not covered by Eq. (4.10) equation (4.22) leads to other expressions:

1. If $e_{22}=0$ and $e_{12}\neq 0$, then we use Eq. (4.11)

$$2e_{12}\left(\bar{\Omega}_{,1}-e_{11,2}+e_{12,1}\right)-\left(\bar{\Omega}_{,2}-e_{12,2}+e_{22,1}\right)e_{11}=0. \tag{4.24}$$

2. If $e_{22}=0$ and $e_{12}=0$, then we use Eq. (4.12)

$$\bar{\Omega}_{,2}-e_{12,2}+e_{22,1}=0. \tag{4.25}$$

It should be noted that condition (4.23) depends on the derivatives of the strain field. This is the reason why for a homogeneous state of stress this condition is satisfied as an identity and then the solution is given by a straight line which can be obtained from condition Eq. (4.10).

In order to simplify the notation we define a function $F$ as:

$$F=\begin{cases} e_{22}\left(\bar{\Omega}_{,1}-e_{11,2}+e_{12,1}\right)+\left(\bar{\Omega}_{,2}-e_{12,2}\right. & \\ \quad \left.+e_{22,1}\right)\left(\bar{\Omega}-e_{12}\right) & \text{if } e_{22}\neq 0, \\ 2e_{12}\left(\bar{\Omega}_{,1}-e_{11,2}+e_{12,1}\right)+ & \text{if } e_{22}=0 \\ \quad -\left(\bar{\Omega}_{,2}-e_{12,2}+e_{22,1}\right)e_{11} & \text{and } e_{12}\neq 0, \\ \bar{\Omega}_{,2}-e_{12,2}+e_{22,1} & \text{if } e_{22}=0 \\ & \text{and } e_{12}=0. \end{cases} \tag{4.26}$$

With this definition of function $F$ we can simply write conditions Eq. (4.23), Eq. (4.24), and Eq. (4.25) as:

$$F=0. \tag{4.27}$$

We have shown that if some line $\Gamma$ is the sought interface then along this line, condition (4.27) has to be satisfied. However we have not shown that the inverse is true. In fact, it can be shown by just one example that it is not. Therefore, the condition (4.27) is only the necessary condition, but lines along which condition (4.27) is satisfied are the only possible locations of the sought interface. As a consequence of this, we have reduced the problem of stress redistribution from searching among the infinite number of possible locations of $\Gamma$ to a finite number of its locations.

### 4.4. Practical use of derived condition

The solution of the primary problem gives us stresses $\tilde{\sigma}_{ij}$ as functions of coordinates. The values of $e_{ij}$ can be obtained from stresses $\tilde{\sigma}_{ij}$ which determine $\varepsilon_{ij}$ and $\tilde{\varepsilon}_{ij}$. The value of $\tilde{\varepsilon}_{ij}$ was originally defined in $\mathcal{D}_2$ only. However, one can compute $\tilde{\varepsilon}_{ij}$ from $\sigma^I_{ij}$ everywhere in $\mathcal{D}$, although it can be meaningless in the neighbourhood of the kinematic boundary conditions. This makes it possible to obtain $e_{ij}$ without the prior knowledge of $\Gamma$. Then the field(s) of $\bar{\Omega}$ and its derivatives can be computed. Substituting all these functions into Eq. (4.26), a parametric equation for $F$ can be obtained:

$$F\left(e_{ij}(x,y), e_{ij,k}(x,y), \bar{\Omega}(x,y), \bar{\Omega}_{,i}(x,y)\right) = F(x,y). \tag{4.28}$$

It is quite difficult and apparently not necessary to solve this parametric equation. The most practical way to obtain the location of lines where condition Eq. (4.27) is satisfied is to draw contour lines of the surface given by $F$ over the entire domain.

When drawn, the contour lines of zero level show us all possible locations of $\Gamma$.

The absence of the zero level contour informs us that a solution does not exist. When one or more zero level contours appear, it is neccessary to verify each one separately. In fact, we should consider two such surfaces $F^+$ and $F^-$, according to the choice of the sign in Eq. (4.18)

This approach is very efficient. In fact we need to solve a simple linear static problem (primary), then compute the values and draw the contours of $F^+$ and $F^-$ and finally verify by direct computation every line satisfying Eq. (4.27). Prior to this verification we can exclude some lines when they violate assumptions (g) or (h).

## 5. Example

The formula (4.27) gives a solution for the problem of finding the shape of $\Gamma$. We will now show an example of a solution predicted by Eq. (4.27). This example is a case of an inhomogeneous state of stress, in order to actually verify condition Eq. (4.27) rather than Eq. (4.10). We show a simple example obtained in a rather artificial way. We find an example which is a solution of the redistribution problem and then compute the functions given by Eq. (4.27) in order to check if we obtain the correct solution.

We assume the shape of $\Gamma$ and determine the stress which satisfies Eq. (4.27). For the sake of simplicity, the shape of $\Gamma$ is chosen as a straight line described by the function:

$$y = x - 1. \tag{5.1}$$

We will seek the solution in a class of linearly varying fields of stress. After lengthy but simple derivations, one of the possible stress fields is found as:

$$\begin{aligned} \sigma_{11} &= -2137x, \\ \sigma_{22} &= 1645x + 3362y, \\ \sigma_{12} &= -3572 - 3362x + 2137y. \end{aligned} \tag{5.2}$$

The following material constants are adopted: $E = 20$ GPa, $\nu = 0.1$, $\tilde{E} = 210$ GPa, $\tilde{\nu} = 0.3$. After computing the displacements for the primary problem and the secondary problem it is verified that the displacements along the material interface are equal, which makes us sure that it is the complete solution of the redistribution problem.

Therefore, any part of plane $xy$ (finite or not) can be considered as a primary problem as long as we guarantee that the stresses inside are given by Eq. (5.2). Then, the static boundary conditions at the appropriate part of the boundary can be obtained from Eq. (5.2). The kinematic boundary conditions (if any) have to be determined from the displacements resulting from Eq. (5.2), but again the rigid body motion is arbitrary. Then the solution of the redistribution problem is given by Eq. (5.1) provided that the chosen domain contains any part of this line and the chosen kinematic boundary condition does not violate assumption (h).

In order to demonstrate the application of the presented approach, the domain $0 \leq x \leq 2$ and $0 \leq y \leq 4$ is chosen arbitrarily. The static boundary conditions are prescribed at all boundaries. In addition to this, one can assume appropriate pointwise supports at lower corners of the rectangle in order to prevent the rigid body motions. They do not influence the presented example, however they might be essential in case of (numerical) verification of the obtained solution.

Then, we can verify the validity of formula (4.27), by computing $F$ using stresses given by Eq. (5.2). After applying the procedure described previously, the surfaces created by functions $F(x, y)$ are drawn over the domain. The values of $F^{-}(x, y)$ are negative everywhere in this domain and the solution does not exist. Figure 8 (left) shows the contour lines of function $F^{+}(x, y)$. In Fig. 8 (right) only the zero contours are left. This shows us two lines satisfying Eq. (4.27). Then we should verify each line separately, by solving the secondary problem, if it is the actual solution of the redistribution problem. It should be noted that the known solution of the redistribution problem (5.1) has been detected by this approach.

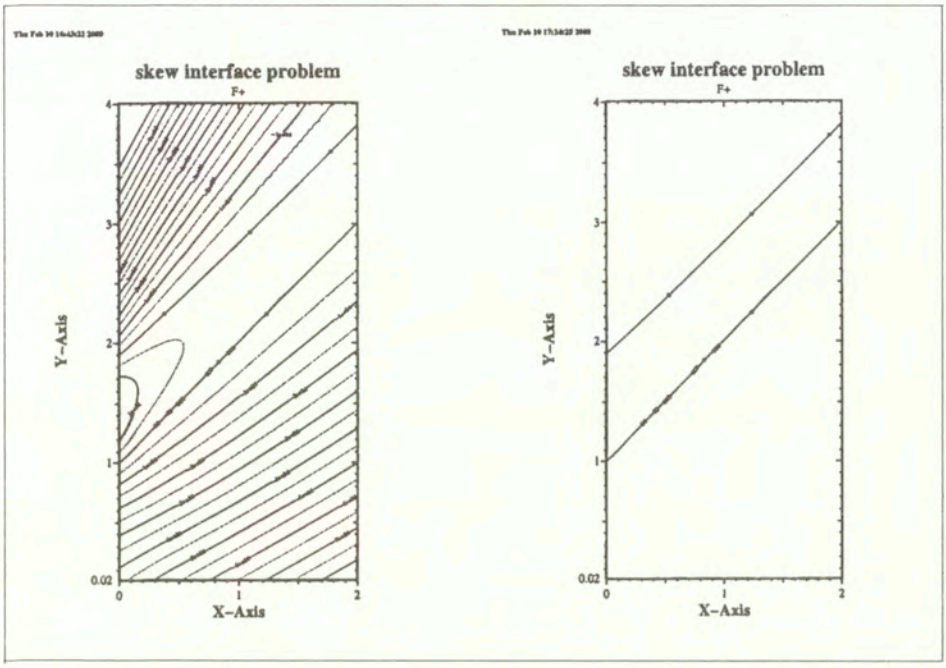


FIG. 8. Plot of contour lines of $F^+(x, y) = \text{const}$ (left) and contours of zero level (right)

## 6. Conclusions

In this paper we have formulated the problem of stress redistribution, i.e. the problem of finding a shape of a partial material replacement which preserves the same stress as in the body before replacement. We have shown some trivial examples which prove that this problem may have a solution. The paper demonstrates how significantly we can influence the redistribution caused by a bimaterial interface. It is also a proof that the solution of such a problem does not violate the fundamental laws of mechanics and, moreover, it contradicts the common belief that a bimaterial interface has to lead to stress redistribution, as long as the material properties of both materials are different.

Then we have discussed the question of searching for such a specific material interface. For a simplified problem we have derived the neccessary condition for the existence of a solution. This converts the problem of searching among an infinite number of interface locations to the verification of finite number of lines. We have demonstrated that the use of this condition is a practical method of finding that interface. However, the proposed method of solution has obvious limitations. The application of this approach is strongly limited by the set of adopted assumptions.

The article presents the ultimate approach to the problem of redistribution: we can obtain no redistribution or no solution at all. In practice, a partial solution of the problem focused on the reduction of redistribution could be equally worthwhile.

The redistribution problem brings some side effects, such like undesired deformations. The significance of these effects can be assessed in case of a given application, since the same effects may be irrelevant for one problem while they can disqualify the solution for other problems.

## References

1. A. C. ERINGEN, *Mechanics of continua*, John Wiley & Sons, 1967.
2. Y. C. FUNG, *Foundations of solid mechanics* (Polish translatation), PWN, 1969.
3. H. A. C. JACOB and H. HUGGLER, *An investigation into biomechanical causes of prosthesis stem loosening within the proximal end of the human femur*, J. Biomech., **13**, 159-173, 1980.
4. A. E. LOWE, *A Treatise on the mathematical theory of elasticity*, Dover Publications, New York, $4^{th}$ edition, 1927.
5. A. MATUSZAK, *Numerical approach to the problem of stress redistribution*, In $2^{nd}$ European Conference on Computational Mechanics, Cracow, 26-29 June 2001.
6. I. MOHAMMED and K. M. LIECHTI, *The effect of corner angles in bimaterial structures*, International Journal of Solids and Structures, **38**, 4375-4394, 2001.
7. T. J. REITER, *A model for the functional adaptations of bone and application in optimal structural design*, PhD thesis, Technical University Wien, 1996.
8. S. TIMOSHENKO and J. N. GOODIER, *Theory of elasticity* (Polish translation), Arkady, 1962.

*Received December 29, 2000; revised version December 27, 2001.*

Arch. Mech., **54**, 1, pp. 55–74, Warszawa 2002

# Thermal radiation effects on free convection over a rotating axisymmetric body with application to a rotating hemisphere

M. A. HOSSAIN [1], M. ANGHEL [2] and I. POP [3]

[1] *Department of Mathematics University of Dhaka*
*1000 Dhaka, Bangladesh*

[2] *Faculty of Mathematics University of CLUJ*
*R-3400 CLUJ, CP 253, Romania*

[3] *Faculty of Mathematics University of CLUJ*
*R-3400 CLUJ, CP 253, Romania*
*e-mail: popi@math.ubbcluj.ro*

THIS PAPER DEALS with the interaction of thermal radiation with free convection, laminar boundary-layer flow past a heated rotating axisymmetric round-nosed body of uniform surface temperature. The fluid considered is a gray, absorbing-emitting but nonscattering medium, and Rosseland approximation is used to describe the radiative heat flux. The difficulty of having a unified mathematical treatment of this problem is due to the nonsimilarity nature of the governing equations arising from the buoyant force-field and the transverse curvature of the body. The important parameters of this problem are the Planck number, $R_d$, the buoyancy parameter, $\lambda$, and the wall to free stream temperature ratio, $\theta_w$. Numerical solution of the boundary-layer equations are performed using the Keller-box method as well as the local nonsimilarity method. The theory is applied to a rotating hemisphere for a gas with Prandtl number of 0.72. The effects of the parameters $\lambda$, $R_d$ and $\theta_w$ are shown on the velocity and temperature profiles, as well as on the local skin friction coefficient and local rate of heat transfer.

## Notations

| | |
|---|---|
| $a$ | Rosseland mean absorption coefficient |
| $f$ | dimensionless stream function |
| $g$ | acceleration due to gravity |
| $g_x$ | component of the acceleration due to gravity in the $x$ direction |
| $Gr$ | Grashof number |
| $S(x)$ | function of $x$ denotes sine of the angle between the acceleration vector and a component normal to the surface of the body |
| $k$ | thermal conductivity |
| $L$ | characteristic length |
| $Nu$ | Nusselt number |
| $Pr$ | Prandtl number |
| $R_d$ | Planck number or the conduction-radiation parameter defined in Eq. (2.13) |

| | |
|---|---|
| $Re$ | Reynolds number |
| $R$ | radial distance from a surface element to the axis of symmetry |
| $T$ | temperature of the fluid in the boundary-layer |
| $T_w$ | surface temperature |
| $T_\infty$ | temperature of the ambient fluid |
| $u$ | velocity component in the $x$ direction |
| $U_e$ | reference velocity |
| $v$ | velocity component in the $y$ direction |
| $w$ | velocity component in the rotation direction |
| $x$ | coordinate measured from the stagnation point along the surface of the body |
| $y$ | coordinate normal to $x$ |
| $z$ | coordinate measured in the rotation direction |

*Greek letters*

| | |
|---|---|
| $\alpha$ | thermal diffusivity |
| $\beta$ | thermal expansion coefficient |
| $\eta$ | similarity variable defined in Eq. (2.15) |
| $\theta$ | non-dimensional temperature |
| $\theta_w$ | ratio of the surface temperature to the ambient temperature defined in Eq. (2.13) |
| $\nu$ | kinematic viscosity |
| $\lambda$ | buoyancy parameter defined in Eq. (2.12) |
| $\rho$ | density of the fluid |
| $\xi$ | transformed coordinate defined in Eq. (2.15) |
| $\Omega$ | angular velocity |
| $\tau_x, \tau_z,$ | skin friction coefficients in the $x$- and $z$-directions, respectively |
| $\sigma$ | Stephan-Boltzmann constant |
| $\sigma_s$ | scattering coefficient |
| $\psi$ | stream function |

## 1. Introduction

THE THERMAL RADIATION EFFECTS on free convection flow are important in the context of space technology and processes involving high temperatures, and very little is known about the effects of radiation on the boundary-layer flow of radiating fluid past a body of general geometry. The inclusion of thermal radiation effects in the energy equation leads to a highly nonlinear partial differential equation. In absence of the effect of radiation, investigations have been made on the laminar heat transfer from rotating axisymmetric round-nosed bodies either for forced convection or for natural convection in refs. [1-5]. The density difference arising as a result of temperature difference gives rise to a buoyancy force. The neglect of buoyancy effect on forced convection heat transfer may not be justified when the velocity is small and the temperature difference between the surface and ambient fluid is large. It may be expected that this buoyancy force will affect the momentum and the heat transfer.

Several authors [6-11] have discussed the effect of buoyancy forces on non-rotating bodies. For rotating bodies, LEE *et al.* [5] have investigated the laminar boundary-layer and heat transfer in forced flow, neglecting the buoyancy forces. They have used MERK's [10] series, modified by CHAO and FAGBENLE [11], and their results compare favorably with previous theoretical and experimental studies. SUWONO [12] considered the problem of buoyancy effects on the flow and heat transfer in rotating axisymmetric round-nosed bodies for both aiding and opposing flows. He has shown that spinning a vertical axisymmetric body in a convective flow, the fluid near the surface is forced outwards in the radial direction due to the presence of centrifugal force. Application of this idea in order to develop rotating systems for enhancing the heat transfer rate is important in the analysis of the rotary machine design. The problem posed by SUWONO [12] has later been investigated by HOSSAIN *et al.* [13] for a viscous and electrically conducting fluid, using the implicit finite difference method.

The majority of studies on interaction of thermal radiation and natural convection have been confined to the case of a vertical semi-infinite flat plate [14-20]. HOSSAIN and TAKHAR [21] have analyzed the effect of radiation on the forced and free convection flow of an optically dense viscous and incompressible fluid past a heated vertical flat plate with uniform free stream velocity and surface temperature using the Rosseland diffusion approximation, which leads to nonsimilarity solutions. The convection-radiation effects on free convection boundary-layer flow from an inclined surface with small angle of inclination to the horizontal has been investigated by HOSSAIN *et al.* [22]. In this analysis, solutions are obtained in the upstream, the downstream and the entirely mixed regimes. Very recently, HOSSAIN and ALIM [23] have studied the problem of natural convection interaction in the boundary-layer flow along a thin vertical cylinder employing two methods, namely, the implicit finite-difference method and the local non-similarity method, taking up terms to the third level of truncation.

The purpose of the present paper is to investigate the effect of the conduction-radiation interaction on the laminar free convection flow of an optically dense, viscous incompressible fluid with heated rotating axisymmetric round-nosed bodies of uniform surface temperature. The difficulty of having a unified mathematical treatment of this problem is due to the nonsimilarity nature of the governing equations arising from the buoyant force-field and the transverse curvature of the bodies. Numerical simulations of the boundary-layer equations are performed using the implicit finite-difference method, known as the KELLER-box (see CEBECI and BRADSHAW [24]) method, as well as the local nonsimilarity method, taking terms up to the second level of truncation. The results are then applied to the case of a rotating hemisphere.

## 2. Basic equations

Consider the steady free convection boundary-layer flow over a rotating axisymmetric round-nosed body, which rotates with the constant angular velocity $\Omega$ around its vertical axis of symmetry in an optically dense, viscous and incompressible fluid of constant ambient temperature $T_\infty$. It is assumed that the surface of the body has the uniform temperature $T_w$, where $T_w > T_\infty$. Let $x, y$ and $z$ be a non-rotating orthogonal curvilinear coordinate system with the $x$-coordinate measured from the lower stagnation point along the surface of the body, $y$ measured normal to $x$ and $z$ measured in the rotation direction, as shown in Fig. 1. It is also assumed that the radiative heat flux in the $x$-direction is negligible in comparison with that in the $y$-direction (see SPARROW and CESS[19]).

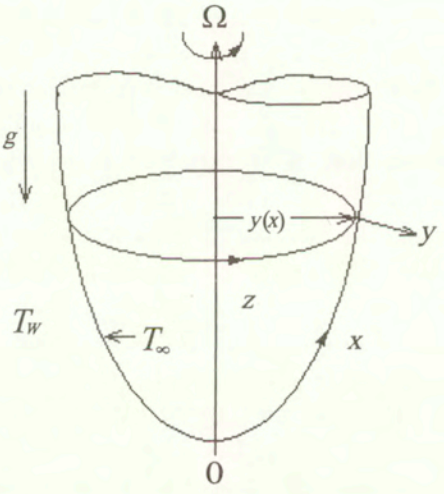


FIG. 1. Physical model and coordinate system.

$$\frac{\partial u}{\partial x} + \frac{\partial v}{\partial y} + \frac{u}{r}\frac{dr}{dx} = 0, \tag{2.1}$$

$$u\frac{\partial u}{\partial x} + v\frac{\partial u}{\partial y} - \frac{w^2}{r}\frac{dr}{dx} = \nu\frac{\partial^2 u}{\partial y^2} + g_x\beta(T - T_\infty), \tag{2.2}$$

$$u\frac{\partial w}{\partial x} + v\frac{\partial w}{\partial y} + \frac{uw}{r}\frac{dr}{dx} = \nu\frac{\partial^2 w}{\partial y^2}, \tag{2.3}$$

$$u\frac{\partial T}{\partial x}+v\frac{\partial T}{\partial x}=\frac{\nu}{Pr}\frac{\partial}{\partial y}\left[\left(1+\frac{16\sigma T^3}{3k(a+\sigma_s)}\right)\frac{\partial T}{\partial y}\right], \tag{2.4}$$

where $u$, and $w$ are the velocity components along the $x, y$ and $z$ axes, $T$ is the fluid temperature, $g_x$ is the $x$-component of the local gravitational acceleration vector in the direction of increasing $x$, $r(x)$ is the radial distance from the axis of symmetry to the surface of the body, $Pr$ is the Prandtl number; $\rho$, $\beta$, $\nu$, $a$, $\sigma$, $\sigma_s$ are, respectively, the fluid density, thermal expansion coefficient, kinematic viscosity of the fluid, Rosseland mean absorption coefficient, Stefan-Boltzmann constant and the scattering coefficient, respectively. We assume that $g_x = gS(x)$ where $S(x)$ is a non-dimensional function of $x$ and $g$ is the constant gravitational acceleration. Radiation effects are considered here using the Rosseland diffusion approximation (see SIEGEL and HOWEL [25]). Under this approximation, the situation is not valid where scattering is expected to be non-isotropic as well as in the immediate vicinity of the wall.

The boundary conditions to be satisfied by Eqs. (2.1) – (2.4) are

$$\begin{aligned} &u=v=0,\quad w=r\Omega,\quad T=T_w \ \text{ at } y=0,\\ &u\to 0,\quad w\to 0,\quad T\to T_\infty \ \text{ as } y\to\infty, \end{aligned} \tag{2.5}$$

where $\Omega$ is the angular velocity.

We now define the following non-dimensional variables:

$$\begin{aligned} &\bar{x}=x/L,\quad \bar{y}=Re^{1/2}\,(y/L),\quad \bar{r}=r/L,\\ &\bar{u}=u/U,\quad \bar{v}=Re^{1/2}\,(v/U),\quad \bar{w}=w/U,\\ &\theta=(T-T_\infty)/(T_w-T_\infty), \end{aligned} \tag{2.6}$$

with $L$ and $U = L\Omega$ being reference length and reference velocity, respectively. Substituting these variables into Eqs. (2.1) – (2.4) and dropping the bar for brevity, we get

$$\frac{\partial u}{\partial x}+\frac{\partial v}{\partial y}+\frac{u}{r}\frac{dr}{dx}=0, \tag{2.7}$$

$$u\frac{\partial u}{\partial x}+v\frac{\partial u}{\partial y}-\frac{w^2}{r}\frac{dr}{dx}=\frac{\partial^2 u}{\partial y^2}+\lambda S(x)\theta, \tag{2.8}$$

$$u\frac{\partial w}{\partial x}+v\frac{\partial w}{\partial y}+\frac{uw}{r}\frac{dr}{dx}=\frac{\partial^2 w}{\partial y^2}, \tag{2.9}$$

$$u\frac{\partial\theta}{\partial x}+v\frac{\partial\theta}{\partial y}=\frac{1}{Pr}\frac{\partial}{\partial y}\left[\left\{1+\frac{4}{3}R_d(1+K\theta)^3\right\}\frac{\partial\theta}{\partial y}\right], \tag{2.10}$$

and the boundary conditions (2.5) become

$$u=v=0,\ w=r,\ \theta=1 \text{ at } y=0,\ u\to 0,\ w\to 0,\ \theta\to 0 \text{ as } y\to\infty, \tag{2.11}$$

where $\lambda$, $Gr$ and $Re$ are the buoyancy parameter, the Grashof number and the Reynolds number which are defined by

$$\lambda=\frac{Gr}{Re^2},\quad Gr=\frac{g\beta(T_w-T_\infty)L^3}{\nu^2},\quad Re=\frac{UL}{\nu}. \tag{2.12}$$

Also the parameters $R_d$ and $K$ in Eq. (2.10) are defined as

$$R_d=\frac{4\sigma T_\infty^3}{k(a+\sigma_s)},\qquad \mathrm{K}=\frac{T_w}{T_\infty}-1=\theta_w-1 \text{ (say)}, \tag{2.13}$$

and they are known as the Planck number and the surface temperature parameter, respectively. Further, in Eq. (2.13) $\theta_w$ is the ratio of the surface temperature to the temperature of the ambient fluid. Throughout the present investigation we assume that $K>0$. However, when the wall temperature $T_w$ is very close to the ambient temperature $T_\infty$ (i.e., $K=0$), the energy equation (2.10) takes the following form (see, ALI *et al.* [26]):

$$u\frac{\partial\theta}{\partial x}+v\frac{\partial\theta}{\partial y}=\frac{1}{Pr}\left(1+\frac{4}{3}R_d\right)\frac{\partial^2\theta}{\partial y^2}, \tag{2.14}$$

We now introduce the new coordinates $(\xi,\eta)$ in place of the non-dimensional coordinates $(x,y)$ defined as

$$\xi=\int_0^x [r(x)]^3dx,\quad \eta=r^2\frac{y}{(2\xi)^{1/2}} \tag{2.15}$$

along with the non-dimensional functions:

$$(\psi(x,y)=(2\xi)^{1/2}f(\xi,\eta),\quad w(x,y)=\frac{(2\xi)^{1/2}}{r}h(\xi,\eta), \tag{2.16}$$

where $\psi$ is the stream function and is defined in the usual way as

$$u=\frac{1}{r}\frac{\partial\psi}{\partial y},\quad v=-\frac{1}{r}\frac{\partial\psi}{\partial x}. \tag{2.17}$$

Using these transformations, the momentum and energy Eqs. (2.8) – (2.10) can be written in the following form:

$$f''' + ff'' - P(\xi)\left(f'^2 - h^2\right) + \lambda Q(\xi)\theta = 2\xi\left(f'\frac{\partial f'}{\partial \xi} - f''\frac{\partial f}{\partial \xi}\right), \tag{2.18}$$

$$h'' + fh' - 2P(\xi)f'h = 2\xi\left(f'\frac{\partial h}{\partial \xi} - h'\frac{\partial f}{\partial \xi}\right), \tag{2.19}$$

$$\left[\left\{1 + \frac{4}{3}R_d\left(1 + K\theta\right)^3\right\}\theta'\right]' + Prf\theta' = 2Pr\xi\left(f'\frac{\partial \theta}{\partial \xi} - \theta'\frac{\partial f}{\partial \xi}\right), \tag{2.20}$$

subject to the boundary conditions (2.11) which become

$$\begin{gathered} f(\xi,0) = f'(\xi,0) = 0,\ h(\xi,0) = 1,\ \theta(\xi,0) = 1, \\ f'(\xi,\infty) = 0,\ h(\xi,\infty) = \theta(\xi,\infty) = 0, \end{gathered} \tag{2.21}$$

where

$$P(\xi) = \frac{2\xi}{r}\frac{dr}{d\xi},\quad Q(\xi) = \frac{2\xi K(\xi)}{r^5}. \tag{2.22}$$

Here primes denote partial differentiation with respect to $\eta$. If the wall temperature $T_w$ is very close to the ambient temperature $T_\infty$, the energy Eq. (2.20) takes the form:

$$\left(1 + \frac{4}{3}R_d\right)\theta'' + Pr\, f\theta' = 2Pr\,\xi\left(f'\frac{\partial \theta}{\partial \xi} - \theta'\frac{\partial f}{\partial \xi}\right). \tag{2.23}$$

Once the solution of Eqs. (2.18) – (2.23) is known, it becomes important from the experimental point of view to determine the physical quantities like skin friction coefficients and the local heat transfer at the surface of the body. These quantities are given by

$$Re^{1/2}\tau_x = \frac{r^3}{(2\xi)^{1/2}}f''(\xi,0),\quad Re^{1/2}\tau_z = \frac{r^3}{(2\xi)^{1/2}}h'(\xi,0), \tag{2.24}$$

and

$$NuRe^{-1/2} = \frac{r^2}{(2\xi)^{1/2}}\left(1 + \frac{4}{3}R_d(1+K)^3\right)\theta'(\xi,0), \tag{2.25}$$

where $\tau_x$ and $\tau_z$ are the skin friction coefficients along the $x$- and $z$-directions, and $Nu$ is the local Nusselt number.

## 3. Application to a rotating hemisphere

As an example, in this section, we discuss the application of the present analysis to the case of a rotating hemisphere of radius $R$ with the rotating axis being parallel to the gravitational vector $\mathbf{g}$. If we select $R$ as the reference length, i.e. $L = R$, we then have the following non-dimensional variables:

$$r(x) = \sin x, \quad K(x) = \sin x, \quad \xi = \frac{1}{3}\left(\cos^3 x - 3\cos x + 2\right). \tag{3.1}$$

Substituting (3.1) into Eqs. (2.18) – (2.20), we get

$$f''' + ff'' - P(x)\left(f'^2 - h^2\right) + \lambda Q(x)\theta = 2xI(x)\left(f'\frac{\partial f'}{\partial x} - f''\frac{\partial f}{\partial x}\right), \tag{3.2}$$

$$h'' + fh' - 2P(x)f'h = 2xI(x)\left(f'\frac{\partial h}{\partial x} - h'\frac{\partial f}{\partial x}\right), \tag{3.3}$$

$$\left[\left\{1 + \frac{4}{3}R_d\left(1 + K\theta\right)^3\right\}\theta'\right]' + Pr\, f\theta' = 2Pr\, xI(x)\left(f'\frac{\partial \theta}{\partial \xi} - \theta'\frac{\partial f}{\partial \xi}\right), \tag{3.4}$$

subject to the boundary conditions

$$\begin{gathered} f(\xi,0) = f'(\xi,0) = 0, \quad h(\xi,0) = 1, \quad \theta(\xi,0) = 1, \\ f'(\xi,\infty) = 0, \quad h(\xi,\infty) = \theta(\xi,\infty) = 0, \end{gathered} \tag{3.5}$$

where $P(x)$, $Q(x)$ and $I(x)$ are now given by

$$\begin{aligned} P(x) &= \frac{2\cos x}{3\sin^4 x}\left(\cos^3 x - 3\cos x + 2\right), \\ Q(x) &= \frac{2}{3}\frac{\left(\cos^3 x - 3\cos x + 2\right)}{\sin^4 x}, \\ I(x) &= \frac{\left(\cos^3 x - 3\cos x + 2\right)}{3x\sin^3 x}. \end{aligned} \tag{3.6}$$

We notice in passing that, when the conduction-radiation is absent (i.e., $R_d = 0$), Eqs. (3.2) – (3.4) reduce to those reported by SUWONO [12].

## 4. Numerical solution

In the absence of the effect of thermal radiation (i.e. $R_d = 0$), the partial differential Eqs. (2.18) – (2.20) subject to the boundary conditions (2.21) were solved by SUWONO [12] using Görtler's series method for small values of $\xi$ (i.e. $\xi \ll 1$), and the results were then applied to the case of a rotating hemisphere. Here we are solving the transformed Eqs. (3.2) – (3.4) subject to the boundary conditions (3.5) numerically following two distinct methods, namely: the implicit finite-difference method, known as Keller-box method (see CEBECI and BRADSHAW [24]), and the local nonsimilarity method, respectively. The latter method has been recently used very efficiently by HOSSAIN and ALIM [23]. The results obtained by employing these method are compared with those of SUWONO [12] for the case when the radiation is absent (i.e. $R_d = 0$).

### 4.1. Keller-box method

To employ this method, the system of partial differential Eqs. (3.2) – (3.4) is first converted to a system of seven first-order partial differential equations by introducing new unknown functions of $\eta$ derivatives. This system is then put into a finite-difference form in which the nonlinear difference equations are linearized by the Newton's quasi-linearization method. The resulting linear difference equations along with the appropriate boundary conditions are finally solved by an efficient block-tridiagonal factorization technique. The details of the computational procedure have been discussed by HOSSAIN *et al.* [8, 16–19] and will not be repeated here. We note that for initiating this method, the profiles at $x = 0$ (the lower stagnation point of the hemisphere) for the functions $f(\eta)$, $g(\eta)$ and $\theta(\eta)$ and their derivatives are obtained from the exact solutions of the similarity equations:

$$f''' + ff'' + \frac{1}{2}\left(f'^2 - h^2\right) + \frac{1}{2}\lambda\theta = 0, \tag{4.1}$$

$$h''' + fh'' - f'h' = 0, \tag{4.2}$$

$$\left[\left\{1 + \frac{4}{3}R_d\left(1 + K\theta\right)^3\right\}\theta'\right]' + Prf\theta' = 0, \tag{4.3}$$

which are obtained from Eqs. (3.2) – (3.4) as $x \to 0$. The appropriate boundary conditions to be satisfied by Eqs. (4.1) – (4.3) are

$$\begin{aligned} &f(0) = f'(0) = 0, \quad h'(0) = 1, \quad \theta(0) = 1, \\ &f'(\infty) = 0, \quad h'(\infty) = \theta(\infty) = 0, \end{aligned} \tag{4.4}$$

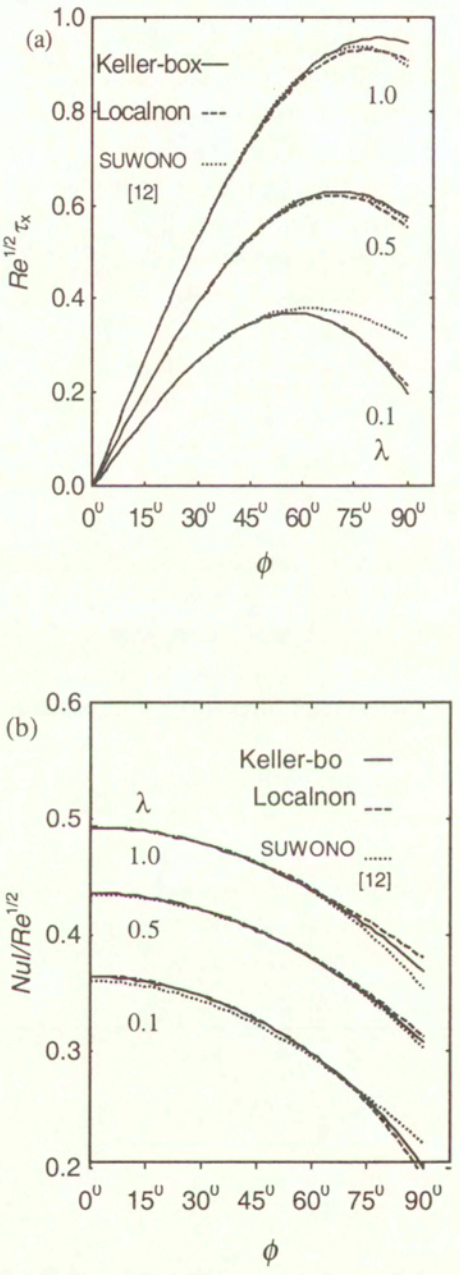


FIG. 2. Comparisonof the results without the effect of radiation ($R_d = 0$)obtained fc $Pr$=0.72 and $\lambda = 0.1, 0.5$ and 1.0. (a) The local skin friction coefficient along the $x$-direcion, and (b) the local Nusselt number.

**4.2. Local nonsimilarity method**

The formulation of the local nonsimilarity method for heat transfer problems has been first given by SPARROW and YU [27]. More extensive and successful use of this method has ben made recently by HOSSAIN *et al.* [23, 28]. With reference to the present problem, we derive here the equations up to the second level of truncation. To do it, we introduce the following functions:

$$F(x,\eta) = \frac{\partial f}{\partial x}, \quad G(x,\eta) = \frac{\partial h}{\partial x}, \quad \Theta(x,\eta) = \frac{\partial \theta}{\partial x}. \tag{4.5}$$

The governing Eqs. (3.2)–(3.4) can then be written as

$$f''' + ff'' + P(x)\left(f'^2 - g^2\right) + \lambda Q(x)\theta = I_1(x)\left(f'F' - f''F\right), \tag{4.6}$$

$$h'' + fh' - 2P(x)f'h = 2xI_1(x)\left(f'G - h'F\right), \tag{4.7}$$

$$\left[\left\{1 + \frac{4}{3}R_d\left(1 + K\theta\right)^3\right\}\theta'\right]' + Prf\theta' = \Pr I_1(x)\left(f'\Theta - \theta'F\right), \tag{4.8}$$

subjected to the boundary conditions.

The equations for $F, G$ and $\Theta$ can be derived by taking the derivatives of Eqs. (4.6) – (4.8) with respect to $x$ and neglecting the terms with the derivative functions $F, G$ and $\Theta$ with respect to $x$. To this end, we get

$$\begin{aligned} F''' + fF'' + (1 + 2I_2(x))\, f''F - (2P(x) + I_2(x))\, f'F' + 2P(x)gG \\ - P_1(x)\left(f'^2 - g^2\right) + \lambda\left(+Q(x)\Theta + Q_1(x)\theta\right) = I_1(x)\left(F'^2 - FF''\right), \end{aligned} \tag{4.9}$$

$$\begin{aligned} G'' + fG' + (1 + I_2(x))\, h'F - (2P(x) + I_2(x))f'G - 2P_1(x)f'h \\ = I_1(x)\left(F'G - G'F\right), \end{aligned} \tag{4.10}$$

$$\begin{aligned} &\left\{1 + \frac{4}{3}R_d\left(1 + K\theta\right)^3\right\}\Theta'' + 4R_d\left(1 + K\theta\right)^2\theta'' \\ &+ 8R_dK\left(1 + K\theta\right)\left[\left(1 + K\theta\right)\theta'\Theta' + K\theta'^2\Theta\right] + Pr\left[f\Theta' + (1 + I_2(x))\,\theta'F\right] \\ &- PrI_2(x)f'g = PrI_1(x)\left(Ff\Theta - \Theta'F\right). \end{aligned} \tag{4.11}$$

The boundary conditions to be satisfied by the equations for $F, G$ and $\Theta$ are

$$\begin{aligned} F(x,0) = F'(x,0) = G(x,0) = \Theta(x,0) = 0, \\ F'(x,\infty) = G(x,\infty) = \Theta(x,\infty) = 0, \end{aligned} \tag{4.12}$$

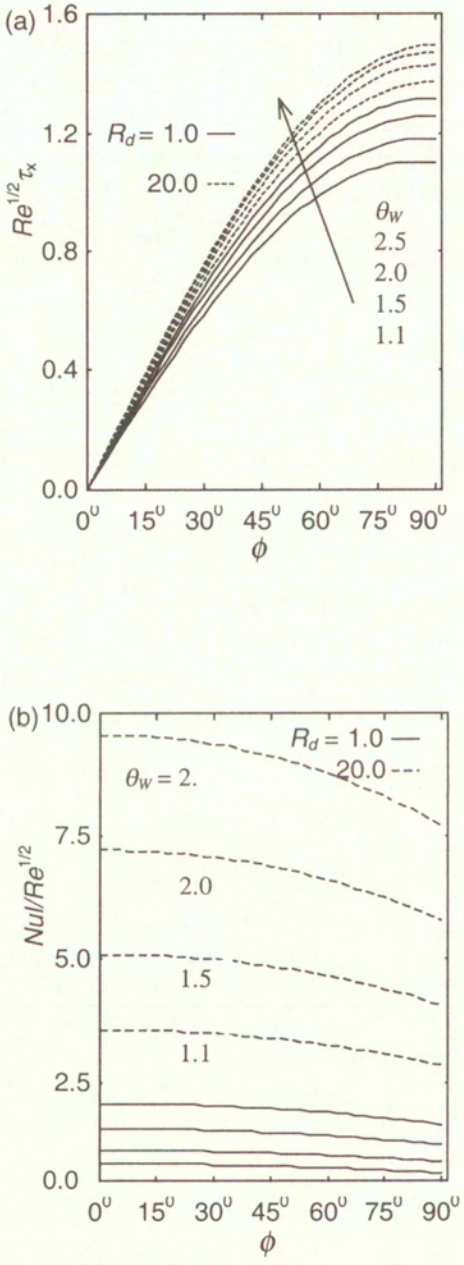


FIG. 3. Variation with $\phi$ of: (a) skin friction coefficient along the $x$-direction and (›) the local Nusselt number for some values of $R_d$ and $\theta_w$ with $Pr = 0.7$ and $\lambda = 0.1$

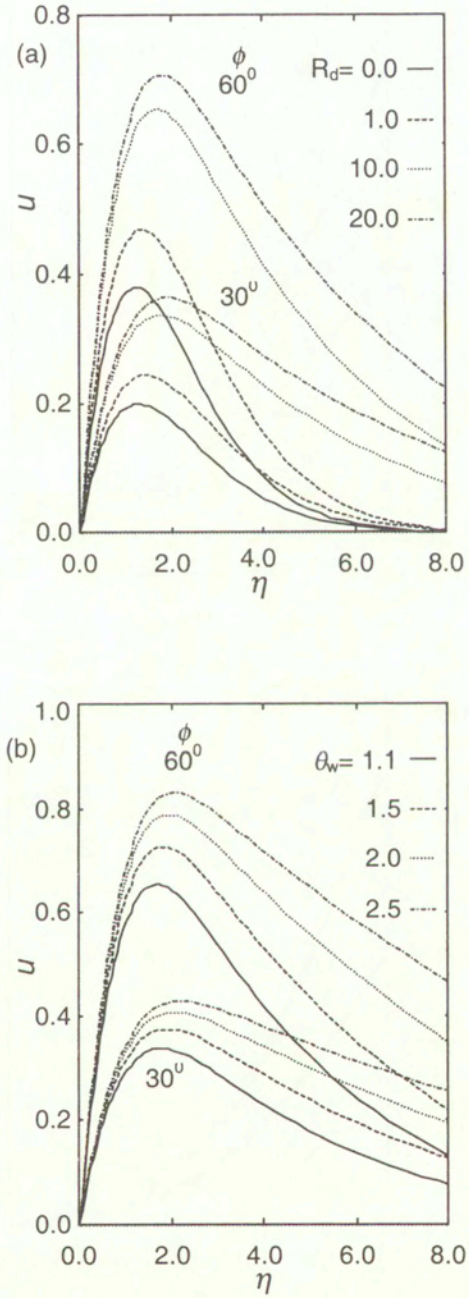


FIG. 4. Non-dimensional velocity profiles $u$ at $\phi = 30°$ and $60°$ with $Pr = 0.72$ and $\lambda$ =1.0: (a) for some values of $R_d$ with $\theta_w = 1.1$, and (b) for some values of $\theta_w$ with $R_d$= 10.0.

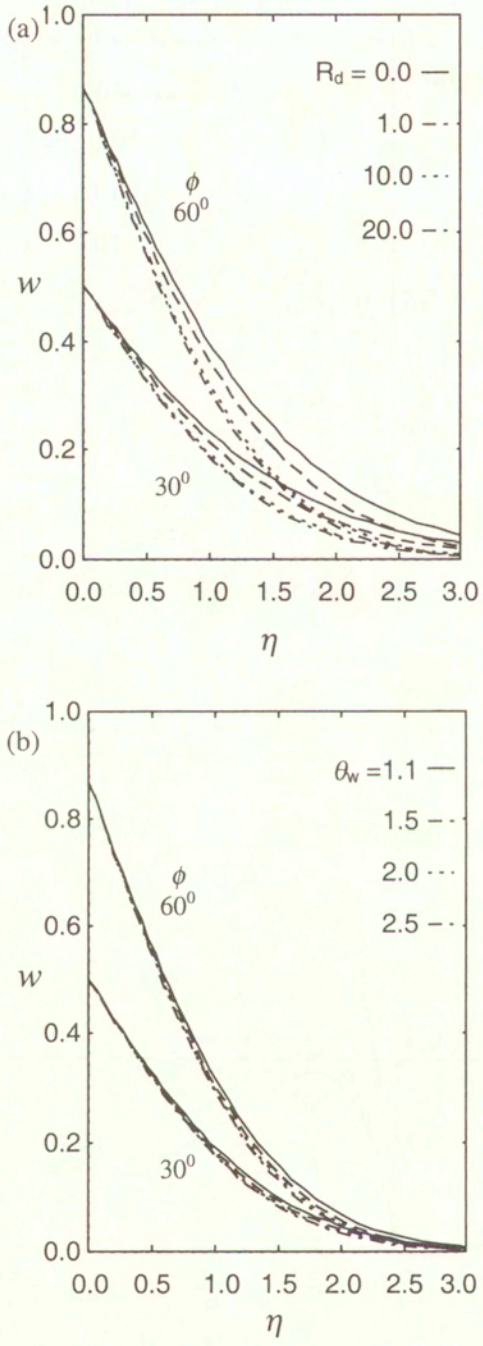


FIG. 5. Non-dimensional velocity profiles $w$ at $\phi = 30°$ and $60°$ with $Pr = 0.72$ and $\lambda$ =1.0: (a) for some values of $R_d$ with $\theta_w = 1.1$, and (b) for some values of $\theta_w$ with $R_d$= 10.(

The functions $P(x)$ and $Q(x)$ in Eqs. (4.6) – (4.11) were defined in the relations (3.6) and the other coefficients $P_1(x)$, $Q_1(x)$, $I_1(x)$ and $I_2(x)$ are given by

$$P_1(x) = \frac{4(\cos x - 1)^3}{3\sin^5 x},$$

$$Q_1(x) = 0.5926\frac{\left(\cos^4 x - 6\cos^2 x + 8\cos x - 3\right)}{2\sin^4 x},$$

(4.13)

$$I_1(x) = \frac{3\left(\cos^3 x - 3\cos x + 2\right)}{2\sin^3 x},$$

$$I_2(x) = \frac{dI_1}{dx} = \frac{9}{2}\frac{(\cos x - 1)^2}{2\sin^3 x}.$$

Equations (4.6) – (4.11) are coupled and highly nonlinear. The numerical solution of these equations has been obtained for some values of the involved parameters $\lambda$, $R_d$, $\theta_w$ and $Pr$ using the Nachsteim-Swigert iteration technique together with the sixth order Runge-Kutta-Butcher, initial value solver, see HOSSAIN *et al.* [16-19].

## 5. Results and discussions

Here we discuss the effects of thermal radiation on free convection boundary-layer flow characteristics of an optically dense fluid in a rotating hemisphere by two distinct methods, namely, the Keller-box method and the local nonsimilarity scheme with second level of truncation, respectively. The numerical results for the velocity components $u$ and $w$ along the $x$- and $z$-directions as well as for the local skin-friction coefficient $Re^{1/2}\tau_x$ in the $x$-direction and the local Nusselt number $Nu/Re^{1/2}$, are obtained for some values of the involved parameters $\lambda$, $R_d$ and $\theta_w$ for a heated surface only ($T_w > T_\infty$) with $Pr = 0.72$. It should be noted that for both $CO_2$ – air in the temperature range $100 \approx 650°F$ (with the corresponding Prandtl number range $0.76 \approx 0.6$) and $NH_3$ – vapor in the temperature range $120 \approx 400°F$ (with corresponding Prandtl number range $0.88 \approx 0.84$) at 1 atm, the value of the parameter $R_d$ varies approximately from 10 to 30; whereas for water vapor in the temperature range $220 \approx 900°F$ (with the corresponding Prandtl number $Pr \approx 1.0$), the value of $R_d$ lies between 30 to 200 (see CESS [14]).

As we have mentioned before, in the absence of the effect of conduction-radiation (i.e., $R_d = 0$), the present problem has been studied by SUWONO [12] using Görtler's series expansion method. He showed the effect of the buoyancy parameter $\lambda$ on the flow and heat transfer characteristics at some selected values of $\phi$-positions in the interval $[0, \pi/2]$. Comparison between the present and

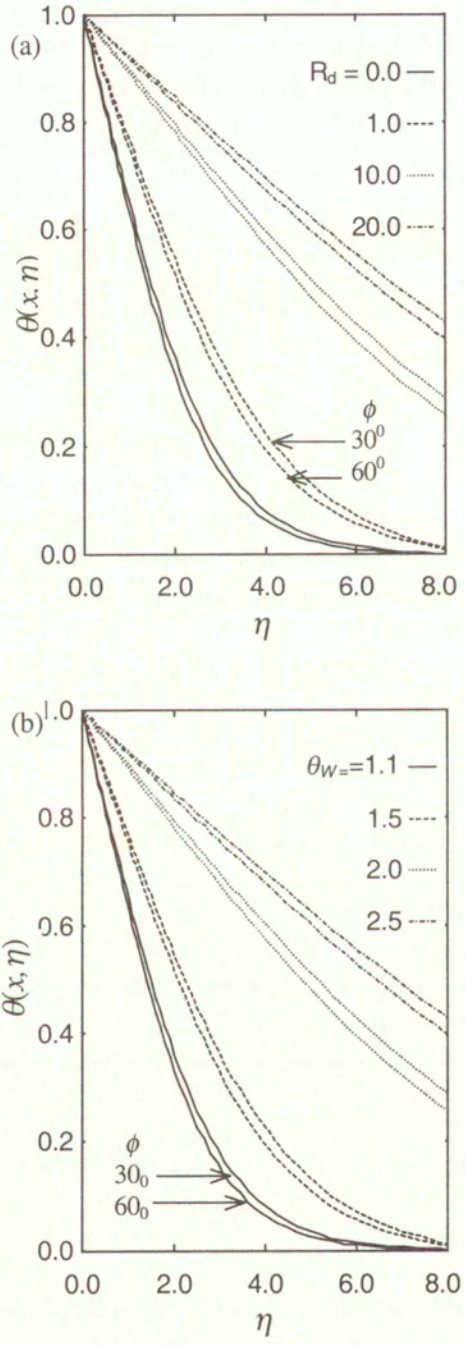


FIG. 6. Non-dimensional temperature profiles $\theta$ at $\phi = 30°$ and $60°$ with $Pr = 0.72$ and $\lambda$ =1.0: (a) for some values of $R_d$ with $\theta_w = 1.1$ and (b) for some values of $\theta_w$ with $R_d$= 10.0.

Suwono's results, interval $[0, \pi/2]$ obtained in terms of the local skin friction coefficient in the $x$-direction $Re^{1/2}\tau_x$ and the local Nusselt number $Nu/Re^{1/2}$ are shown in Fig. 2 (a) and 2 (b), respectively, for the values of the buoyancy parameter $\lambda = 0.1$, 0.5 and 1.0 with $Pr = 0.72$. It can be seen from these figures that the results obtained using the, Keller-box method, are very close to those of the local nonsimilarity method. They are also in good agreement with the results reported by SUWONO [12]. However, the results obtained by the Keller-box scheme are more accurate than the other methods because this method does not require any approximation.

Further results are obtained for $R_d = 1.0$ and 20.0, but for $\theta_w = 1.1$, 1.5, 2.0, 2.5 at selected axial positions $\phi$ in the range $[0, \pi/2]$ with $\lambda = 1.0$ and $Pr = 0.7$ by the Keller-box method only. Figure 3(a) illustrates the variation of the local skin friction coefficient $\tau_x Re^{1/2}$ as a function of $\phi$, and Fig. 3(b) represents that of the local Nusselt number $NuRe^{-1/2}$ for $\theta_w = 1.1$, 1.5, 2.0, 2.5. The solid lines show the values of the mentioned physical quantities for $R_d = 1.0$, while the broken lines are those for $R_d = 20.0$. It is seen from these figures that an increase in the radiation effect leads to decrease in the local skin friction coefficient $\tau_x Re^{1/2}$. On the other hand, this leads to increase in the value of the local Nusselt number $NuRe^{-1/2}$ at every station of the angular distance $\phi$ in the range $[0, \pi/2]$. This tendency is higher for the skin friction coefficient and is less for the local Nusselt number when the value of $\phi$ increases. Further observations drawn from these figures are that values of both the local skin friction and the local Nusselt number at every $\phi$ station increase, owing to an increase of the values of the parameter $\theta_w$.

Representative velocity and temperature profiles are shown in Figs. 4 to 6 in which the non-dimensional velocity components $u$ and $w$ as well as the non-dimensional temperature profiles $\theta$ are plotted against $\eta$ for some values of the conduction-radiation parameter $R_d = 0.0$, 1.0, 10.0 and 20 and the surface temperature parameter $\theta_w$ = 1.1, 1.5 2.0 and 2.5 with $\phi$ = 30° and 60°, and the buoyancy parameter $\lambda$=1.0. It can be seen from these figures that the transverse velocity profiles u and the temperature profiles $\theta$ increase with the increase of the parameters $R_d$ and $\theta_w$ at all values of $\phi$. On the other hand, the increase in the value of the parameters $\theta_w$ and $R_d$ leads to decrease in the value of the circumferential velocity profile $w$. We also see that both the momentum and the thermal boundary layer thickness increase owing to the increase of the parameters $R_d$ and $\theta_w$. However, it is important to notice that the present results are available only for values of the angle $\phi < 90°$. For increasing values of the angle $\phi$ and, in particular, at $\phi > 90°$, the solution of the governing equations becomes unstable. Unfortunately, we are not able to compare the present results with any experimental data since we are not aware of any existing experimental results for the present problem.

## 6. Conclusions

Effect of the radiation-conduction interaction on free convection boundary-layer flow over rotating axisymmetric round-nosed bodies of uniform surface temperature of a gray, absorbing-emitting but nonscattering fluid medium with Rosseland approximation, has been analyzed. The nonsimilarity equations governing the flow and heat transfer have numerically been solved employing the implicit finite difference method known as the Keller-box method and the local nonsimilarity method. Solutions are obtained for different values of the pertinent parameters, such as the Planck number (radiation-conduction parameter) $R_d$, the surface temperature parameter $\theta_w$ and the buoyancy parameter $\lambda$. From the present investigation, the following conclusions may be drawn:

(i) Increase in the radiation parameter $R_d$ leads to decrease of the local skin friction coefficient $\tau_x Re^{1/2}$

(ii) The rate of heat transfer $Nu/Re^{1/2}$ increases owing to the increase of the parameters $\mathrm{R}_d$ and $\theta_w$

(iii) Both the tangential velocity u and the temperature $\theta$ profiles of the fluid increase, whereas the circumferential velocity w profiles decrease due to the increase of either of the value of the parameter $R_d$ or $\theta_w$. Furthermore, increase of the values of the parameters $R_d$ and $\theta_w$ leads to increase in both the momentum and the thermal boundary layer thickness.

## Acknowledgements

The authors are grateful to the Referee for his valuable comments.

## References

1. W. H. BANKS, *The laminar boundary layer on a rotating sphere*, Acta Mechanica, **24,** 273-283, 1976.

2. L. A. DORFMAN and V. A. MIRNOVA, *Solutions of equations for the thermal boundary layer at rotating axisymmetric surface*, Int. J. Heat Mass Transfer, **13,** 81-92, 1970.

3. B. T. CHAO, and R. GREIF, *Laminar forced convection over rotating bodies*, Trans. ASME J. Heat Transfer, **96,** 463-466, 1974.

4. C. CREMERS and D. L. FINLEY, *Natural convection about isothermal sphere*, In: Fourth Int. Heat Transfer Conference, Paris-Versailles , **4**, Paper No. 1.5, Elsevier, Amsterdam 1970.

5. M. H. LEE, D. R. JENG and K. G. DE WITT, *Laminar boundary layer transfer over rotating bodies in forced flow*, Trans. ASME J. Heat Transfer, **100,** 496-502, 1978.

6. A. A. KRANSE and J. SCHENK, *Thermal free convection from a solid sphere*, Appl. Sci. Res. **A15**, 397-403, 1966.

7. T. CHIANG, A. OSSIN and C. L. TIEN, *Laminar free convection from a sphere*, Trans. ASME J. Heat Transfer, **84**, 537-542, 1964.

8. T. S. CHEN and A. MUCOGLU, *Analysis of mixed, forced and free convection about a sphere*, Int. J. Heat Mass Transfer, **20**, 867-875, 1977.

9. A. MUCOGLU and T. S. CHEN, *Mixed convection about a sphere with uniform surface heat flux*, Trans. ASME J. Heat Transfer, **100**, 542-544, 1978.

10. H. J. MERCK, *Rapid calculation for boundary layer transfer for wedge solutions and asymptotic expansions*, J. Fluid Mech., **5**, 460-480, 1959.

11. B. T. CHAO and R. O. FAGBENLE, *On Merk's method of calculating boundary layer transfer*, Int. J. Heat Mass Transfer, **17**, 223-240, 1974.

12. A. SUWONO, *Buoyancy effects on flow and heat transfer on rotating axisymmetric round-nosed bodies*, Int. J. Heat Mass Transfer, **23**, 819-831, 1980.

13. M. A. HOSSAIN, S. K. DAS and I. POP, *MHD free convection flow near rotating axisymmetric round-nosed bodies*, Magnitnaya Gidrodinamika, **2**, 68-73, 1996.

14. R. D. CESS, *Interaction of thermal radiation with free convection heat transfer*, Int. J. Heat Mass Transfer, **9**, 1269-1277, 1966.

15. V. S. ARPACI, *Effect of thermal radiation on the laminar free convection from a heated vertical plate*, Int. J. Heat Mass Transfer, **11**, 871-881, 1968.

16. E. H. CHENG and M. N. OZISIK, *Radiation with free convection in an absorbing, emitting and scattering medium*, Int. J. Heat Mass Transfer, **15**, 1243-1252, 1972.

17. S. HASEGAWA, R. ECHIGO and K. FAKUD, *Analytic and experimental studies on simultaneous radiative and free convective heat transfer along a vertical plate*, Proc. Japanese Soc. Mech. Engng., **38** 2873-2883, 1972 and **39**, 250-257, 1973.

18. J. D. BANKSTON, J. R. LOYD and J. L. NOVOTNY, *Radiation convectioninteraction in an absorbing-emitting liquid in natural convection boundary layer flow*, Trans. ASME J. Heat Transfer, **99**, 125-127, 1977.

19. E. M. SPARROW and R. D. CESS, *Radiation heat transfer-augmented media*, Int. J. Heat Mass Transfer, **5**, 179-806, 1962.

20. R. D. CESS, *The interaction of thermal radiation in boundary layer heat transfer*, [in:] Proc. Third Int. Heat Transfer Conference, **5**, 154-163, 1966.

21. M. A. HOSSAIN and H. S. TAKHAR, *Radiation effect on mixed convection along a vertical plate with uniform surface temperature*, Heat and Mass Transfer, **31**, 243-248, 1966.

22. M. A. HOSSAIN, D. A. S. REES and I. POP, *Free convection-radiationinteraction from an isothermal plate inclined at a small angle to the horizontal*, Acta Mechanica, **127**, 63-73, 1998.

23. M. A. HOSSAIN and M. A. AALIM, *Natural convection-radiation interaction on boundary layer flow along a thin vertical cylinder*, Heat and Mass Transfer, **32**, 515-520, 1997.

24. T. CEBECI and P. BRADSHAW, *Physical and computational aspects of convective heat transfer*, Springer, New York 1994.

25. R. SIEGEL and J. R. HOWEL, *Thermal radiation heat transfer*, McGraw-Hill, New York 1987.

26. M. M. ALI, T. S. CHEN and B. F. ARMALY, *Natural convection-radiation interaction in boundary layer flow over horizontal surface*, AIAA J., **22**, 1797-1803, 1984.

27. E. M. SPARROW and H. S. YU, *Local non-similarity boundary layer solutions*, Trans. ASME J. Heat Transfer, **93**, 328-334, 1971.

28. M. A. HOSSAIN, N. BANU and A. NAKAYAMA, *Non-Darcy forced convection boundary layer flow over a wedge embedded in a saturated porous medium*, Num. Heat Transfer, Part A **26**, 399-414, 1994.

*Received August 22, 1991; revised version January 6, 2002.*

Arch. Mech., **54**, 1, pp. 75–91, Warszawa 2002

# Deformation behavior of TiNi shape-memory alloy under strain- or stress-controlled conditions

H. TOBUSHI [1], K. OKUMARA [1], M. ENDO [1] and K. TANAKA [2]

[1] *Department of Mechanical Engineering,*
*Aichi Institute of Technology*
*1247 Yachigusa, Yagusa-cho, Toyota 470-0392, Japan*
*e-mail : tobushi@me.aitech.ac.jp*

[2] *Department of Aerospace Engineering,*
*Tokyo Metropolitan Institute of Technology*
*Asahigaoka 6-6, Hino, Tokyo, 191-0065, Japan*

THE DEFORMATION PROPERTIES of TiNi shape-memory alloy subjected to strain control and stress control were investigated experimentally. The results obtained are summarized as follows. (1) In the case of a full loop, the stress-strain curves under stress-controlled conditions are similar to those under strain-controlled conditions with high strain rate. The overshoot and undershoot do not appear at the start points of the stress-induced martensitic transformation in these curves. (2) In the case of subloop under stress-controlled conditions, temperature decreases and therefore the strain increases owing to the martensitic transformation at the early stage of the unloading process. At the early stage in the reloading process, temperature increases and therefore the strain decreases owing to the reverse transformation. (3) In the case of subloop under stress-controlled conditions, the starting stresses of the martensitic transformation and the reverse transformation in the loading and unloading processes coincide with the transformation stresses under strain-controlled conditions with low strain rate, respectively. (4) The deformation behaviours for a subloop under stress-controlled conditions are prescribed by the condition for progress of the martensitic transformation based on the transformation kinetics. (5) The deformation behaviors subjected to cyclic loading under stress-controlled conditions at constant temperature are also prescribed by the conditions for progress of the martensitic transformation.

**Key words:** Shape Memory Alloy, Titanium-Nickel Alloy, Stress-Induced Martensitic Transformation, Superelasticity, Strain-Controlled Conditions, Stress-Controlled Conditions, Subloop, Transformation Kinetics

## 1. Introduction

IN A SHAPE-MEMORY alloy (SMA), the shape-memory effect (SME) and superelasticity (SE) appear [1-4]. The strain of 6-8% is recovered by heating in SME and is recovered by unloading in SE. In both cases, strain appears owing to the stress-induced martensitic transformation (SIMT) in the loading process and disappears due to the reverse transformation by heating or unloading.

The recovery stress and recovery strain of SMA which appear due to SIMT are applied to working elements of actuators, robots and solid-state heat engines. In these applications of SMA, the deformation properties of the material are important. The deformation properties due to SIMT vary, depending on temperature and strain rate [5-6]. The basic deformation modes are strain-controlled and stress-controlled conditions. The difference in deformation behaviors between both conditions was reported recently [7]. Most deformation behaviors have been investigated under strain-controlled conditions till now, but few behaviors under the stress-controlled conditions. In the case of subloop under stress-controlled conditions, the SIMT starting stress in the subsequent reloading process does not coincide with the stress from which partial unloading started [7]. In the case of strain variation during SIMT, the thermomechanical state varies due to SIMT. Therefore the progress of deformation due to SIMT cannot be prescribed only by the mechanical condition. Since SMA elements work repeatedly, the cyclic deformation properties of SMA are particularly important [8-9].

In the present study, by the tensile test under strain-controlled and stress-controlled conditions, the deformation behaviours of TiNi SMA subjected to various strain rates, cyclic loading and various strain variations are investigated. The thermomechanical condition for the progress of SIMT is discussed basing on the constitutive equation of the material. The difference in deformation behavior between strain-controlled condition and stress-controlled condition is considered. The subsequent strain variation after cyclic deformation is discussed.

## 2. Condition for progress of martensitic transformation

In the present study, the deformation behavior of SMA due to martensitic transformation (MT) is discussed basing on the condition for progress of MT. The constitutive relationships proposed by Tanaka [10, 11] are as follows. The constitutive equation is

$$\dot{\sigma} = D\dot{\varepsilon} + \Theta\dot{T} + \Omega\dot{\xi} \tag{2.1}$$

and the transformation kinetics for the MT is

$$\frac{\dot{\xi}}{1-\xi} = b_M C_M \dot{T} - b_M \dot{\sigma} \geq 0 \tag{2.2}$$

or, for the reverse transformation,

$$-\frac{\dot{\xi}}{\xi} = b_A C_A \dot{T} - b_A \dot{\sigma} \geq 0 \tag{2.3}$$

where $\sigma, \varepsilon$ and $T$ represent the stress, strain and temperature, respectively. The coefficients $D$ and $\Theta$ represent the modulus of elasticity and the thermoelastic constant, respectively. $\xi$ represents the volume fraction of the martensitic (M) phase. Therefore, volume fraction of the parent phase is 1–$\xi$. The dot over the symbol denotes the time derivative. The material parameters $b_M$, $C_M$, $b_A$ and $C_A$ are determined from expriments. Equation (2.2) is applied to the MT and Eq. (2.3) to the reverse transformation.

If these equations are integrated by assuming these parameters to be constant, Eq. (2.2) and Eq. (2.3) become respectively as follows:

$$\xi = 1 - \exp\{b_M C_M (Ms - T) + b_M \sigma\}, \tag{2.4}$$

$$\xi = \exp\{b_A C_A (As - T) + b_A \sigma\}, \tag{2.5}$$

where $M_S$ and $A_S$ stand for the temperatures at which the MT and the reverse transformation start under the stress-free conditions. From Eq. (2.4), the MT starting and completing lines become as follows:

$$\sigma = C_M (T - M_s), \tag{2.6}$$

$$\sigma = C_M (T - M_s) - 2 \ln 10 / b_M, \tag{2.7}$$

and are expressed by the straight lines with a slope of $C_M$. From Eq. (2.5) the reverse-transformation starting and completing lines become as follows:

$$\sigma = C_A (T - A_s), \tag{2.8}$$

$$\sigma = C_A (T - A_s) - 2 \ln 10 / b_A, \tag{2.9}$$

and are expressed by the straight lines with a slope of $C_A$. On deriving Eqs. (2.7) and (2.9) we have assumed that the transformation is completed when the fraction of induced phase reaches 0.99. The transformation lines and the transformation region are prescribed by Eqs. (2.6)-(2.9). If they are drawn on the stress-temperature plane shown in Fig. 1, Eqs. (2.6)-(2.9) are expressed respectively by the straight lines $M_S$, $M_F$, $A_S$ and $A_F$, and each transformation progresses in the transformation strip between the starting line and the completing line.

From Eq. (2.2), the condition for progress of the MT becomes as follows:

$$b_M C_M \dot{T} \geq b_M \dot{\sigma}, \quad b_M < 0$$

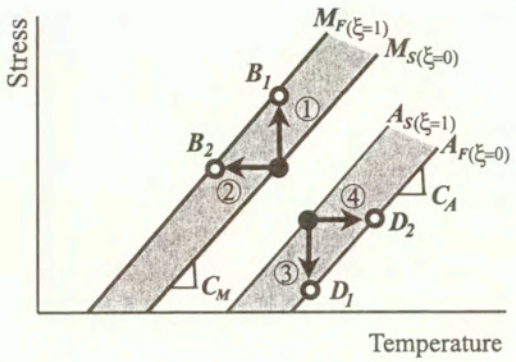


FIG. 1. Transformation lines.

and therefore

$$\begin{aligned} &\frac{d\sigma}{dT} \geq C_M \quad \text{for} \quad dT > 0, \\ &\frac{d\sigma}{dT} \leq C_M \quad \text{for} \quad dT < 0. \end{aligned} \tag{2.10}$$

From Eq. (2.3), the condition for progress of the reverse transformation becomes as follows:

$$b_A C_A \dot{T} \geq b_A \dot{\sigma}, \quad b_A > 0$$

and therefore

$$\begin{aligned} &\frac{d\sigma}{dT} \leq C_A \quad \text{for} \quad dT > 0, \\ &\frac{d\sigma}{dT} \geq C_A \quad \text{for} \quad dT < 0. \end{aligned} \tag{2.11}$$

The MT progresses if the condition (2.10) is satisfied and the reverse transformation progresses if the condition (2.11) is satisfied. Both transformations progress in the transformation strips which are shadowed on the stress-temperature plane in Fig. 1. For example, in the case of loading or unloading from points $A$ or $C$ at constant temperature, the loading path ① or unloading path ③ satisfies the conditions (2.10) or (2.11) and each transformation progresses along the path. In the case of heating or cooling under constant stress, the MT progresses along the cooling path ② and the reverse transformation along the heating path ④.

The conditions for progress of the phase transformation in the subloop during the phase transformation are shown in Fig. 2. The points $A$ and $C$ in Fig. 2(a)

represent respectively the progressing state of the MT and the reverse transformation, and the volume fractions of the M-phase at each point are $\xi_A$ and $\xi_C$. The dashed lines $M_m$ and $A_m$ denote the states with the volume fractions $\xi_A$ and $\xi_C$, respectively. The conditions for progress of the transformation prescribed by Eq. (2.10) and Eq. (2.11) mean that stress and temperature vary from the points $A$ and $C$ to the directions shown by the arrows in Fig. 2(a).

The conditions for progress and stop of the subsequent transformation are shown in Fig. 2(b). In Fig. 2(b), the MT progress in the loading path ① and unloading path ② and stops in the unloading path ③. The reverse transformation progresses in the unloading path ④ and loading path ⑤ and stops in the loading path ⑥.

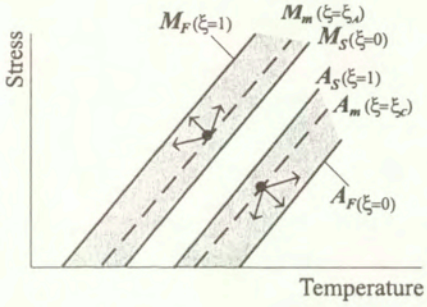


(a) Path for progress of phase transformation

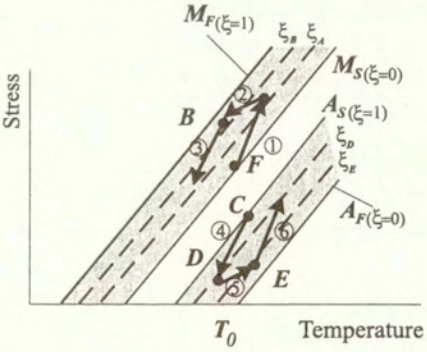


(b) Path for progress and stop pf phase transformation

FIG. 2. Conditions for progress of phase transformation in the subloop during phase transformation.

## 3. Experimental method

### 3.1. Materials and specimen

The material was a Ti-55.4wt%Ni SMA wire, 0.75mm in diameter. The specimens were given the shape memory of a straight line through shape memory processing. This was carried out by holding the wires in the straight line at 673K for 60 min and then cooling in a furnace. The specimens were straight lines with uniform cross-sections. The reverse-transformation completion temperature $A_f$ was about 323K.

### 3.2. Experimental apparatus

The experimental apparatus was an SMA property testing machine composed of a tensile machine and a heating-cooling device [12]. Temperature was measured with a thermocouple, 0.1mm in diameter, on the surface in the central part of the specimens. Displacement and load were measured with an extensometer of 20mm gauge length and a load cell, respectively.

### 3.3. Experimental procedure

The following five experiments were performed.

1. Exp. I: Dependence on the rate
   Tensile tests under constant rate were carried out at test temperature $T_0 = 353$K for maximum strain $\varepsilon_m = 8\%$. Strain rates $\dot{\varepsilon}$ were 1 and 10%/min, and stress rates $\dot{\sigma}$ were 1 and 10MPa/s.
2. Exp. II: Cyclic full-loop behavior
   Loading, and unloading were repeated 100 times at test temperature $T_0 = 353$K for maximum strain $\varepsilon_m = 8\%$. Strain rate $\dot{\varepsilon}$ was 1%/min and stress rate $\dot{\sigma}$ was 30MPa/s.
3. Exp. III: Subloop behavior
   Loading and unloading under subloop were carried out at test temperature $T_0 = 353$K. Strain rate $\dot{\varepsilon}$ was 10%/min and stress rates $\dot{\sigma}$ were 1, 10 and 30MPa/s.
4. Exp. IV: Cyclic subloop behavior
   Loading to the strain $\varepsilon_1 = 4\%$ and subsequent unloading to the strain $\varepsilon_2 = 1\%$ were repeated seven times at test temperature $T_0 = 353$K. After the cyclic deformation, loading to the maximum strain $\varepsilon_m = 8\%$ was performed. Stress rate $\dot{\sigma}$ was 30MPa/s.
5. Exp. V: Subloop behavior after cyclic deformation
   After cyclic deformation to maximum strain $\varepsilon_m = 8\%$ (100 times), loading and unloading under subloop were performed at the test temperature $T_0 = 353$K. Stress rates were 1 and 30MPa/s.

## 4. Experimental results and discussion

In performing the experiment and dealing with the experimental data, stress and strain were treated in terms of nominal stress and nominal strain, respectively. Therefore the stress-controlled and strain-controlled conditions mean the load-controlled and displacement-controlled conditions, respectively.

### 4.1. Deformation behavior under strain- and stress-controlled conditions

In order to investigate the dependence of SIMT on the rate under strain-controlled and stress-controlled conditions, Exp. I was performed. The stress-strain curves obtained by Exp. I are shown in Fig. 3.

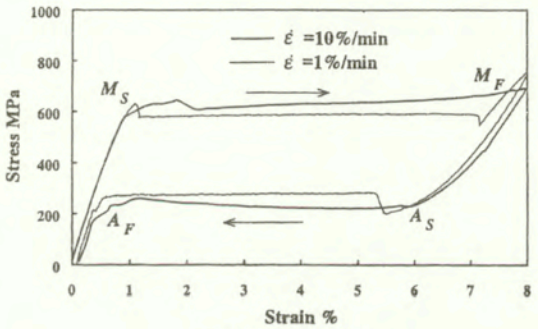


(a) Strain-controlled

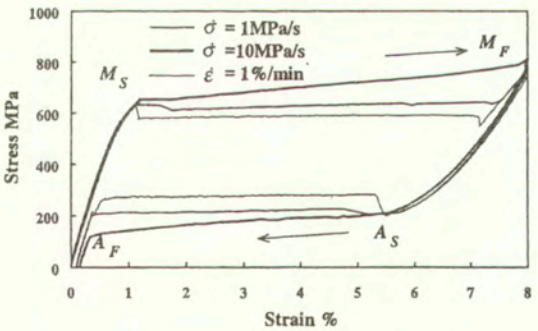


(b) Stress-controlled and strain-controlled

FIG. 3. Stress-strain curves under various strain rates and stress rates.

As seen in Fig. 3(a), in the case of low strain rate $\dot{\varepsilon}$ under strain-controlled condition, an overshoot appears at the point $M_s$ and an undershoot at the point $A_s$. On the other hand, in the case of high strain rate, the overshoot and undershoot do not appear. In the case of low strain rate, the interface between the M-phase

and the parent phase moves under constant stresses which are expressed by stress plateaus following the points $M_s$ and $A_s$. At the points $M_s$ and $A_s$, an excessive energy is necessary to create a nucleus of the induced phase compared with the movement of the interface, and therefore an overshoot and an undershoot appear. The MT is exothermic and the reverse transformation is endothermic. In the case of low strain rate, heat generated by SIMT in the interface is radiated and therefore the temperature does not increase. On the contrary, in the case of high strain rate, because the interface at the temperature increased by SIMT moves, temperature of the material increases during the MT and therefore the MT stress increases. In the case of reverse transformation, the higher the strain rate, the larger is the decrease in temperature, resulting in decrease in the transformation stress. Basing on these reasons, the overshoot and undershoot do not appear in the case of high strain rate.

As it is seen in Fig. 3(b), both the overshoot and undershoot do not appear under the stress-controlled condition. This is due to the stress-controlled condition that stress increases in the loading process and decreases in the unloading process. In this case, the MT and the reverse transformation start respectively under the same stresses as those at the starting points $M_s$ and $A_s$ for a low strain rate. Because the amount of variation in stress is small in the transformation region, the deformation (strain) rate becomes high, resulting in the same deformation behavior as that under high strain rate.

### 4.2. Cyclic deformation property

The stress-strain curves obtained by Exp. II are shown in Fig. 4. The curves are parameterized by the number of cycles $N$. As it can be seen in Fig. 4(a) for the strain-controlled conditions, the MT stress decreases and residual strain increases with an increase in $N$. Both the rate of decrease in the MT stress and the rate of increase in residual strain decrease with an increase in $N$. The MT stress and residual strain have the inclination to satulate a certain value. It is ascertained by the previous study [13] under strain-controlled condition that dislocations accumulate around the infinitesimal defects in the material with cyclic deformation and both the internal stress and residual strain appear. These cyclic deformation properties under strain-controlled condition are also observed in the case of stress-controlled condition, as shown in Fig. 4(b). In the case of strain-controlled condition, both the overshoot and undershoot diminishes with an increase in $N$. Therefore, after a certain number of cycles, the deformation behavior under the stress-controlled condition becomes similar as that under the strain-controlled condition [14] except for the difference in the slope of the stress-strain curve in the transformation region.

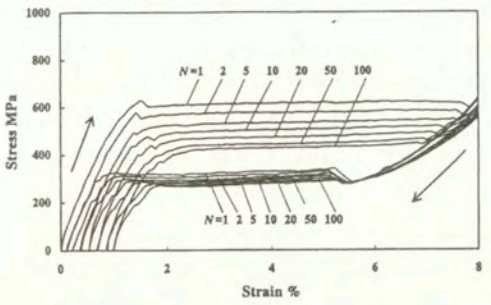


(a) $\dot{\varepsilon}$=1%/min

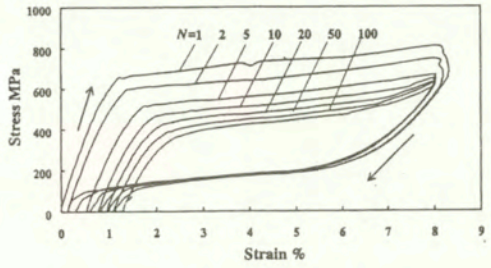


(b) $\dot{\sigma}$=30MPa/s

FIG. 4. Stress-strain curves under cyclic loading.

### 4.3. Deformation behavior in subloop

**4.3.1. Deformation behavior under strain-controlled conditions.** The stress-strain curves obtained by Exp. III under strain-controlled conditions are shown in Fig. 5. In Fig. 5, the path from point $A_i$ to point $D_i$ denotes the unloading process and the path from point $D_i$ to point $A_{i+1}-$ the reloading process. As seen in Fig. 5, in the unloading process, strain decreases owing to elastic deformation between the points $A_i$ and $C_i$, and owing to the reverse transformation between the points $C_i$ and $D_i$. In the reloading process, strain increases owing to elastic deformation between the points $D_i$ and $F_i$, and owing to the MT between the points $F_i$ and $A_{i+1}$. The stress $\sigma_A$ at the start points $C_1$ and $C_2$ of the reverse transformation coincides with the stress of the plateau in $N$=1 under strain rate $\dot{\varepsilon}$=1%/min. The stress $\sigma_M$ at the start points $F_1$ and $F_2$ of the MT coincides with the stress of the plateau in $N$=2 under $\dot{\varepsilon}$=1%/min. Therefore the starting stresses of the MT and the reverse transformation in the subloop are prescribed by the transformation stresses under low strain rate. In the case of unloading from a point $A_1$, stress returns to the point $A_1$ and the MT progresses on the curve which is extended from the initial loading curve. This phenomenon appears as follows. In the initial

loading, the MT progresses to the region which corresponds to the point $A_1$. In the reloading after the point $A_1$, the MT progresses in the non-transformed region under the stress level in $N$=1. The SIMT starting stress in the subsequent reloading process coincides with the stress from which partial unloading starts in the case of low strain rate [15]. This phenomenon is pointed out as the return-point memory effect [7] and is observed for plastic deformation.

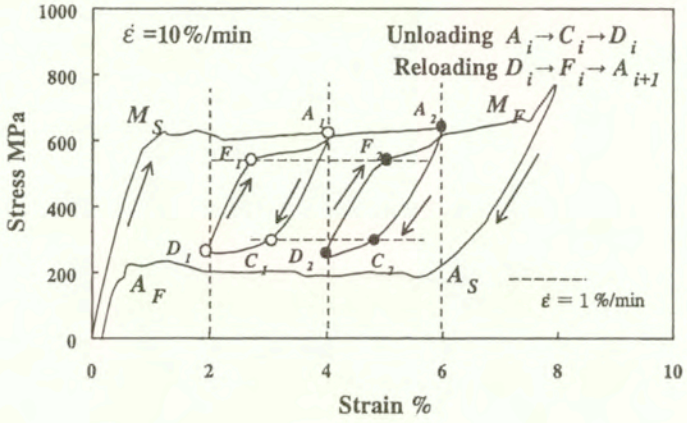


FIG. 5. Stress-strain curves for subloop under strain-controlled conditions.

**4.3.2. Deformation behavior under stress-controlled conditions.** The stress-strain curves obtained by Exp. III under stress-controlled condition are shown in Fig. 6. In Fig. 6, the path from a point $A_i$ to a point $D_i$ denotes the unloading process and the path from a point $D_i$ to $A_{i+1}$– the reloading process. As seen in Fig. 6, in the unloading process of the subloop, strain increases between the points $A_i$ and $B_i$ and decreases owing to elastic deformation between the points $B_i$ and $C_i$, and the curve between the points $C_i$ and $D_i$ is almost parallel to the reverse transformation curve in full loop. The smaller is the strain at a point $A_i$ and the lower is the stress rate $\dot{\sigma}$, the larger will be the amount of strain increment between the points $A_i$ and $B_i$. In the reloading process, strain decreases between the points $D_i$ and $E_i$ and increases owing to elastic deformation between the points $E_i$ and $F_i$, and the curve between the points $F_i$ and $A_{i+1}$ is almost parallel to the initial MT curve. The stresses at a point $F_1$ and a point $F_2$ do not depend on $\dot{\sigma}$ and are equal to the stress $\sigma_M$ of the MT plateau in $N$=2 under the strain-controlled conditions with a low strain rate. The stresses at a point $C_1$ and a point $C_2$ do not depend on $\dot{\sigma}$ and are equal the stress $\sigma_A$ of the reverse transformation plateau under strain-controlled condition with low strain rate.

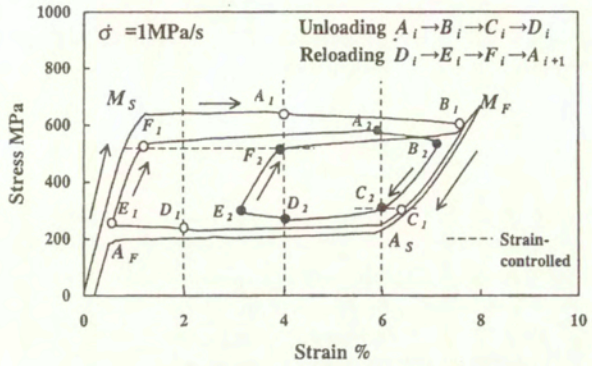


(a) $\dot{\sigma}$ =1MPa/s

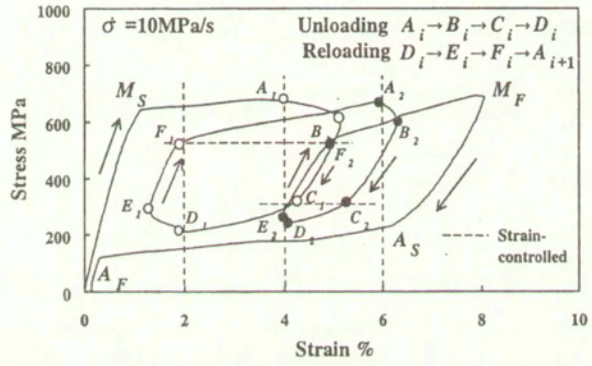


(b) $\dot{\sigma}$ =10MPa/s

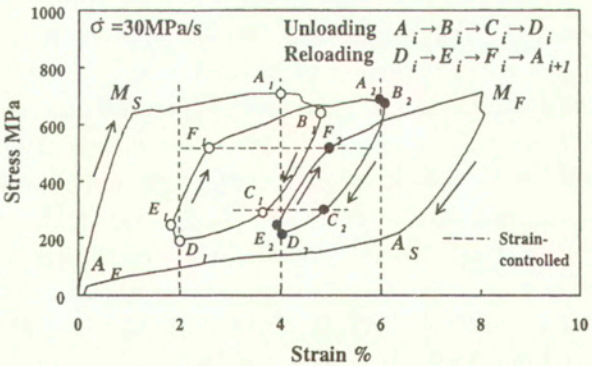


(c) $\dot{\sigma}$ =30MPa/s

FIG. 6. Stress-strain curves for subloop under stress-controlled conditions.

The variation in temperature during subloop under $\dot{\sigma}$=1MPa/s in Exp. III is shown in Fig. 7. In Fig. 7, the abscissa axis expresses the accumulated strain path $S$. $S$ is determined by the following equation:

$$S = \int |d\varepsilon/dt|\, dt \tag{4.1}$$

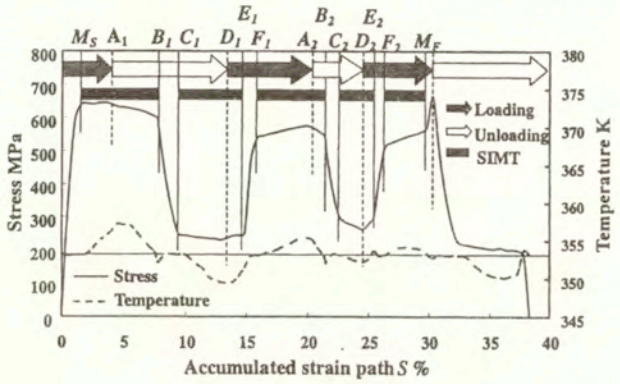


FIG. 7. Temperature variation for subloop under stress-controlled conditions.

where $t$ denotes time. In Fig. 7, variation in stress is shown simultaneously. The symbols $A_i \sim F_i$ in Fig. 7 correspond to those in Fig. 6. As seen in Fig. 7, temperature increases between the points $F_i$ and $A_{i+1}$ in the loading process, decreases between the points $A_i$ and $B_i$ in the unloading process and returns to the ambent temperature at point $B_i$. Temperature decreases between the points $C_i$ and $D_i$ in the unloading process, increases between the points $D_i$ and $E_i$ in the loading process and returns to the ambient temperature at point $E_i$. Temperature does not vary during elastic deformation. Temperature variation $\Delta$T from a point $A_1$ to a point $B_1$ is –4K. From the experiment performed under various strain rates, temperature rise measured with a thermocouple pressed on the surface of a wire, 0.75mm in diameter, is about 4K [6], and the temperature rise on the surface of a ribbon measured with an infrared thermograph is about 20K [16]. Therefore, the actual temperature variation $\Delta$T from point $A_1$ to point $B_1$ is about –20K. Stress variation $\Delta\sigma$ from point $A_1$ to point $B_1$ is –35MPa. The slope of the MT line $C_M$ of TiNi SMA is 6.13MPa/K. Therefore the condition for progress of MT prescribed by Eq. (2.10) is satisfied between the points $A_1$ and $B_1$. From this fact it follows that MT progresses and strain increases between the points $A_1$ and $B_1$ in the unloading process. In the similar manner, from Eqs. (2.10) and (211) which prescribe the condition for progress of MT and the reverse transformaton,

it follows that MT progresses between the points $F_i$ and $A_{i+1}$ and between the points $A_i$ and $B_i$, and the reverse transformation progresses between the points $C_i$ and $D_i$ and between the points $D_i$ and $E_i$.

Basing on the above-mentioned discussion, the path under the stress-controlled condition on the stress-temperature plane is shown in Fig. 8.

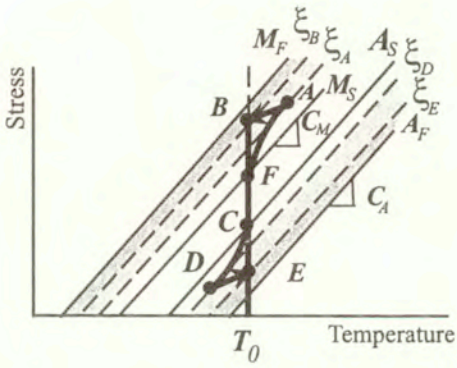


FIG. 8. Stress-temperature path in subloop under stress-controlled conditions.

The symbols $A \sim$F in Fig. 8 correspond to those in Figs. 2, 6 and 7. As seen from Figs. 2, 6, 7 and 8, MT starts at the point $M_s$ and progresses to the point $B_1$ in the unloading process through the unloading start point $A_1$. The reverse transformation starts at the point $C_1$ and progresses to the point $E_1$ through the reloading start point $D_1$. Because MT in the loading process between the points $M_s$ and $A_1$, the points $F_1$ and $A_2$ and the points $F_2$ and $M_F$ is the exothermic transformation, temperature of the material increases. In the unloading process between the points $A_i$ and $B_i$, because temperature increased owing to MT in the loading process returns to the ambient temperature, temperature of the material decreases. According to the decrease in temperature, MT progresses to the point $B_i$. Because the reverse transformation in the unloading process between the points $C_i$ and $D_i$ and the points $A_s$ and $A_F$ is the endothermic transformation, temperature of the material decreases. In the reloading process from the point $D_i$, because temperature decreased owing to the reverse transformation in the unloading process returns to ambient temperature, temperature of the material increases, resulting in progress of the reverse transformation to the point $E_i$.

As seen in Fig. 6, the higher is the stress rate $\dot{\sigma}$, the smaller will be the amount of variation in transformation strain between the points $A_i$ and $B_i$ and the point $D_i$ and $E_i$. This phenomenon appears according to the difference in the time necessary to reach the transformation stop points $B_i$ and $E_i$ depending on $\dot{\sigma}$. In the case of high $\dot{\sigma}$, because the time necessary to reach the transformation stop points $B_i$ and $E_i$ is short, the strain transformed during this time is small.

As seen in Fig. 6, strain increment between the points $A_1$ and $B_1$ is larger than that between the points $A_2$ and $B_2$. This phenomenon appears according to the difference in volume fraction of the M-phase at the point $A_i$. As found from Eq. (2.2), the smaller is the volume fraction of the M-phase $\xi$, the larger will be the amount of variation in $\xi$. The fraction at the point $A_1$ with strain of 4% is smaller than that at the point $A_2$ with strain of 6%. Therefore the amount of variation in $\xi$ from the point $A_1$ is larger than that from $A_2$, and larger transformation strain increment appears.

**4.3.3. Cyclic property.** The stress-strain curves obtained by Exp. IV under cyclic subloop are shown in Fig. 9. In Fig. 9, the thin curve expresses the full loop in $N$=1 under strain rate $\dot{\varepsilon}$=1%/min. The thin dashed line shows the stress at the

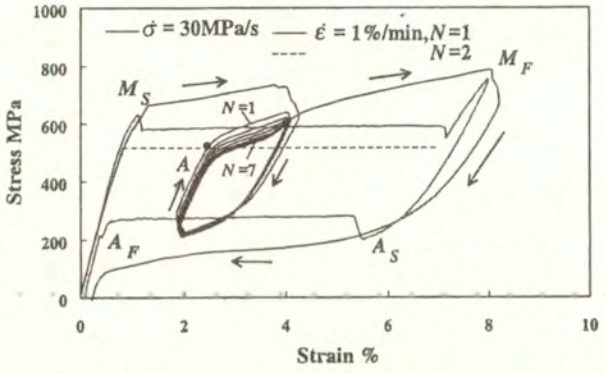


FIG. 9. Stress-strain curves for cyclic subloop.

MT plateau in $N$=2 under the same strain rate. The stress at the MT start point $A$ in the reloading process is equal to the MT stress in $N$=2 under low strain rate. At the initial MT start point $M_s$, high stress is necessary to create a nucleus of the M-phase in the parent phase. In the case of subloop, MT progresses under stress which is lower than that in the case of initial creation of a nucleus. Because the M-phase exists in the material during the subloop, MT starts under the stress in the case of low strain rate. The MT stress decreases with repeating cycles. Compared with Exp. II under cyclic full loop shown in Fig. 4, the amount of decrease in the MT stress under cyclic subloop is small. This occurs according to the fact that because the MT stress of 600MPa in subloop is lower than the MT stress of 800MPa in full loop, the dislocations generated are small and thus the internal stress is small, resulting in a small decrease in the MT stress.

**4.3.4. Deformation after cyclic loading.** The stress-strain curves obtained by Exp. V are shown in Fig. 10. In Fig. 10, the path between the points $A_i$ and $D_i$ denotes the unloading process and the path between the points $D_i$ and $A_{i+1}$– the reloading process. As seen in Fig. 10, MT starts at the point $M_s$ and progresses to the point $B_i$ through the unloading start point $A_i$. The reverse transformation

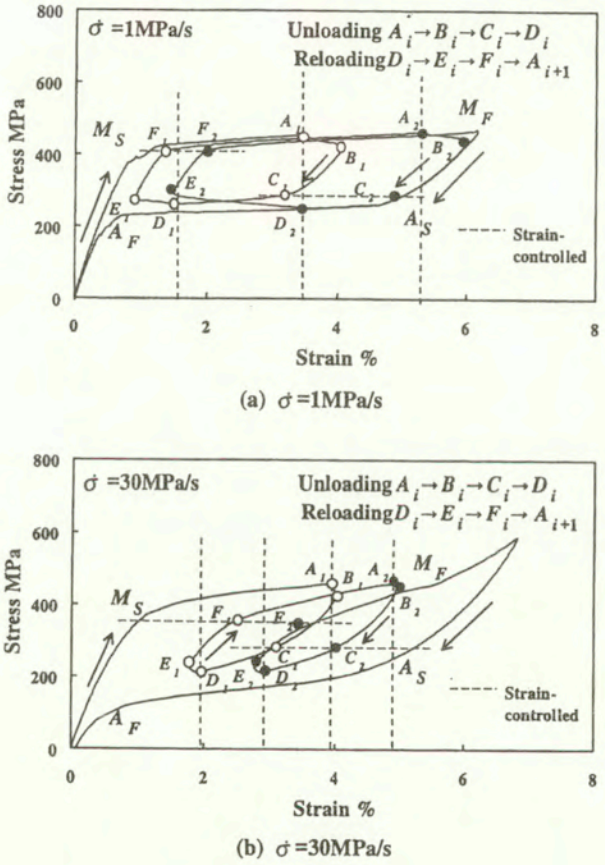


FIG. 10. Stress-strain curves under stress-controlled conditions after cyclic loading.

starts at the point $C_i$ and progresses to the point $E_i$ through the reloading start point $D_i$. As seen in Figs. 10(a) and (b), the higher is the stress rate, the higher is also the MT stress and the lower is the reverse transformation stress. This occurs according to the fact that if the stress rate is high, temperature of the material increases owing to MT, resulting in an increase in the MT stress and temperature of the material decreases owing to the reverse transformation, resulting

in a decrease in the reverse transformation stress. These deformation properties are similar to those without cyclic deformation shown in Fig. 6. In the case of subsequent subloop after cyclic loading, the condition for the transformation is stable, and therefore the stress levels at the points $M_s$ and $F_i$ and those at the points $A_s$ and $C_i$, respectively, coincide.

## 5. Conclusions

The deformation properties of TiNi SMA subjected to strain control and stress control were investigated experimentally. The results obtained are summarized as follows. (1) In the case of a full loop, the stress-strain curves under stress-controlled conditions are similar to those under strain-controlled conditions with high strain rate. The overshoot and undershoot do not appear at the start points of SIMT in these curves. (2) In the case of a subloop under stress-controlled condition, temperature decreases and therefore the strain increases owing to the martensitic transformation at the early stage in the unloading process. At the early stage in the reloading process, temperature increases and therefore the strain decreases owing to the reverse transformation. (3) In the case of subloop under stress-controlled condition, the starting stresses of MT and the reverse transformation in the loading and unloading processes coincide with the transformation stresses under strain-controlled condition with low strain rate, respectively. (4) The deformation behaviors for subloop under stress-controlled condition are prescribed by the condition for progress of MT based on the transformation kinetics. (5) The deformation behavior subjected to cyclic loading under stress-controlled condition at constant temperature is also prescribed by the condition for progress of SIMT.

## Acknowledgements

The experimental work of this study was carried out with the assistance of the students of Aichi Institute of Technology, to whom the authors wish to express their gratitude. The authors also want to extend their thanks to the Scientific Foundation of the Japanese Ministry of Education, Science, Sports and Culture for financial support.

## References

1. H. FUNAKUBO, *Shape memory alloys*, Gordon and Break Science Pub., 1987.
2. T. DUERIG, K. MELTON, D. STOCKEL and C. WAYMAN [Eds.] *Engineering aspects of shape memory alloys*, Butterworth-Heinemann, 1990.

3. K. OTUKA and C.M. WAYMANN [Eds.] *Shape memory materials*, Cambridge University Press, 1998.

4. T. SABURI [Ed.] *Shape memory materials*, Trans Tech Pub., 2000.

5. J. A. SHAW and S. KYRIAKIDES, *Thermomechanical aspects of TiNi*, J. Mech. Phys. Solids, **43**, 8, 1243-1281, 1995.

6. H. TOBUSHI, Y. SHIMENO, T. HACHISUKA and K. TANAKA, *Influence of strain rate on superelastic properties of TiNi shape memory alloy*, Mech. Mater., **30**, 141-150, 1998.

7. G. SOCHA, B. RANIECKI AND S. MIYAZAKI, *Influence of control parameters on inhomogenity and the deformation behavior of Ti-51.0at%Ni SMA undergoing martensitic phase transformation at pure tension*, 33rd Solid Mechanics Conference, 369-370, 2000.

8. H. TOBUSHI, H. IWANGA, K. TANAKA, T. HORI and T. SAWADA, *Deformation behavior of TiNi shape memory alloy subjected to variable stress and temperature*, Continuum Mech. Thermodym., **3**, 79-93, 1991.

9. K. TANAKA, F. NISIMURA, T. HAYASHI, H. TOBUSHI and C. LEXCELLENT, *Phenomenological analysis on subloops and cyclic behavior in shape memory alloys under mechanical and/or thermal loads*, Mech. Mater., **19**, 281-292, 1995.

10. K. TANAKA, S. KOBAYASHI and Y. SATO, *Thermomechanics of transformation pseudoelasticity and shape memory effect in alloys*, Inter. J. Plasticity, **2**, 59-72, 1986.

11. K. TANAKA, *A Thermomechanical sketch of shape memory effects: one-dimensional tensile behavior*, Res Mechanica, **18**, 251-263, 1986.

12. H. TOBUSHI, K. TANAKA, K. KIMURA, T. HORI and T. SAWADA, *Stress-strain-temperature relationship associated with the R-phase transformation in TiNi shape memory alloy*, JSME Inter. J., I, **35**-3, 278-284, 1992.

13. S. MIYAZAKI, T. IMAI, Y. IGO and K. OTSUKA, *Effect of cyclic deformation on the pseudoelasticity characteristics of Ti-Ni alloys*, Metall. Trans. A, **17A**, 115-120, 1986.

14. H. TOBUSHI, S. YAMADA, T. HACHISUKA, A. IKAI and K. TANAKA, *Thermomechanical properties due to martensitic and R-phase transformations of TiNi shape memory alloy subjected to cyclic loadings*, Smart Mater. Struct., **5**, 788-795, 1996.

15. P.H. LIN, H. TOBUSHI, K. TANAKA, T. HATTORI and M. MAKITA, *Pseudoelastic behavior of TiNi shape memory alloy Subjected to Strain Variations*, J. Intelligent Mater. Systems Struct., **5**, 694-701, 1994.

16. S. P. GADAJ, W. K. NOWACKI and H. TOBUSHI, *Temperature evolution during tensile test of TiNi shape memory alloy*, Arch. Mech., **51**-6, 649-664, 1999.

*Received May 25, 2001; revised version August 1, 2001.*

IUTAM

**International Congress**
**of Theoretical and Applied Mechanics**
**August 15 - 21, 2004 ♦ Warsaw, Poland**


| *President:* | *Co-Chairman:* | *Co-Chairman:* | *Secretary-General:* |
|---|---|---|---|
| Witold Gutkowski | Michał Kleiber | Włodzimierz Kurnik | Tomasz Kowalewski |
| *PAN, Warszawa* | *IPPT PAN, Warszawa* | *Politechnika Warszawska* | *IPPT PAN, Warszawa* |

# Preliminary Announcement

## Scientific Program

The scientific program will start and end with opening and closing lectures, presented by prominent scientists. Titles of lectures and names of lecturers will be announced in October 2002, in the First Announcement and Call for Papers for the Congress.

The program will consist, moreover, of sectional lectures, mini-symposia and contributed papers presented in lecture and seminar presentation sessions. Invitations to present the contributed papers will be made on the recommendation of the International Paper Committee, based on their reviews of submitted abstracts and extended summaries.

## Mini-Symposia

- Smart materials and structures.
- Tissue, cellular and molecular biomechanics.
- Mechanics of thin films and nanostructures.
- Microfluidics.
- Microgravity flow phenomena.
- Atmosphere and ocean dynamics.

## Pre-Nominated Sessions

### In Fluid Mechanics

Biological fluid dynamics • Boundary layers • Combustion and flames • Complex and smart fluids • Compressible flow • Computational fluid dynamics (jointly with IACM) • Convective phenomena • Drops and bubbles • Environmental fluid mechanics • Experimental methods in fluid mechanics • Flow control • Flow in porous media • Flow instability and transition • Flow in thin films • Fluid mechanics of materials processing • Granular flows • Low-Reynolds-number flow • Magnetohydrodynamics • Multiphase flows • Solidification and crystalgrowth • Stirring and mixing • Suspension mechanics • Topological fluid mechanics • Turbulence • Vortex dynamics • Waves

**In Solid Mechanics**

Computational solid mechanics (jointly with IACM) • Contact and friction problems (jointly with IAVSD)g • Control of multibody systems • Control of structures • Damage mechanics • Dynamic plasticity of structures • Elasticity • Experimental methods in solid mechanics • Fatigue • Fracture and crack mechanics (jointly with ICF) • Functionally graded materials • Impact and wave propagation • Material instabilities • Mechanics of composites • Mechanics of phase transformations (jointly with IACM) • Mechanics of porous materials • Multibody dynamics • Plasticity and viscoplasticity • Plates and shells (jointly with IACM) • Rock mechanics and geomechanics • Solid mechanics in manufacturing • Stability of structures • Stochastic micromechanics • Structural optimization (jointly with ISSMO) • Structural vibrations • Viscoelasticity and creep

**Topics involving both fluid mechanics and solid mechanics**

Acoustics • Chaos in fluid and solid mechanics • Continuum mechanics • Fluid-structure interaction • Mechanics of foams and cellular materials • Multiscale phenomena in mechanics

Details on preparation of manuscripts will be provided in the First Announcement and Call for Papers in October 2002.

**It is planned to provide all future information mostly by e-mail. If you are interested in receiving future information, *please pre-register on the Congress World Wide Web site*:**

**http://ictam04.ippt.gov.pl**

**On this site, you can already find many interesting information concerning the Congress**

Correspondence related to the Congress should be sent to:

**Prof. Tomasz Kowalewski, ICTAM04 Secretary-General**

Institute of Fundamental Technological Research

Świętokrzyska 21, 00-049 Warszawa, Poland

e-mail: ictam04@ippt.gov.pl

*Centre International des Sciences Mecaniques* — *International Centre for Mechanical Sciences*

# International Centre for Mechanical Sciences (CISM)
## Programme 2002

| | |
|---|---|
| Advanced Dynamics and Control of Structures and Machines<br>*H. Irskik (Linz), K. Schlacher (Linz)* | **April 15-19** |
| Light Gauge Metal Structures: Recent Advances<br>*J. Rondal (Liege), Dubina D. (Timisoara)* | **June 3-7** |
| Deformation in the Earth's Continental Crust: Theory, Experiment and Modeling<br>*Y. Leroy (Palaiseau), F.K. Lehner (Salzburg)* | **June 17-21** |
| Cardiovascular Fluid Mechanics<br>*G. Pedrizzetti (Trieste), K. Perktold (Graz)* | **July 1-5** |
| Multiscale Modeling in Continuum Mechanics and Structured Deformations<br>*G. Del Piero (Ferrara), D.R. Owen (Pittsburgh)* | **July 15-19** |
| Modern Trend in Composite Laminates Mechanics<br>*H. Altenbach (Halle), W. Becker (Siegen)* | **July 22-26** |
| Phase Change with Convection: Modelling and Validation<br>*T.A. Kowalewski (Warsaw), D. Gobin (Orsay)* | **Sept. 2-6** |
| Modeling and Control of Two-Phase Flow Phenomena<br>*V. Bertola (Turin)* | **Sept. 9-13** |
| Computational Micromechanics of Materials<br>*P. Wriggers (Hannover), C. Schwab (Zurich), T.I. Zohdi (Hannover)* | **Sept. 23-27** |
| Mechanics and Thermomechanics of Rubberlike Solids<br>*G. Saccomandi (Lecce), R.W. Ogden (Glasgow)* | **Sept.30-Oct.4** |
| Moving Discontinuities in Crystalline Solids<br>*F.D. Fischer (Leoben), M. Berveiller (Metz)* | **October 7-11** |
| Liquid Films Theory, Experiments and Industrial Applications<br>*N. Aksel (Bayreuth)* | **October 14-18** |

*Palazzo del Torso, Piazza Garibaldi, 18, 33100 Udine(Italy)* • *e-mail: cism@cism.it* • *http://www.cism.it*
Tel. : +390432248511(6 lines)/Fax + 390432248550• Printing Office Tel. and Fax +39 0432572206 • Partita IVA 00401650304


## The 7th Conference "Shell Structures, Theory and Applications"
### Gdańsk-Jurata, Poland, 9-11 October 2002

organized by

Polish Academy of Sciences, Committee for Civil Engineering, Section of Structural Mechanics
Technical University of Gdańsk, Faculty of Civil Engineering, Structural Mechanics Department
Polish Society of Theoretical and Applied Mechanics, Gdańsk Branch

# Call For Papers

Conferences "Shell Structures, Theory and Applications" (SSTA in short) have been organized in Poland since 1974. The aim of these meetings is always the same: to bring together scientists, designers, engineers and other specialists of shell structures in order to discuss important results and new ideas in this broad field of activity. The goal is to pursue more accurate theoretical models, to develop more powerful and versatile numerical methods for computerized analysis, and to disseminate expertise in design and maintenance of various shell structures and elements commonly used in science, technology and everyday life.

While earlier SSTA Conferences were primarily Polish national meetings, the last 6th SSTA98 in Jurata became a truly international event. It was attended by 170 participants from 14 countries. This confirmed our feeling that there is a need for a specialized international meeting in the field of shell structures, and the SSTA Conference may be an adequate forum for it. It is expected that the next 7th SSTA 2002 will bring together even more specialists of shell structures from international scientific and engineering community.

**CONFERENCE TOPICS**

- The theory and analysis of shells, including:
  - linear and nonlinear theory;
  - constitutive laws;
  - shells and plates with internal microstructure;
  - hybrid and branched structures;
  - beam - shell interaction;
  - stability, dynamics, optimization, reliability, sensitivity, limit load analysis etc.
- Numerical analysis of shell structures and elements, including:
  - computer methods: FEM, BEM and others;
  - analysis of nonstandard problems;
  - development of software packages.
- Design and maintenance of shell structures, including:
  - industrial applications in civil, power, mining and mechanical engineering, as well as in automotive, shipbuilding, aerospace and chemical processing industries;
  - shell design codes and procedures (e.g. Eurocode);
  - case studies of various shell structures and failure problems.

**SCIENTIFIC COMMITTEE**

Wojciech Pietraszkiewicz - chairman

Jan Awrejcewicz, Jacek Chróścielewski, Michał Kleiber,

Paweł Kłosowski, Piotr Konderla, Marian Królak,

Tomasz Lewiński, Czesław Szymczak,

Krzysztof Wiśniewski, Rościsław Tribiłło,

Zenon Waszczyszyn, Czesław Woźniak, Jerzy Ziółko

**THE MAIN DEADLINES**

- Submission of registration form: December 31, 2001
- Second announcement: March 31, 2002
- Submission of 2 pages abstract: April 30, 2002
- Notification to accepted authors: June 30, 2002

**GENERAL INFORMATION**

- The Conference program will include general lectures and contributed papers presented as lectures. The Conference lecture can be delivered in English or in Polish.
- All the contribution abstracts (2 pages) will be rigorously reviewed prior to acceptance. The accepted abstracts will be included in the Conference book of abstracts. Full length manuscripts of the selected papers will be further considered for publication in a special volume of a recognized technical journal.
- An exhibition related to the Conference themes provided by contractors, system manufacturers and consultants will be organized during the event.
- The Conference venue will be the comfortable hotel "Neptun" located in the attractive leisure region of the Hel Peninsula (www.hotelneptun.gda.pl).
- The registration fee, which will cover the full board accommodation and the book of abstracts, will be approximately 300 US dollars and 250 US dollars for accompanying person.
- The second announcement with more details about the Conference fees, general lectures and the abstract format will be sent to persons who return the preliminary registration form.
- Registration by Internet Homepage (http://www.pg.gda.pl/ssta2002) will be welcomed.
- For more details please visit our Internet Homepage or contact the conference secretariat.

**ADDRESS FOR CORRESPONDENCE**

SSTA2002 Organizing Committee
Department of Structural Mechanics
Faculty of Civil Engineering
Technical University of Gdańsk
ul. G. Narutowicza 11/12
80-952 Gdańsk, POLAND

http://www.pg.gda.pl/ssta2002
E-mail: ssta2002@pg.gda.pl
Phone.:+48-58-347-21-47, Fax:+48-58-347-16-70

INSTITUTE OF FUNDAMENTAL TECHNOLOGICAL RESEARCH
publishes the following periodicals:

ARCHIVES OF MECHANICS — bimonthly (in English)
ARCHIVES OF ACOUSTICS — quarterly (in English)
ARCHIVES OF CIVIL ENGINEERING — quarterly (in English)
ENGINEERING TRANSACTIONS — quarterly (in English)
COMPUTER ASSISTED MECHANICS AND ENGINEERING SCIENCES
— quarterly (in English)
JOURNAL OF TECHNICAL PHYSICS — quarterly (in English)

Subscription orders for all journals edited by IFTR may be sent directly to:
*Editorial Office*
*Institute of Fundamental Technological Research*
*Świętokrzyska 21, p. 508*
*00-049 Warszawa, POLAND*

## DIRECTIONS FOR THE AUTHORS

The journal *ARCHIVES OF MECHANICS* (ARCHIWUM MECHANIKI STOSOWANEJ) deals with the printing of original papers which should not appear in other periodicals.

As a rule, the volume of a paper should not exceed 40 000 typographic signs, that is about 20 type-written pages, format: 210×297 mm, leaded. The papers should be submitted in two copies. They must be set in accordance with the norms established by the Editorial Office. Special importance is attached to the following directions:

1. The title of the paper should be as short as possible.
2. The text should be preceded by a brief introduction; it is also desirable that a list of notations used in the paper should be given.
3. The formula number consists of two figures: the first represents the section number and the other the formula number in that section. Thus the division into subsections does not influence the numbering of formulae. Only such formulae should be numbered to which the author refers throughout the paper, and also the resulting formulae. The formula number should be written on the left-hand side of the formula; round brackets are necessary to avoid any misunderstanding. For instance, if the author refers to the third formula of the set (2.1), a subscript should be added to denote the formula, viz. $(2.1)_3$.
4. All the notations should be written very distinctly. Special care must be taken to write small and capital letters as precisely as possible. Semi-bold type should be underlined in black pencil. Explanations should be given on the margin of the manuscript in case of special type face.
5. It has been established to denote vectors by semi-bold type. Trigonometric functions are denoted by sin, cos, tg and ctg, inverse functions – by arc sin, arc cos, arc tg and arc ctg; hyperbolic functions are denoted by sh, ch, th and cth, inverse functions – by Arsh, Arch, Arth and Arcth.
6. Figures in square brackets denote reference titles. Items appearing in the reference list should include the initials of the first name of the author and his surname, also the full title of the paper (in the language of the original paper); moreover;
   a) In the case of books, the publisher's name, the place and year of publication should be given, e.g., 5. S. ZIEMBA, *Vibration analysis*, PWN, Warszawa 1970;
   b) In the case of a periodical, the full title of the periodical, consecutive volume number, current issue number, pp. from ... to ..., year of publication should be mentioned; the annual volume number must be marked in black pencil so as to distinguish it from the current issue number, e.g., 6. M. SOKOŁOWSKI, *A thermoelastic problem for a strip with discontinuous boundary conditions*, Arch. Mech., **13**, 3, 337–354, 1961.
7. The authors should enclose a summary of the paper. The volume of the summary is to be about 100 words.
8. The authors are kindly requested to enclose the figures prepared on diskettes (format WMF, EMF, GIF, PCX, BitMaP, EPS or PostScript).

Upon receipt of the paper, the Editorial Office forwards it to the reviewer. His opinion is the basis for the Editorial Committee to determine whether the paper can be accepted for publication or not.

The printing of the paper completed, the author receives 25 copies of reprints free of charge. The authors wishing to get more copies should advise the Editorial Office accordingly, not later than the date of obtaining the galley proofs.

**The papers submitted for publication in the journal should be written in English. No royalty is paid to the authors.**

**Please send us, in addition to the typescript, the same text prepared on a diskette (floppy disk) 3 1/2″ as an ASCII file, preferably in the TEXor LATEXformat in Dos or Unix format.**

*EDITORIAL COMMITTEE*
*ARCHIVES OF MECHANICS*
*(ARCHIWUM MECHANIKI STOSOWANEJ)*

Archives of Mechanics

## Contents of issue 1 vol. 54



Arch. Mech., **54**, nr 1, str. 1–100, Warszawa 2002